2013

Application of Genetically-Encoded Photoactivatable Crosslinkers to Map Ligand-Binding Sites on G Protein-Coupled Receptors

Amy Grunbeck

APPLICATION OF GENETICALLY-ENCODED PHOTOACTIVATABLE CROSSLINKERS TO MAP LIGAND-BINDING SITES ON G PROTEIN-COUPLED RECEPTORS

A Thesis Presented to the Faculty of

The Rockefeller University

in Partial Fulfillment of the Requirements for

the degree of Doctor of Philosophy

by

Amy Grunbeck

June 2013

APPLICATION OF GENETICALLY-ENCODED PHOTOACTIVATABLE CROSSLINKERS TO MAP LIGAND-BINDING SITES ON G PROTEIN-COUPLED RECEPTORS

Amy Grunbeck, Ph.D.

The Rockefeller University 2013

G protein-coupled receptors (GPCRs) are dynamic membrane proteins that bind extracellular molecules to transduce biological signals. Although GPCRs represent the largest class of targets for therapeutic agents, ligand-binding sites have been precisely defined for only a small percentage of the receptors in the human genome. A general cell-based photocrosslinking approach was developed to investigate the binding interfaces necessary for the formation of GPCR signaling complexes. Amber codon suppression was extended to facilitate the incorporation of photoactivatable unnatural amino acids, *p*-benzoyl-L-phenylalanine and *p*-azido-L-phenylalanine, into engineered GPCRs expressed in mammalian cells in culture. Proof-of-concept studies were carried out in chemokine receptors C-X-C chemokine receptor 4 (CXCR4) and C-C chemokine receptor 5 (CCR5), which are known HIV-1 co-receptors required for HIV-1 cellular entry in $CD4^+$ cells. A cyclic peptide CXCR4-specific inhibitor, T140, photocrosslinked primarily to a specific site on CXCR4 and the result was reconciled with existing structural biology data. A small molecule drug, maraviroc, photocrosslinked to multiple sites on CCR5 and the results were extended to develop a computer homology model of the CCR5-maraviroc complex. In summary, the application of a novel targeted cell-

based photocrosslinking strategy provided detailed information about receptor-ligand complexes in two chemokine receptors. The general approach described here using genetically-encoded photoreactive molecules to study the binding interactions between GPCRs and ligands represents a significant advance in the application of photocrosslinking reagents to address problems in biochemistry and pharmacology.

To my Mom and Dad…

I would never be where I am today without your endless love and support.

Acknowledgments

I would like to acknowledge my advisor, Dr. Thomas P. Sakmar, for giving me the opportunity to carry out my Ph.D. in his lab. I value the guidance and support he has given me throughout my Ph.D. project. In addition, I have really enjoyed working in the collaborative environment that he has created both within the lab and with other scientists in both academic and industrial settings.

I owe most of what I have learned at the bench to the other members of the Sakmar Lab. Dr. Thomas Huber has been an especially great mentor during the course of my Ph.D. I appreciate all the help he has given me with troubleshooting my experiments and teaching me how to critically evaluate my results before moving to the next step. I also want to recognize Manija Kazmi, Pallavi Sachdev, and Saranga Naganathan for their expertise in various areas and for their patience in answering all of my questions. I would like to acknowledge Adam Knepp, Jennifer Peeler, Sarmistha Ray, W Vallen Graham, and Shixin Ye for their helpful comments and feedback. I want to thank all the members of the lab for making the lab environment such an exciting and fun place to work.

During my Ph.D. I have had the opportunity to work on several collaborative projects, which have all been great learning experiences. I want to thank all the scientists I have worked with for their contributions to these projects. These include Dr. John Moore's Lab at Weill Cornell Medical College, which includes Dr. Reem Berro and Sarya Abi-Habib, Anchor Therapeutics, especially Dr. Jay Janz, Dr. Martin Teintze at Montana State University, and Dr. William Goddard's Lab at Caltech, especially Dr. Ravi Abrol. I also want to thank Dr. Stephen Hill at the University of Nottingham and his post-docs Dr. Joelle Goulding and Dr. Leigh Stoddardt for giving me the opportunity to visit the lab and learn some new techniques from them.

Finally, I would like to acknowledge my friends and family for their continued love and support, especially my parents Patrice and George Grunbeck, my sister Marie Grunbeck, and my fiancée Carlos Perea.

Table of Contents

List of Figures

List of Tables

CHAPTER 1: Introduction

1.1. Physiological Role of GPCRs in Biology and Disease.

Adapted in part with permission from (Grunbeck, A., et al. (2012) *ACS Chem. Biol. 7*, 967-972).

G protein-coupled receptors (GPCRs), the largest group of cell-surface receptors, are ubiquitously expressed throughout the human body. These transmembrane proteins have a characteristic heptahelical structure and couple to a cytoplasmic heterotrimeric G protein, which is comprised of an α, β, and γ subunit (Figure 1-1). GPCR-dependent

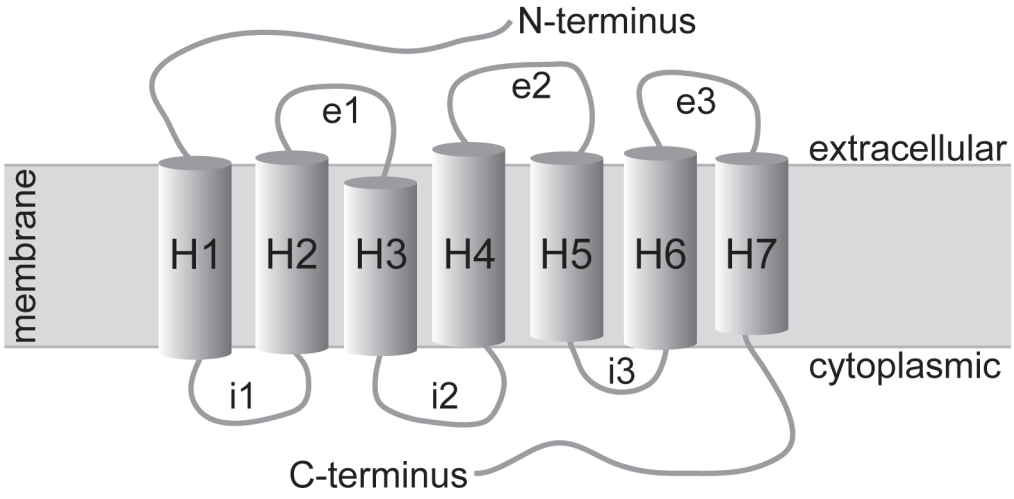

Figure 1-1. Schematic of a prototypical G protein-coupled receptor structure. The seven transmembrane spanning helices are labeled with **H**. Some GPCRs have also been reported to have an eighth helix, but this is not pictured here. Every receptor has three loop regions on the extracellular surface of the receptor, which are designated here with an **e**. Each receptor also has three loops on the cytoplasmic surface of the receptor, which are labeled here with an **i**.

signaling pathways regulate many critical biological processes by responding to environmental signals. A few examples of GPCR modulators are hormones, odorants, neurotransmitters, light, and cytokines. In the prototypical GPCR signaling paradigm, binding of an extracellular ligand to a receptor results in G protein activation by catalyzing GDP-GTP exchange [1]. The G protein subunits then dissociate and stimulate activity of other cellular components [2]. Research over the last several decades has found that the GPCR signaling network is much more complex and diverse than the classical paradigm suggests [3]. Therefore further investigations into the structure and function of GPCR signaling complexes are necessary to understand the molecular mechanisms of specific signaling events, especially those involved in disease.

The onset and progression of many diseases involves the mutation and dysfunction of GPCRs. The infamous role of GPCRs in disease has resulted in this class of proteins being the largest group of molecular targets for drug research [4]. To design and develop drugs to target a specific receptor requires knowledge of the receptor's structure and function. The β-adrenergic receptors, for instance, are important pharmaceutical targets due to their role in regulating the circulatory system and the wealth of information known about their structure and dynamics. The Nobel Prize in Chemistry was awarded in 2012 to Robert Lefkowitz and Brian Kobilka for their research on the β-adrenergic receptor system and the contributions they made towards the understanding of GPCR function in general. Rhodopsin, a light activated receptor, is another well-characterized GPCR. One of the initial discoveries in the rhodopsin field, which had a significant impact on the GPCR field, was the finding that light induces conformational changes in rhodopsin, which in turn transduce a signal in the photoreceptor cell [5]. Following this

discovery, it was quickly appreciated that the functional activity of rhodopsin was directly dependent on its conformational state. Structure-function studies on rhodopsin and the β-adrenergic receptors have provided some insight into how GPCRs are activated, but have raised many unanswered questions about the activation process of other GPCRs.

There are over one thousand proteins expressed in humans that are characterized to have a heptahelical structure. Only a handful of these have been investigated to the extent of rhodopsin and the β-adrenergic receptors, and a large percentage remains to be orphan receptors [6]. Two inherent qualities of GPCRs that make them exceptionally difficult to investigate are their low expression levels and requirement of an amphipathic membrane for function. Researchers spend years optimizing conditions to circumvent these hurdles. One probable solution is to develop novel techniques to investigate GPCRs in their native environment and on a small scale. In the Sakmar Lab, we are interested in creating a set of tools to probe the structure and function of low expressing GPCRs in their native membrane environment.

1.1.1. Chemokine Receptors and HIV Entry

For this thesis project, we focused our studies on the two Family A or rhodopsin-like GPCRs, C-C chemokine receptor 5 (CCR5) and C-X-C chemokine receptor 4. CCR5 is a member of the C-C chemokine receptor family and is activated by the chemotactic cytokines, also referred to as chemokines, which include macrophage inflammatory protein-1α (MIP)-1α, MIP-1β, and regulated-and-normal-T cell-expressed and secreted (RANTES) [7]. The native chemokine ligand for CXCR4 is stromal cell derived factor-1α

(SDF-1α) or CXCL12 [8,9]. Both CXCR4 and CCR5 couple to the inhibitory heterotrimeric G protein, G_i, in the cytoplasm. Ligand binding to the receptor catalyzes G protein activation as in the classical paradigm. Desensitization of the receptor-signaling pathways is initiated through phosphorylation of the C-terminus of the receptor. The cytoplasmic protein β-arrestin then binds to the phosphorylated receptor, which results in decoupling of the G protein and subsequent endocytosis [10,11]. The receptors are then either degraded or recycled back to the plasma membrane.

Chemokine receptors play an important role in the immune response by directing the migration of T lymphocytes to the site of infection. In the case of inflammation, the chemotactic response of immune cells is in response to a chemokine gradient that is created from the site of infection [7]. Due to the importance of CCR5 and CXCR4 in the immune response, these receptors have been hijacked by immune deficiency viruses and cancer to facilitate disease progression[12]. The human immunodeficiency virus (HIV) requires CCR5 or CXCR4 as a co-receptor along with CD4 for viral entry into the host cell[13-15]. The use of either CCR5 or CXCR4 as a co-receptor for viral entry is dependent on the stage of the virus. CCR5 is reported to be the primary co-receptor, whereas CXCR4 is used in later stages of the virus [16]. The discovery of the role of CCR5 and CXCR4 in HIV entry has made these receptors important pharmaceutical targets.

The first proof-of-concept HIV-1 entry blocker was the small molecule CXCR4 antagonist, AMD3100[17], which led to the development of CCR5-targeted entry blockers [18]. Maraviroc, a CCR5-specific small molecule, is the first patient approved GPCR-specific HIV-1 entry inhibitor [19]. Several of the GPCR-specific HIV-1 therapeutics that failed drug trials are often used as experimental tools to probe receptor function. One

example is the conformationally sensitive antibody 2D7, which binds to an extracellular epitope on CCR5 [20]. 2D7 binds to the native structure of CCR5 and is a common tool to determine if CCR5 is correctly folded [21]. A cyclic-peptide called T140, a CXCR4 inhibitor, is another popular investigative tool that was identified due to its anti-HIV activity [22]. For instance, an analogue of T140 was used to stabilize CXCR4 for crystallographic studies [23]. Pepducins are another class of GPCR ligands that are interesting experimental tools and have shown therapeutic potential. Pepducins are palmitoylated peptides with agonist or antagonist potential, whose sequence mimics that of an intracellular loop of the target receptor [24]. A CXCR4-specific pepducin, ATI-2341, mimics intracellular loop 1 of CXCR4 and is reported to be a CXCR4-agonist [25]. Investigating the mechanism of action of ATI-2341 is important for the development of these ligands as GPCR therapeutics in addition to providing insight into the role of receptor intracellular loops for GPCR function. GPCR therapeutic agents are useful tools to study the structure and function of receptor signaling complexes.

1.1.2. Importance of GPCR-ligand Interactions

GPCRs are regulated by ligands of various sizes and structures. Some are peptides or small proteins, such as hormones and chemokines, while others are small molecules, like neurotransmitters, odorants, and pharmaceutical drugs. The mechanism of how a ligand binds to a GPCR and elicits a specific intracellular response is still unknown, although it has been well described that binding of a ligand on a GPCR results in a conformational change in the receptor's structure. Receptor activation was originally

viewed as a 'two state model,' which described GPCRs to only have two conformations, active and inactive [26]. Recent research has shown that the downstream signaling characteristics of a receptor are dependent on the identity of the bound ligand, suggesting the receptor has multiple conformational states [27,28]. Investigating the functional selectivity of these conformational states will provide information about formation of the ternary complex, which includes a ligand, receptor, and G protein, and rationale for future drug design.

Determining the structure of GPCR complexes is important for developing GPCR-specific small molecule therapeutics and biologicals[29]. Some GPCR-targeted drugs bind to orthosteric sites and inhibit the binding interactions with endogenous agonist ligands that are necessary to form productive signaling complexes. However, GPCR-mediated signaling can also be affected by allosteric modulators[30,31]. Targeting potential allosteric sites on GPCRs opens up new avenues for structure-based drug design[29]. To facilitate future drug development and to understand the mechanism of action of existing drugs it is important to identify the binding sites of both orthosteric and allosteric GPCR modulators[32,33]. However, it is not straightforward to identify the precise binding sites and mechanisms of action of GPCR ligands. For example, GPCRs bound to antagonists or agonists are known to display different packing within the 7-helix bundle, and receptor activation proceeds through a series of agonist-GPCR conformations. In addition, computational predictions suggest that binding of various antagonists to CCR5 stabilize different packing within the 7-helix bundle, which might lead to changes in function (*e.g.,* coupling to β-arrestin or G protein) [34]. The focus of this thesis project is on

the optimization and application of a chemically-precise technique in live cells, involving photoactivatable crosslinkers, to define a ligand-binding site on a GPCR.

1.2. Probing GPCR-Ligand Interactions with Targeted Photoactivatable Crosslinkers

Adapted from Grunbeck, A. and Sakmar, T.P. "Probing GPCR-Ligand Interactions with Targeted Photoactivatable Crosslinkers," *in preparation*.

Photoactivatable crosslinking reagents have been used to study binding interactions within biological systems since the 1960s. Westheimer and colleagues pioneered early work by applying photoreactive molecules to map an enzyme's active site [35]. One of the advantages of using photoactivatable probes in a biological system is they react instantaneously with surrounding chemical bonds upon photolysis [36]. The ability to photoactivate a crosslinker reagent allows, at least in principle, for control over "when and where" a crosslinking reaction takes place. Therefore, these reagents enable the investigation of the structures of transient complexes in a cellular environment, for example, which is not possible with standard chemical or crystallographic techniques. Most physiologically relevant GPCR-ligand complexes require the native plasma membrane environment for complex formation. Photolabile probes with high affinity for receptors under native conditions and with minimal alteration to the structure of the original ligand or of the ligand-receptor complex are required to gain maximal information.

There are several different reagents that are reactive upon photolysis, but only a handful of these are stable within a biological environment. A few of the most common ones that have been used to study biological interactions include diazoacyl ester [35], aryl azide [37-39], benzophenone [40], and diazirine [41]. Each of these molecules has their own inherent advantages and disadvantages, which have been described in detail elsewhere [36,42,43]. The primary characteristics that differ among these molecules and determine their effectiveness to probe biological interactions are size, reactivity, and stability. Over the past forty years or so photocrosslinking reagents have been popular tools for the study of GPCR-ligand interactions. The two obvious general strategies for investigating GPCR-ligand interactions with chemical crosslinkers are either by attaching the photoactivatable moiety to the ligand or to the receptor (Figure 1-2). In this section we will cover the methodologies that have been used to generate photoactivatable GPCR ligands, in addition to the recent advances in the site-specific incorporation of photogenerated crosslinkers into proteins expressed in mammalian cells.

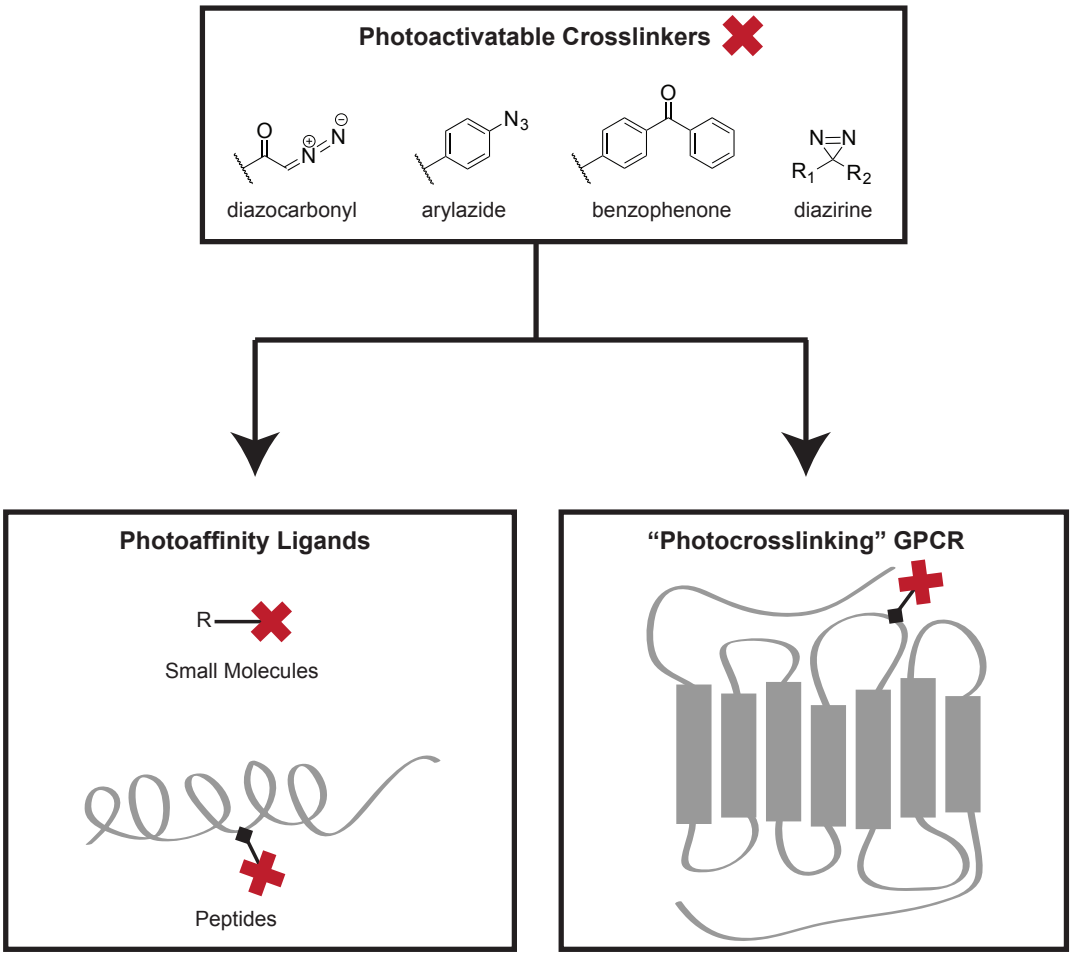

Figure 1-2. A diagram demonstrating how photoactivatable crosslinkers have been used to investigate GPCR-ligand interactions. The top panel shows the four most commonly used photocrosslinking molecules to study biological systems. These groups have been used to study GPCR-ligand interactions in two ways either by incorporating them into the ligand or into the receptor.

1.2.1. Photoactivatable GPCR Ligands

Photoaffinity labeling is a potentially powerful technique for identifying the receptors for orphan ligands and for determining a ligand-binding site on a receptor. To perform these studies an analogous ligand needs to be designed that contains a photoactivatable crosslinking moiety while retaining binding affinity to the cognate receptor. Photoaffinity ligands have been synthesized in several different ways depending on whether the ligand is a small molecule, a peptide, or a protein (Figure 1-3). In the sections below we describe a few examples of how photoactivatable GPCR ligands have been generated.

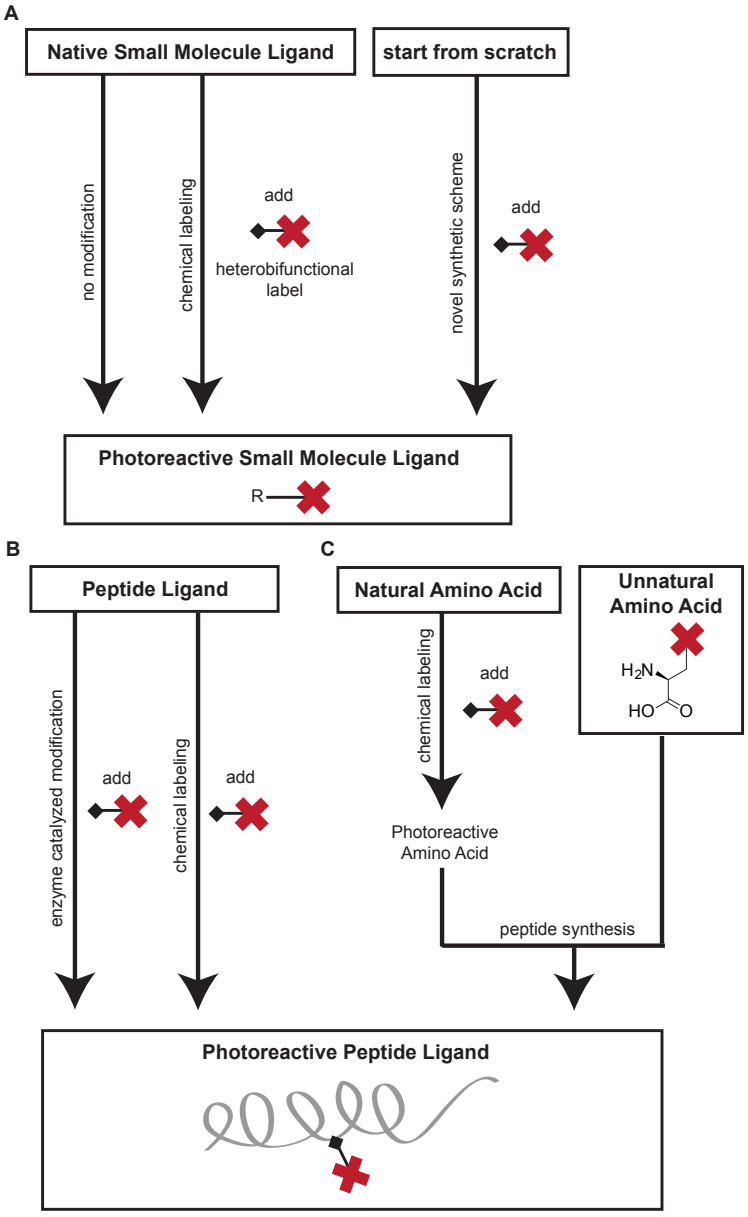

Figure 1-3. An overview of the methods discussed to create photoaffinity GPCR ligands. (A) Some native small molecule ligands naturally contain photoreactive groups. Other photoreactive small molecule ligands are generated by chemically labeling a molecule with a heterobifunctional group or synthesizing a photoactivatable analogue from scratch. (B) Peptide ligands are labeled post-peptide synthesis through an enzyme catalyzed reaction or chemical modification. (C) Photoreactive peptide ligands are also created by synthesizing a peptide using natural amino acids derivatized with photocrosslinking groups or photoactivatable unnatural amino acids

1.2.1.a. Synthetic Small Molecule Ligand Analogues

Many of the native ligands for family A, or rhodopsin-like GPCRs, are small molecules. For example, the prototypical GPCR rhodopsin serves as the dim-light photoreceptor in the rod cells and binds the chromophore 11-*cis*-retinal, which acts like a pharmacological inverse agonist. To create an analogue of a small molecule that contains a photogenerated crosslinker generally requires extensive organic synthesis, as was the case in studies to determine the binding site and orientation of 11-*cis*-retinal in the transmembrane core of rhodopsin. Several analogues of 11-*cis*-retinal were synthesized to contain a diazirine group as a substituent on the β-ionone ring [38]. These molecules were characterized for their ability to regenerate opsin. Only one of the analogues was able to bind to opsin to regenerate a pigment and found to crosslink to opsin upon exposure to ultraviolet (UV) light. After further analysis the orientation of 11-*cis*-retinal was determined to be such that the β-ionone ring was directed towards TM helices 3 and 6 [39]. Crosslinking an 11-*cis*-retinal analogue to opsin is a classic example of how it is possible to retain binding of a small molecule ligand to its receptor after introducing a photocrosslinking group. In addition, this work demonstrates how synthetic ligand analogues can determine the absolute orientation of a molecule in the ligand-binding site of a receptor without extensive site-directed mutagenesis and ligand binding assays on receptor mutants, or a high-resolution crystal structure of a receptor-ligand complex.

Rhodopsin is unique compared to many other GPCRs because it is found in large abundance within the disc membrane of the retinal rod cell and can be purified to homogeneity in detergent solution. Other receptors are expressed at much lower levels in the native tissues, which complicates their identification, isolation, and characterization.

In such cases, the development of photoaffinity ligands is advantageous to identify target receptors and probe ligand specificity. One particular demonstrative example is the identification of the sex pheromone receptor in the silk moth *Antheraea polyphemus*. Ganjian *et al.* synthesized a diazoacetate derivative of the sex pheromone, HDA, and demonstrated that this molecule retained 10% of the native activity of the pheromone [44]. UV irradiation of the diazoacetate HDA analogue when bound to sensory hairs from the silk worm resulted in the identification of a 69-kDa membrane protein [45]. Prior to this discovery the involvement of a membrane receptor in the sex pheromone transduction mechanism was only a theory.

1.2.1.b. Native or Native-like Ligands

Native ligands, in some cases, are able to crosslink without the addition of specific reactive functional groups. For example, dopamine is an example of a native photoaffinity ligand. Nishikori *et al.* were the first to discover that UV illumination of mammalian nervous tissues in the presence of dopamine led to the covalent attachment of dopamine to specific cellular proteins. Dopamine does not contain one of the common photoactivatable crosslinking groups, and this report proposed that the photocrosslink occurs between the oxygen in the catechol moiety of dopamine and an amino acid residue in the dopamine receptor. Through the use of dopamine as a photoaffinity probe Nishikori and colleagues were also able to apply [^{3}H]-dopamine to quantify the amount of purified receptor and identify that the D1 and D2 dopamine receptors are co-expressed

in mammalian nervous tissues [46]. Others followed up this study and used the photoactive properties of dopamine to determine that dopamine binds specifically to a 57-kDa protein subunit in striatal membranes that they suggested was the D1 dopamine receptor [47]. There are many advantages to performing photocrosslinking studies when the native structure of the ligand is retained, especially with small molecule ligands where addition of even a small chemical group significantly alters the structure of the molecule.

Some drugs are themselves photoactivatable crosslinkers without further modification, although efficiency of the photolysis and crosslinking can be very low. Members of the adrenergic receptor subfamily of GPCRs have been extremely popular drug targets because of their significance in regulating the cardiac, pulmonary and circulatory systems. For example, the β-adrenergic receptors have been the focus of many photocrosslinking studies involving photoreactive drug analogues. Isoprenaline, a β-adrenergic receptor agonist used as a cardiac iontropic agent and pressor substance, is one example of a GPCR drug that has been shown to label covalently a receptor upon photolysis without further modification of the molecule [48]. Other β-adrenergic receptor antagonists, generally termed β-blockers, have required alternative syntheses to incorporate a photoreactive group, resulting in the development of a plethora of β-adrenergic azide-containing [49-53] and diazirine-containing [54] probes. Obviously, the ideal probe ligand contains a photoreactive moiety at a location distinct from its pharmacophore so that pharmacological activity is maintained. Such synthetic ligand tools have been useful for the study of the β-adrenergic, and other types of related receptors, and exemplify how a variety of different photocrosslinkers based on small molecule analogues of GPCR ligands can be used to study ligand-binding sites.

1.2.1.c. Derivatizing Peptide Ligands with Photoactivatable Groups

A large number of GPCRs are activated by endogenous peptide hormones, neuropeptides, or peptide-derived ligands (peptides that are post-translationally modified). Peptide ligands that target GPCRs have been labeled with photocrosslinking groups post-synthesis either through enzyme-catalyzed reactions or chemical modifications. The application of modifying enzymes for labeling purposes provides unique specificity and allows for labeling at positions that cannot generally be targeted with chemical reagents. For example, Gorman *et al.* demonstrated the use of guinea pig liver transglutaminase for the attachment of aryl azides onto the γ-carboxamide of glutamine residues in peptide ligands. Novel substrates for transglutaminase were synthesized and then reacted with peptide ligands, such as substance P and glucagon 1-6 [55]. This technique was also applied to generate a photosensitive calcitonin analogue using the transglutaminase substrate N-(β-aminoethyl)-4-2-nitroaniline. Photolysis of this calcitonin analogue when bound to T47D breast cancer cells led to the identification of an 85-kDa calcitonin binding protein [56]. The photoaffinity probe in this example facilitated the identification of the calcitonin receptor, which had not been done previously due to difficultly in stabilizing the receptor-ligand interaction.

Heterobifunctional reagents are perhaps the most common and effective tools for crosslinking peptide ligands to their cognate receptors. These types of reagents can derivatize peptide ligands prior to receptor binding, or once the ligand-receptor complex is formed. The prototypical structure of heterobifunctional reagents commonly includes a chemical crosslinking group attached via a linker to a photoactivatable crosslinking

group. Here we describe several examples of heterobifunctional molecules that have been used to study GPCR-ligand interactions.

Labeling of primary amino groups in peptide ligands, either at the free amino group at the N-terminus or at lysine residues, can be carried out in several different ways. N-hydroxysuccinimide ester or succinidmidyl containing molecules react with all accessible primary amines. The N-terminus of oxytocin was labeled specifically using the N-hydroxysuccinimide ester of 2-nitro-5-azidobenzoylglycine because no lysines are present in this peptide [57]. In other cases where more than one primary amine is present, protecting groups need to be used to label only one position. The parathyroid hormone was labeled specifically on a lysine with succinimidyl *p*-(3-iodobenzoyl) benzoate by using an Fmoc-protecting group on the N-terminal residue [58]. One reagent that specifically labels the ε-amino group of lysines without reacting with the free amino group at the N-terminus is 4-fluoro-3-nitrophenylazide. This reagent was shown to label a lysine in glucagon and the location of the photoactivatable group was characterized by Edman degradation [59,60].

Another common functional group found in peptides is a carboxyl group, but derivatizing peptides at carboxyls is uncommon due to the high abundance of Asp and Glu residues in most peptides. In general, the greater the number of positions in a peptide that are labeled, the more difficult it is to purify a homogeneous analogue and the more likely it is that its binding to the receptor will be perturbed. One reagent used for carboxyl group modification is N-(5-azido-2-nitrophenyl)-2-ethylenediamine. In one report, this reagent labeled the carboxyl groups on α-thrombin via a carbodiimide condensation reaction. The photoreactive α-thrombin derivative was not found to have

significantly altered binding to cell surface receptors. In addition, this ligand was found to crosslink specifically to a ~50-kDa receptor on mouse embryo cells [61]. Alternatively, peptide ligands can also be derivatized on Trp residues. Trp residues can be specifically labeled with sulfenyl chloride reagents that react with the side chain indole ring. Glucagon and corticotropin are two examples of peptide hormones that have been labeled with 2-nitro-5-azidophenylsulfenyl chloride for photoaffinity studies [62,63].

Heterobifunctional reagents can also be added to a receptor-ligand complex after the complex is formed. In this scenario crosslinking should occur between the ligand and receptor of interest. However, since these types of reagents tend to bind relatively non-specifically, the results of positive crosslinks can be complex and difficult to interpret. Despite the obvious drawbacks and low signal-to-noise problem inherent in attempts to crosslink with non-specific reagents, the procedure can be relatively straightforward since tedious chemical synthesis of photoactivatable ligands is not formally needed. Another advantage of this approach is that native complexes between ligand and receptor are formed before the crosslinking reaction and neither the ligand nor the receptor is altered before photolysis. This strategy was used to crosslink glucagon to the glucagon receptor in rat liver membranes. The heterobifunctional crosslinking reagent hydroxysuccinimidyl-p-azidobenzoate was added to membranes that were pre-incubated with [^{125}I]-glucagon. Photolysis resulted in the covalent crosslink of the labeled glucagon to a 53-kDa protein [64].

1.2.1.d. Introducing Photoreactive Side Chains into Peptide Ligands

Photoreactive molecules can also be introduced into peptide ligands during peptide synthesis through the incorporation of amino acid derivatives or unnatural amino acids (UAAs). This strategy enables the incorporation of the photocrosslinker at any position in the peptide, whereas derivatization post-synthesis depends on the location of an available functional group. Benzophenone has been introduced into GPCR ligands in both of these manners. One report derivatized a lysine precursor prior to peptide synthesis with *p*-benzoylbenzoic acid [65]. The benzophenone-labeled lysine was introduced into parathyroid hormone and calcitonin during peptide synthesis [66,67]. Kauer *et al.* synthesized another benzophenone-containing UAA, *p*-benzoyl-L-phenylalanine (BzF) [68,69]. BzF has subsequently been used in the development of many GPCR-targeted photoaffinity ligands. BzF scanning can be carried out where BzF is incorporated successively at each position of a peptide ligand analogue. In one notable example, BzF scanning was carried out on Substance P, which led to the identification of two specific positions where BzF in the peptide sequence resulted in analogues that crosslinked to the NK-1 receptor [70]. Additional analysis of the crosslinked complex using protease digestion and analysis of proteolytic products led to the identification of the location in the receptor where the crosslink occurred [71,72]. The process of identifying the location of the crosslink in the receptor can be extremely involved and complicated and in most cases precise identification of the site of a crosslink is not technically possible. Therefore, newer strategies described later in this report have been devised to improve the likelihood of

identifying sites of crosslinking, which dramatically enhances the utility and sensitivity of crosslinking experiments.

The introduction of BzF into peptide ligands to create photoaffinity probes has been used commonly for the study of class B GPCRs, also known as the secretin- or glucagon-like receptors. The characteristic structure of class B GPCRs includes a medium length N-terminal domain, also referred to as the ectodomain, which is important for binding peptide hormones. Extensive photocrosslinking experiments have been performed to understand how a peptide hormone binds to its cognate ectodomain. For example, the binding of secretin analogues to the ectodomain of the secretin receptor has been studied in detail using crosslinking approaches [73]. In these studies BzF was incorporated at various positions in secretin and the resulting [^{125}I]-labeled analogues were characterized and crosslinked to the receptor in native membranes. The general location of crosslinking in the receptor was identified through extensive digestion of the covalent receptor-analogue ligand complex followed by detection of the [^{125}I]-labeled fragment in the resulting peptide mixture using SDS-PAGE [74]. To improve the localization of the crosslink site additional cyanogen bromide cleavage sites were created in the receptor using site-directed mutagenesis to introduce Met residues [75,76]. A similar strategy was also used to study the binding interactions between the vasoactive intestinal peptide (VIP) and the human VPAC1 receptor [77-79]. A molecular model of the VIP-hVPAC1 complex was created using the NMR structure of VIP and the distance constraints identified from the crosslinking study [80]. This study is a notable demonstration of how photocrosslinking data can be applied to create a more detailed model of a GPCR-ligand complex.

An UAA containing an aryl azide, *p*-azido-L-phenylalanine (azF), has also been synthesized [81]. Since this amino acid is unstable under the conditions required for peptide synthesis [82], another method was needed to incorporate azF into peptides. A precursor ion, L-4-nitrophenylalanine, was incorporated at the position of interest during synthesis and then the nitro group was coverted to an azido group through additional chemical reactions [83]. This method has been used to create photoaffinity analogues of angiotensin II and kinins [84,85].

More recently derivatives of Leu and Met have been generated to contain a diazirine group. These amino acids are referred to as photo-Leu and photo-Met, respectively [86], and were originally created for the incorporation of photoreactive groups into proteins expressed in cells since they can be recognized by the endogenous tRNA synthetases for Leu and Met. Photo-Leu has been incorporated into pepducins to investigate their mechanism of action [31]. This photocrosslinking study demonstrated that the pepducin agonist, ATI-2341, crosslinked to its cognate receptor CXCR4, but the exact site of the crosslink was not identified. In the section that follows, we will discuss the methods available for the site-specific incorporation of photoactivatable crosslinkers into GPCRs to enable the identification or mapping of ligand-binding sites.

1.2.2. GPCRs Engineered to Contain Photocrosslinkers

A complementary technique to the use of photoaffinity ligands is to introduce photoactivatable groups at specific positions in a GPCR itself. An advantage to performing crosslinking experiments from the orientation of the receptor is that the exact

site on the receptor of any potential covalent linkage is known in advance. Since the receptor is much larger than the ligand for any GPCR-ligand complex, and since the general aim of crosslinking experiments is to map the binding site of a ligand to its receptor, knowing the site of origin for a crosslink and the receptor can be a tremendous advantage. In general, as with the case of derivatizing the GPCR ligand, there are also two methods for introducing the photoreactive group into the receptor – either derivatize the receptor post-translationally or incorporate the unique functional group during protein translation (Figure 1-4). These methods both rely on heterologous over-expression of engineered receptors in culture using now standard techniques of molecular biology as discussed below.

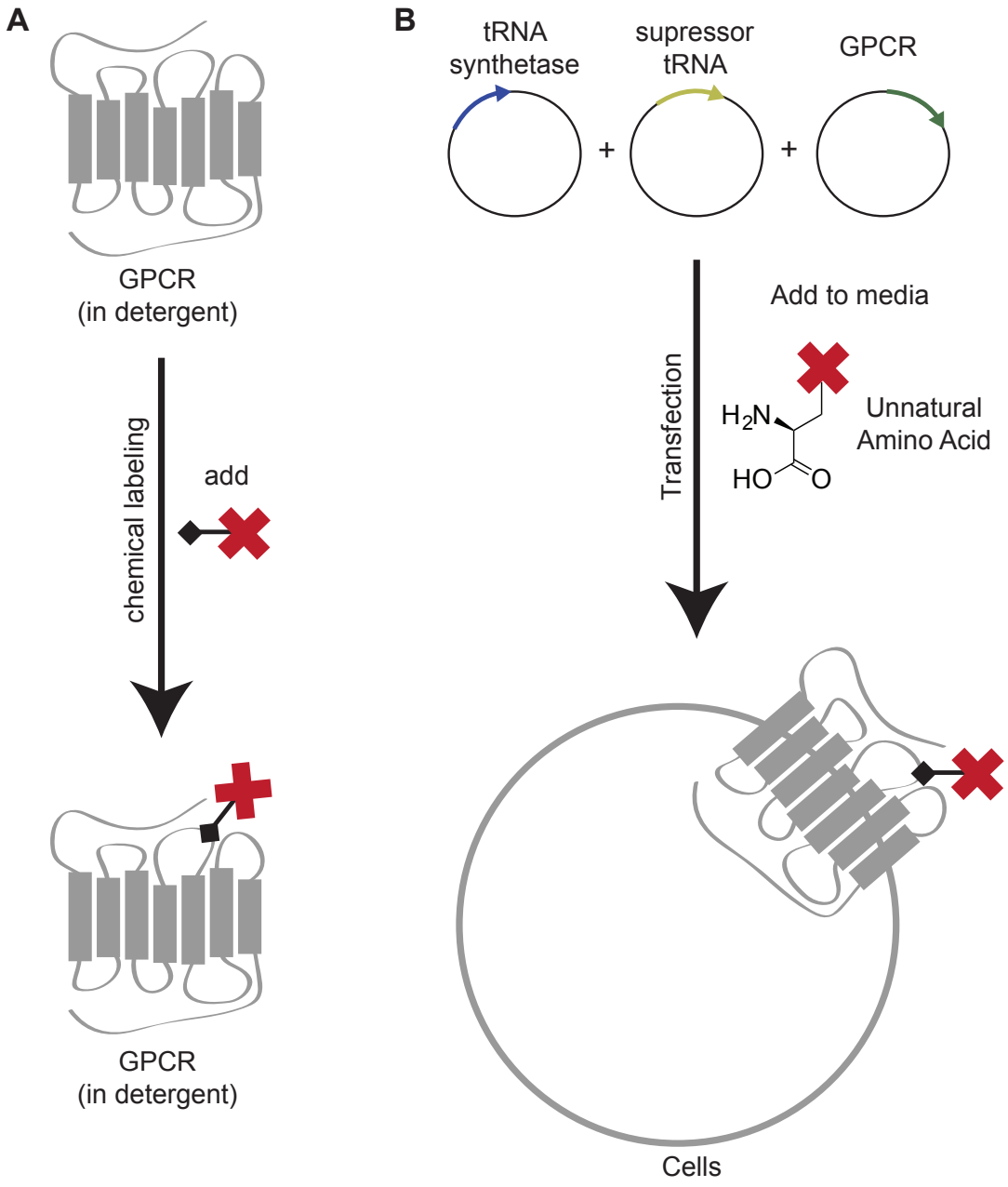

Figure 1-4. Techniques for introducing photocrosslinkers into GPCRs. (A) Photocrosslinking groups have been attached to a specific residue, such as cysteine, in a GPCR through chemical modification of the receptor after extraction from cells. (B) Photoactivatable crosslinkers have also been incorporated into GPCRs expressed in cells as an unnatural amino acid using the amber codon suppression technology.

1.2.2.a. Labeling Cysteines with Photocrosslinkers

One way to introduce a photocrosslinker into a GPCR is to use sulfhydryl chemistry and target the available Cys residues after the receptor has been expressed and purified. Since all known GPCRs contain multiple Cys residues, to attain specific labeling at only one site in the receptor requires that all other Cys residues need to be removed by site-directed mutagenesis. This technique was used to introduce an aryl azide at a specific Cys in rhodopsin with the photocrosslinking group N-((2-pyridyldithio)ethyl-4-azidosalicylamide (PEAS). In this report, the binding interactions between rhodopsin and the G protein, transducin, were investigated [87]. The receptor was first extracted from the cell membrane using detergent and bound to an immunoaffinity resin before being derivatized with the PEAS reagent. In principle this strategy could also be applied to investigate ligand-receptor interactions as long as the labeling reaction did not alter an essential conserved disulfide bond on the extracellular surface of the receptor. However, removal of all but one reactive Cys residue, which can then be strategically situated as desired in the receptor sequence, is a painstaking process that can take years to accomplish. Many GPCRs have atleast one cysteine residue that is essential for the correct formation of a receptor's tertiary structure. [88,89]. In addition, many ligand binding events that lead to a ternary complex between receptor and G protein require the receptor to be in a native-like membrane environment. Incorporating the photoreactive group into a receptor during protein translation overcomes this limitation as discussed in the next section.

1.2.2.b. Unnatural Amino Acid Mutagenesis

The strategy of using amber stop codon suppression to incorporate amino acids with unique functional groups into proteins expressed in cells was developed most notably by Peter G. Schultz and coworkers [90]. This methodology involves the engineering of orthogonal suppressor tRNA and amino acyl tRNA pairs and was originally advanced primarily for use in *E. coli* expression systems. For photocrosslinking studies, the tRNA synthetases were developed for the two relevant UAAs, BzF and azF [91,92]. Since these reports, the amber codon suppression technique has been adapted and enhanced in order to incorporate BzF and azF into GPCRs expressed in yeast [93,94] and mammalian cells [95,96].

The prototypical yeast GPCR, Ste2p, was the first yeast receptor reported to have an UAA incorporated at a specific site in the receptor. In this study BzF was introduced into Ste2p expressed in *Saccharomyces cerevisiae* [93,94]. The Ste2p BzF mutants were then examined for crosslinking to the Ste2p peptide ligand, α factor. Several positions in the receptor were reported to result in covalent crosslinks to biotinylated α factor [93]. This was the first example of a covalent crosslink between an engineered GPCR with UAAs and a ligand.

The introduction of UAAs into GPCRs expressed in mammalian cells was first demonstrated using rhodopsin and CCR5. Heterologous expression of rhodopsin and CCR5 UAA mutants in HEK 293T cells resulted in the expression of functional receptors at the cell surface [95,97]. In this dissertation, we report the application of BzF and azF to identify a ligand-binding interface on a GPCR, a technique we term targeted photocrosslinking. We describe how the complex of CXCR4 and the CXCR4-specific

inhibitor T140 was used to validate the targeted photocrosslinking strategy and how the data were evaluated using the crystal structure of CXCR4 bound to a homologous T140 peptide, CVX15 [23,98]. In addition, we performed a second photocrosslinking study to investigate the binding site of the FDA-approved small molecule drug maraviroc on CCR5. This complex currently has no crystal structure available. The methods described in this report detail how to perform the targeted photocrosslinking experiments, in addition to various strategies for evaluating the functional activity and ligand binding properties of GPCRs in cells, membrane preparations, and detergent. We also discuss the steps that we have taken towards determining the mechanism of action of the CXCR4-specific pepducin. Finally, we review the complementarity of photocrosslinking studies and crystallography and how we would like to develop further the targeting photocrosslinking technique to investigate the binding interactions between GPCRs and other binding partners.

CHAPTER 2: Materials and Methods

2.1 Reagents and Buffers

Materials. All enzymes for molecular biology applications were purchased from New England Biolabs. Protein expression vectors were purchased from Invitrogen. Protease inhibitor tablets were purchased from Roche. The 1D4 antibody was purchased from National Cell Culture Center. 2D7 was purchased from BD Biosciences and 3A9 was from Ebiosciences. The His4 antibody was purchased from Sigma. The FLAG mAb was purchased from Sigma. 2D7 and 3A9 were labeled in house with Atto655. Alexa647-MIP-1α was purchased from Almac group. Fluorescein-labeled maraviroc analogues, FL-maraviroc and FL-MVC-bp, and T140 analogue containing BzF and labeled with fluorescein (FL-T140-BzF) were provided by Dr. Martin Teintze from Montana State University. Fluorescein-T140 (FL-T140) was synthesized by the Proteomics Facility at Rockefeller University. Secondary antibodies conjugated to horseradish peroxidase (HRP) were acquired from KPL Inc..

Buffers:

Buffer N: 20 mM Tris-HCl (pH 7.0), 0.1 M $(NH_4)_2$-SO_4, 10%(v/v) glycerol, 0.07% cholesteryl hemisuccinate (CHS), 0.018% 1,2-dioleoyl-sn-glycero-3-phosphocholine (DOPC), 0.008% 1,2-dioleoyl-sn -glycero-3-phospho-L-serine (DOPS), 0.33% n-dodecyl-β-D-maltoside (DM), and 0.33% 3-[(3-

cholamidopropyl)-dimethylammonio]-1-propanesulfonate (CHAPS)[99].

Buffers for Preparation of Membranes:

a. Buffer HL: 1 mM Tris-HCl pH 6.8, 10 mM EDTA, 0.1 mM PMSF, 10 μg/mL Aprotinin + Leupeptin
b. Buffer MP: 20 mM Tris-HCl pH 6.8, 150 mM NaCl, 1 mM $MgCl_2$, 1 mM $CaCl_2$, 10 mM EDTA, with or without 0.1 mM PMSF

Buffers for [^{35}S]-GTPgS Binding Assay:

a. Buffer R: 50 mM Tris-HCl pH 7.5, 5 mM $MgCl_2$, 0.5 mM EDTA, 60 mM NaCl, 10 μM GDP, 0.1 mg/mL saponin, and 1 mg/mL BSA
b. Buffer W: 10 mM Tris-HCl pH 7.5, 5 mM $MgCl_2$, and 60 mM NaCl

CHAPSO buffer: 1% CHAPSO (Affymetrix-Anatrace) in 50 mM Tris-HCL; pH 8.0, 0.5 mM EDTA, 250 mM NaCl, 0.2 mM PMSF

Buffer X: 1X Hank's Buffered Salt Solution (HBSS) with 20 mM HEPES pH 7.4 and 0.2% BSA

Buffer D: 50 mM HEPES pH 7.4, 1 mM $CaCl_2$, 5 mM $MgCl_2$, and 0.5% BSA

Buffers for Zap1 Purification:

a. Homogenization buffer: 40 mM Tris pH 8, 0.3 M NaCl, 5 mM 2-mercaptoethanol, 2 mM PMSF, and protease inhibitors
b. Buffer T: 25 mM Tris pH 8, 0.3 M NaCl, 20 mM imidazole, 0.5 mM TCEP, and 1% (v/v) Triton X 100
c. Buffer C: 25 mM Tris pH 8, 0.3 M NaCl, 20 mM imidazole, 0.5 mM TCEP, and 20 mM Na Cholate

d. Buffer ND: 25 mM Tris pH 8, 0.3 M NaCl, 20 mM imidazole, and 0.5 mM TCEP
e. Buffer E: 25 mM Tris pH 8, 0.3 M NaCl, 0.5 M imidazole, and 0.5 mM TCEP
f. Buffer G: 10 mM Tris pH 8, 0.15 M NaCl, and 0.5 mM TCEP

Buffer M: 20 mM Tris pH 6.8, 0.1 M $(NH_4)_2SO_4$, 0.6% POPC, 0.4% POPS, 1% CHAPS, and 0.37 mg/mL 1D5 peptide

NABB Buffer: 20 mM Tris pH 6.8, 150 mM NaCl, and 1 mM EDTA

2.2. Mutagenesis

2.2.1. Site-directed mutagenesis and plasmid construction.

Construction of the suppressor tRNA and BzF and azF amino-acyl tRNA synthetase plasmids were described previously [95]. The human CXCR4 gene and human CCR5 are both in a pcDNA3.1(+) plasmid and contain a C-terminal 1D4-epitope, TETSQVAPA. Single site mutations and amber codons were introduced into CXCR4 and CCR5 using the Quikchange Lightning Site-Directed Mutagenesis kit (Stratagene). The plasmid used for expression of the Zap1 protein in *E. coli* is pE28-zap1. Construction of this plasmid has been described elsewhere [100].

2.2.2. Construction of CXCR4/CCR5 Chimera by PCR Splicing by Overlap Extension (SOEing).

A CXCR4 chimeric construct was created by exchanging the sequence between residue Met 63 and Leu 78 with the homologous sequence in CCR5, which corresponds to the residues between Leu 55 and Leu 70. This construct was created through a splicing by overlap extension (SOEing) method, which involves generating DNA fragments with overlapping ends [90,101]. Two DNA fragments encoding upstream of Met 63 and downstream of Leu 78 in CXCR4 were made by PCR amplifying the CXCR4 template plasmid using primers with the sequences CTTAAGCTTGTTACCATGGAGG and CTTTTGCAGTTTATCAGGACCAGGATGACCAATCCATTG for one fragment and primers GACATCTACCTGCTCCACCTGTCAGTGGCCGACC and CTGCAGAATTCTTAGGCG for the other. The DNA fragment encoding the region of CCR5 between residues Leu 55 and Leu 70 was created by PCR amplifying the CCR5 template plasmid with TTGGTCATCCTGGTCCTGATAAACTGCAAAAGGC and GGCCACTGACAGGTGGAGCAGGTAGATGTCAGTC. The three DNA fragments were then spliced together with two additional PCR reactions. Each of these PCR reaction mixtures contained 1 μg of template plasmid, 5 μL of 10X PCR buffer, 2 μL of 10 mM dNTPs, 1 μL of 50 μM primers, and 1 μL of Pfu Turbo in a total of 50 μL reaction volume made up in ddH_2O. The conditions for these PCR reactions involved 5 minutes of denaturation at 95°C followed by 30 cycles of denaturation (30 sec., 95°C), annealing (1 min., 50°C or 55°C) and extension (1 min. or 2 min., 72°C). The final cycle had a 7 minute extension step at 72°C followed by DPN-1 digestion for 1 hour at 37°C. The final PCR product was then reacted with Taq polymerase for 10 minutes at 72°C.

This PCR product was then cloned into a pcDNA3.1 Topo TA vector. The new vector was then transformed into top 10 cells and mini-prepped. The plasmid was then digested at HINDIII and EcoRI restriction sites and ligated into a pcDNA3.1 vector, which had also been digested with the same restriction enzymes. This CXCR4 construct where the intracellular loop 1 region has been replaced with the homologous sequence of CCR5 from now on will be referred to as CXCR4_R5i1.

2.3. Expression of GPCRs in HEK293T Cells

2.3.1. Culturing of HEK293T Cells and Transfection of GPCRs.

HEK293T cells were grown in Dulbecco's Modified Eagle's Medium (DMEM; 4.5 g/L glucose, 2 mM glutamine; Gibco) containing 10% FBS in a 5% CO_2 atmosphere at 37°C. Twenty-four hours prior to transfection cells were split so they were at 70-80% confluency for the day of transfection. For transfection in a 10 cm^2 plate, 3.5 μg of receptor plasmid DNA or empty vector for mock transfections was mixed with 10 μL of plus reagent and 750 μL of DMEM. In a second tube 17 μL of lipofectamine was mixed with 500 μL of DMEM. After a 15 minute incubation at room temperature the two tubes were combined and incubated for another 15 minutes before being brought up to a total of 4 mL with DMEM and added to the cells. The cells were then incubated with the transfection mixture for 4 to 6 hours at 37°C in a 5% CO_2 atmosphere and then supplemented with 4 mL of DMEM containing 20% FBS. Twenty-four hours post-transfection the cell media was then replaced with 8 mL of new DMEM media with 10% FBS. Cells were harvested or used in experiments 48 hours post-transfection.

2.3.2. Expression of CCR5 and CXCR4 Unnatural Amino Acid Containing Mutants in Mammalian Cells.

CCR5 and CXCR4 UAA mutants were expressed as previously described for CCR5 and rhodopsin [95]. Briefly, HEK293T cells were transfected with three cDNA simultaneously, which contained the genes for the receptor amber mutant, BzF or azF amino-acyl tRNA synthetase and suppressor tRNA. Transfections were performed using lipofectamine plus reagent (Invitrogen). The ratio of DNA in μg was 1:0.1:1 CXCR4:UAA synthetase:suppressor tRNA. For transfection in a 10 cm^2 plate, 3.5 μg of receptor DNA were used with 10 μL of plus reagent and 17 μL of lipofectamine. Transfections performed in a 6-well plate used a quarter of these amounts. Four hours post-transfection the media was supplemented to have a final concentration of 10% FBS with or without 0.5 mM BzF or azF in Dulbecco's Modified Eagle's Medium (DMEM; 4.5 g/L glucose, 2 mM glutamine; Gibco). The cells were scraped 48 hours post-transfection in 1X Phosphate Buffered Saline (PBS) containing the protease inhibitors aprotinin and leupeptin and tested for receptor expression through a Western Blot analysis.

> Note: The GPCR UAA mutants express at significantly lower levels than wildtype receptor. To obtain similar expression levels of UAA mutants and wildtype receptor use approximately 1/20 or 1/25 the amount of plasmid for the wildtype receptor as is used for transfection of the amber mutants.

2.3.3. SDS-PAGE and Western Blot Analysis.

Cell pellets were lysed in 1% (w/v) *n*-dodecyl β-D-maltoside in 50 mM Tris-HCl at pH 7.5 containing protease inhibitors for 1 hour at 4°C on a nutator. Following solubilization the lysate was spun at 20,000xg for 5 minutes. For immunopurification experiments, the supernatant fraction was bound to sepharose beads conjugated to the 1D4 antibody overnight at 4°C. Samples were eluted from the beads by shaking in 1X NuPAGE LDS sample buffer containing DTT for 1 hour at 37°C. The samples were then run on an SDS-PAGE gel (NuPage Novex 4-12% Bis-Tris Gel) and then transferred to a polyvinylidene difluoride (PVDF) membrane for immunoblotting. PVDF membrane was blocked in 5% milk in 1X Tris Buffered Saline with Tween-20 (TBST) for 1 hour at 4°C on a shaker followed by incubation with primary and secondary antibodies diluted in 5% milk in 1X TBST. For detection of CCR5 or CXCR4, PVDF membranes were blotted with a 1D4 mAb at a 1:5000 dilution followed by incubation with an anti-mouse antibody (1:10,000) conjugated to horseradish peroxidase (HRP). Molecules conjugated to fluorescein were detected using a polyclonal anti-fluorescein antibody (abcam; #ab19491) at a 1:3000 dilution followed by a secondary antibody anti-rabbit-HRP (1:10,000). The membranes were then incubated in a chemiluminescent substrate (Thermo Scientific) prior to being exposed to HyBlot CL autoradiography film (Denville Scientific Inc.).

> Note: The anti-fluorescein antibody is very specific for fluorescein. The reactivity of this antibody is not dependent on the presence of an aminohexanoyl linker between the fluorescein moiety and the protein. This antibody will also recognize fluorescein-maleimide and proteins labeled with fluorescein-maleimide. Also, exposure of fluorescein to UV light does bleach the fluorescence, but this does not appear to affect the reactivity of the antibody with the fluorophore.

2.4. In vitro Functional Assays

2.4.1. Fluorescent Ligand Binding to CCR5 on Beads.

Biotinylated 1D4 antibody was pre-bound to streptavidin-conjugated magnetic Dynabeads (Invitrogen). Cf2th cells (NIH AIDS Research & Reference Reagent Program [21]) stably expressing CCR5 were solubilized in buffer N containing protease inhibitors. Lysate was sonicated with six 1 second pulses and then incubated on a nutator for 2 hours at 4°C. Lysate was then bound to the 1D4 Dynabeads for 30 minutes at 4°C. After the incubation the bead-lysate suspension was then split into 3 eppendorf tubes, beads were pelleted with a magnet, and supernatant was removed. To each tube 50 nM of Atto655-2D7, Atto655-3A9 or Alexa647-MIP-1α was added. Samples were incubated on a nutator for 10 minutes at room temperature. Beads were then pelleted with a magnet, supernatant was removed, and samples were eluted from the beads with 5% sodium dodecyl sulfate (SDS) in 1X PBS. Eluted samples were transferred to a 384-well plate and the fluorescence was read on the envision plate reader (Perkin Elmer). A representative data set is shown in Figure 2-1.

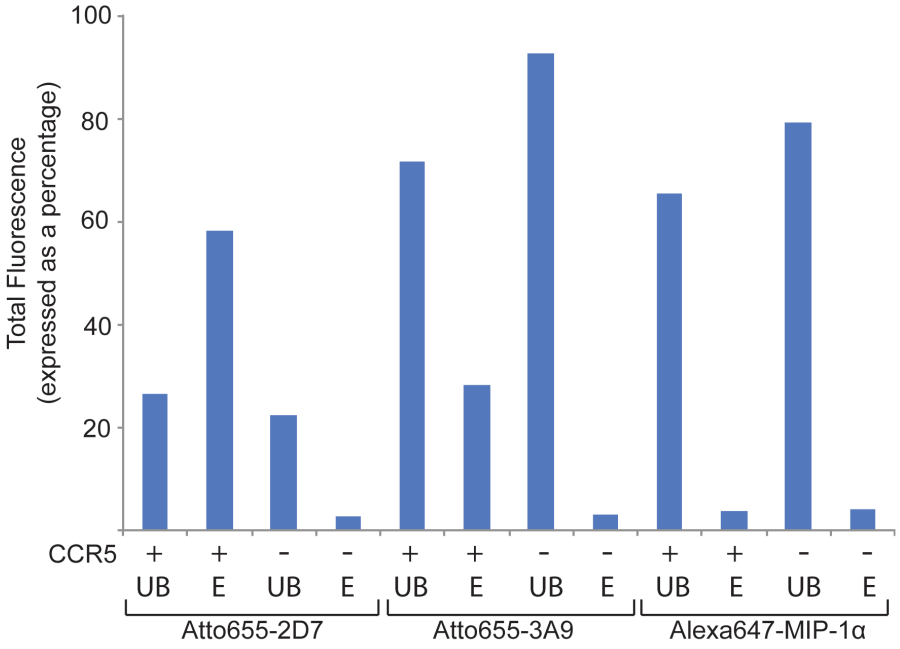

Figure 2-1. Fluorescent ligand binding to CCR5 on beads. This figure is a representative data set measuring binding of fluorescently labeled ligands to CCR5 in detergent. The three fluorescently tagged ligands used in this study were 2D7, a mAb that recognizes a conformational epitope on CCR5, 3A9, a mAb that recognizes a linear epitope at the N-terminus of CCR5, and MIP-1α, one of the native chemokine ligands for CCR5. On the bar graph UB stands for unbound samples and E is for the eluted samples. Non-specific binding was measured by incubating the beads with detergent-containing buffer without CCR5. This graph shows that specific binding of 2D7 and 3A9 can be measured to CCR5 in detergent using fluorescently labeled antibodies. No specific binding of MIP-1α was found to CCR5 containing samples, which agrees with other reports that binding of this ligand to the receptor is dependent on the presence of G protein [102].

2.4.2. Immunopurification of CCR5 by Conformationally Sensitive Antibody on Dynabeads.

Protein G magnetic Dynabeads (Invitrogen) were transferred to an eppendorf tube and washed with 1X PBS. Bead suspension was then split between three or four eppendorf tubes. Beads were separated with a magnet and 200 μL of buffer N or 1X PBS was added. To each tube 5 μg of the 2D7, 1D4, His4, or FLAG monoclonal antibodies were added and allowed to incubate for 20 minutes on the shaker (approximately 5 μg of antibody per approximately 0.2 mg of Dynabeads). Beads were separated with a magnet, supernatant was removed, and beads were washed with buffer N. In the case of using CCR5 in detergent, membrane preparations from CCR5 stably expressing cells were solubilized in buffer N with protease inhibitors for 3 hours at 4°C on a nutator. Lysate was spun down and supernatant was added to the prepared Dynabead samples. If CCR5 containing NABBs were being used, the NABBs were prepared as described below and then added to the prepared Dynabeads. Samples incubated with beads for 1 hour at room temperature. Beads were then separated with a magnet, supernatant was removed, and samples were eluted from beads by shaking for 1 hour at room temperature in 1X NuPAGE LDS sample buffer (Invitrogen) diluted in buffer N. Unbound and eluted samples were then run on an SDS-PAGE gel, transferred to a PVDF membrane, and immunoblotted with the 1D4 antibody to look for the presence of CCR5. A representative data set is shown in Figure 2-2.

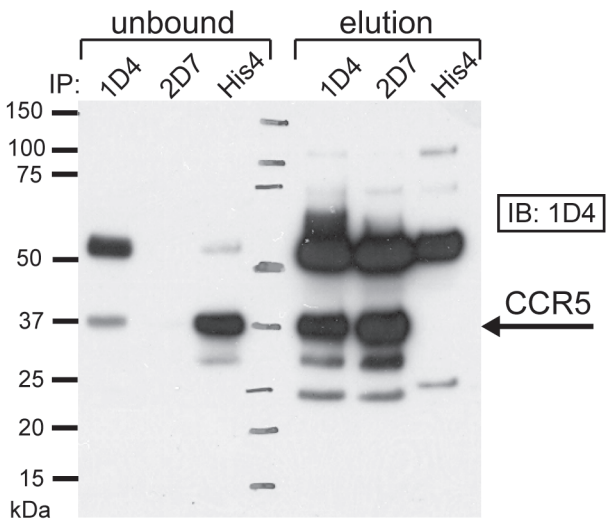

Figure 2-2. Immunopurification of CCR5 by 2D7 on magnetic Dynabeads. In this experiment CCR5 was solubilized in a detergent-containing buffer that had previously been reported to retain CCR5 in its native conformation. This was measured by binding to the conformationally sensitive antibody 2D7[99]. Here we also demonstrate that CCR5 in Buffer N can be immunopurified by 2D7. As a positive control CCR5 was also immunopurified with the 1D4 antibody, which recognizes a linear epitope at the C-terminus of CCR5. A His4 antibody was used to determine non-specific binding of the receptor to the beads. The Western Blot shown is detected with the 1D4 mAb. The bands detected at approximately 37 kDa correspond to monomeric CCR5 and the bands detected above 50 kDa are the antibody heavy chain. The results from this experiment showed that the same amount of CCR5 was immunopurified with 1D4 and 2D7 and no background binding was seen with the His4 antibody. This suggests that CCR5 is in its native conformation in Buffer N. In addition this assay is a useful method for identifying whether CCR5 is correctly folded and for purifying correctly folded receptor from a heterogeneous solution of CCR5 conformations.

2.5. Functional Assays in Membrane Preparations

2.5.1. Preparation of Membranes from HEK293T Cells.

HEK293T cell pellets were lysed with buffer HL. Lysates were forced through a 23-gauge needle, then 26-gauge needle on a 1 mL syringe 3 times. In TLS-55 centrifuge tubes (Beckman, reorder#: 347356), 1 mL of 35.5% (w/w) sucrose solution in buffer MP was added to each tube. The lysed pellets were slowly layered on top of the sucrose solution. Tubes were balanced by adding in extra buffer HL and then spun in the TLS-55 rotor (SN# 2168) on the ultracentrifuge at 22,000 rpm at 4°C for 20 minutes with acceleration and deceleration both set to 5. Membrane layer was removed from tubes with a 23-gauge needle on a 3 mL syringe. Membranes were added to two TLA 100.3 tubes (Beckman, reorder#: 326819) then 3.4 mL of buffer MP with PMSF was added to each tube and tubes were balanced with additional buffer MP with PMSF. Tubes were centrifuged in a TLA 100.3 rotor (SN# 3583) at 60,000 rpm at 4°C for 30 minutes. Supernatant was poured off and pellets were resuspended in buffer MP with PMSF (3.5 mL) using a 1 mL syringe with a 27-gauge needle. Tubes were then centrifuged again in a TLA 100.3 rotor at 60,000 rpm at 4°C for 30 minutes. Each pellet was then resuspended in buffer MP and protein amounts were quantified using the Biorad DC protein assay. Membranes were suspended at a protein concentration of approximately 1.83 mg/mL and suspensions were aliquoted and stored at -80°C until further use.

2.5.2. Quantifying CCR5 Expression in Membrane Preparations or Cells with fluorescein-maraviroc (FL-maraviroc).

For the membrane preparation experiments, an aliquot of CCR5-containing membranes and untransfected cell membranes was thawed. Membranes were combined with buffer N containing 100 nM FL-maraviroc in the presence or absence of 10 μM TAK-779. Samples were resuspended and put at 4°C on a nutator overnight. For the cell-based experiments, the cells were first solubilized in buffer N for 3 hours at 4°C and then lysate was spun down in an ultracentrifuge tube at 14,000 rpm for 20 minutes. The lysate was then incubated with 100 nM FL-maraviroc overnight at 4°C. After incubation with FL-maraviroc the samples were spun down and the supernatant was bound to sepharose beads conjugated to the 1D4 antibody at 4°C on a nutator overnight. After 24 hours the samples were transferred to Ultrafree-MC tubes and the beads were washed with buffer N. The samples were eluted from the beads in 1% SDS in 20 mM Tris-HCl pH 7.5 by shaking for 1 hour at room temperature. The tubes were then spun down and the elution was transferred to a 96-well black round bottom plate and read on the CytoFluor II fluorescence multi-well plate reader (ex: 485nm; em: 530nm). FL-maraviroc dilutions were made to create a standard curve and the amount of specifically bound FL-maraviroc was calculated. A representative data set is shown in Figure 2-3.

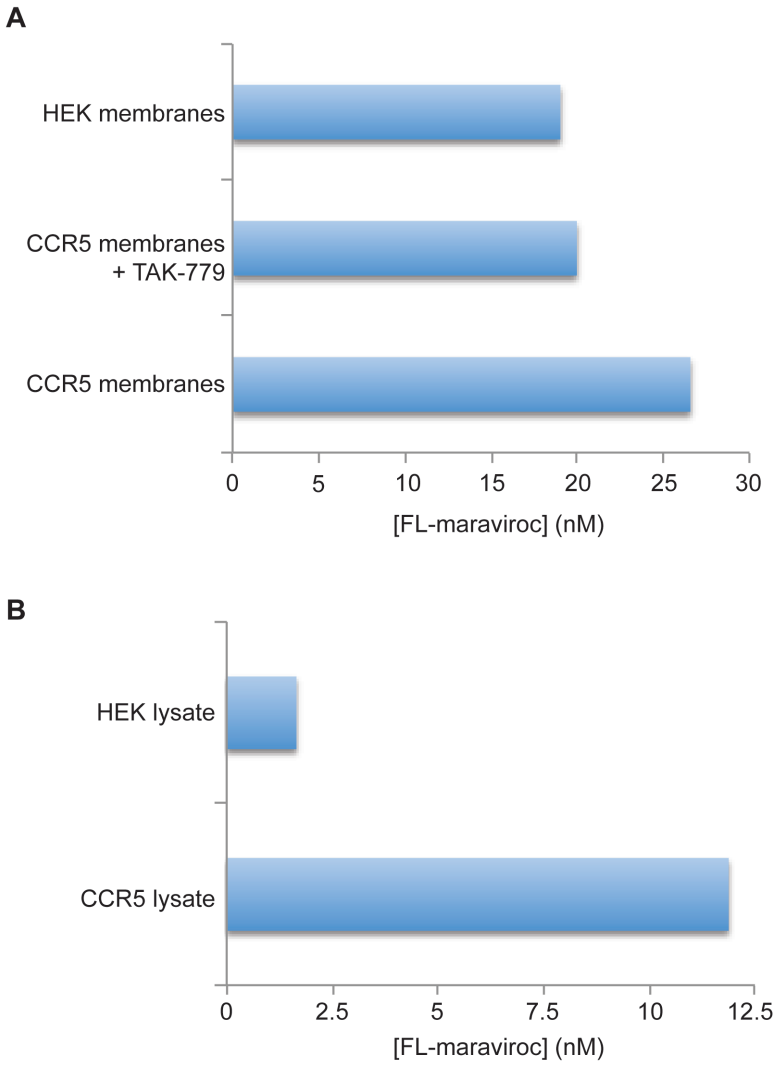

Figure 2-3. Quantifying CCR5 expression with a fluorescein-maraviroc analogue. We have optimized a method for quantifying CCR5 expression using a fluorescein-labeled maraviroc analogue (FL-maraviroc). Panel (A) shows that we can measure the amount of FL-maraviroc that is specifically bound to CCR5 in membrane preparations through competition with another CCR5 inhibitor TAK-779. The amount of non-specific binding detected in the competition experiment also agrees with the amount bound to membrane preparations that do not contain CCR5. Panel (B) displays the amount of FL-maraviroc that was specifically bound to CCR5-containing lysate, which also demonstrates that CCR5 in buffer N is still able to bind FL-maraviroc. These results determine that FL-maraviroc can be used to quantify the amount of CCR5 present in a sample.

2.5.3. [^{35}S]-GTPgS Binding to CCR5 and CXCR4 containing Membrane Preparations.

A 100 nM stock of [^{35}S]-GTPgS was made up in buffer R. For each condition to be tested an eppendorf tube was made up with a 50 μL solution containing 10 μg of membrane protein, the ligand of interest, and 2 nM [^{35}S]-GTPgS. Reactions incubated for 15 minutes in a 30°C water bath and then 49 μL of the reaction was transferred to 2.5 mL of cold buffer W on a nitrocellulose membrane. Solutions were then vacuumed filtered through the membrane and washed three more times with cold buffer W. Nitrocellulose membranes were then transferred to vials with Ecoscint A scintillation fluid (National Diagnostics) and counted on a LKB Wallac Beta Liquid Scintillation Counter. A representative data set is shown in Figure 2-4.

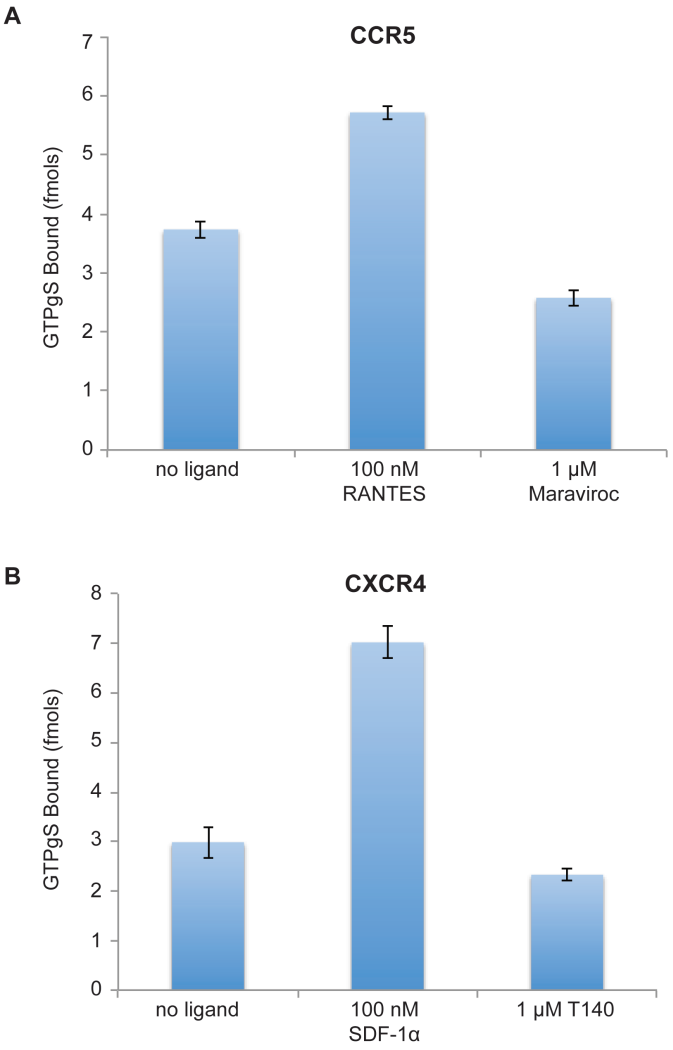

Figure 2-4. Ligand induced [^{35}S]-GTPγS binding to CCR5- and CXCR4-containing membrane preparations. We were able to measure chemokine receptor dependent G protein activity using a radioactive non-hydrolyzable GTP analogue. (A) Membrane preparations containing CCR5 when treated with RANTES, a CCR5 agonist, resulted in an increase in the amount of GTPγS bound to the membranes. Alternatively, when these membranes were treated with maraviroc, a CCR5 inverse agonist, there was a decrease in the amount of GTPγS bound to the membranes. (B) The same trend was also seen with CXCR4-containing membrane preparations when they were treated with SDF-1α, a CXCR4 agonist, and T140, a CXCR4 inverse agonist. This is a proof of concept experiment showing that this assay can be used to measure chemokine receptor function.

2.6 Cell-Based Functional Assays

2.6.1. High-throughput Calcium Flux Assays.

Twenty-four hours post-transfection, cells were plated onto a poly-D-lysine coated 384-well plate at 20,000 cells per well in 20 μL of DMEM with 10% FBS. The plate was spun down for 5 minutes at 700 rpm after plating and put back into a 37°C incubator with a 5% CO_2 atmosphere. The next day the cells were loaded with Calcium 4 dye (Molecular Devices) for 1 hour at 37°C. Calcium 4 dye solution was made up with 0.4% BSA and 20 μL was loaded per well. Ligand dilutions were made up in buffer X. Fluorescence measurements and ligand additions were performed using the FlexStation II (Molecular Devices). The change in fluorescence detected upon ligand addition was plotted versus a log function of the ligand concentration. The plot was then fit to a sigmoidal function using Origin Graphing Software and the EC_{50} values were calculated.

2.6.2. Cell Surface Enzyme-Linked Immunosorbent Assay (ELISA).

Transfected cells were split 24 hours post-transfection into black clear bottom 96-well plates pre-coated with poly-D-lysine. The next day the media was changed on the cells to DMEM without FBS and incubated for 1 hour at 37°C in the incubator. Cells were then washed once with 100 μL per well of 1X Dulbecco's PBS (DPBS) containing calcium and magnesium. Cells were fixed with either paraformaldehyde at room temperature for 15-20 minutes or MeOH for 5 minutes at 4°C. The fixed cells then incubate with primary antibody in 1X DPBS containing 0.5% BSA on ice for 1 hour. The primary antibodies were used at the following dilutions 1D4 (1:2000), 2D7 (1:500), and 12G5 (1:2000).

After incubation the cells were washed twice with 1X DPBS with 0.5% BSA. The secondary antibody anti-mouse conjugated to horseradish peroxidase was then added to the cells at a 1:2500 dilution in 1X DPBS with 0.5% BSA and incubated for 30 minutes at room temperature. The cells were washed three times with 1X DPBS with 0.5% BSA and then the amplex-red solution was added to the wells. The amplex-red solution was made up with 4.5 mL of 1X PBS, 0.5 mL of 20 mM H_2O_2, and 50 μL of 10 mM amplex red reagent (Molecular Probes). The cells incubated for 15 to 20 minutes at room temperature with the amplex red solution and then the plates were read on the CytoFluor II fluorescence mult-well plate reader (ex: 530nm, em: 590nm).

2.6.3. [^{125}I]-RANTES Binding to CCR5 Expressing Cells.

(This work was done in collaboration with Dr. Reem Berro at Weill Cornell Medical College in Dr. John Moore's Lab.) Two days post-transfection cells were scraped, washed once with 1X DPBS and then resuspended in 1X DPBS. Cells were then counted and transferred to a 96-well V-bottom plate so that each well contained 800,000 cells. The plate was then spun down at 1900 rpm and the media was aspirated. The cells were then resuspended in 50 μL of buffer D with or without a known concentration of vicroviroc. The cells incubated with vicroviroc at room temperature for 30 minutes and then [^{125}I]-RANTES was added for a final concentration of 400 pM or otherwise indicated. The cells incubated with [^{125}I]-RANTES for 1 hour at room temperature. The plate was then spun down at 1900rpm for 2 minutes and washed four times with 200 μL of 1X DPBS. After the last wash the cells were resuspended in 200 μL of 1X DPBS and transferred to scintillation vials and read on a Packard Gamma Counter Model 5530. A representative data set is shown in Figure 2-5 [103].

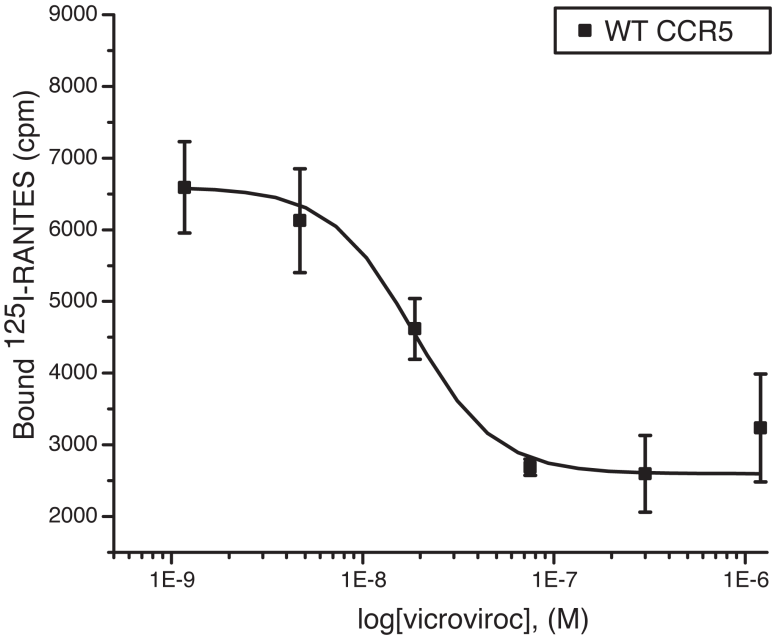

	IC_{50} (nM)
WT CCR5	18.2 ± 2.7

Figure 2-5. [^{125}I]-RANTES binding to CCR5 expressing cells. In this experiment we measured the IC_{50} of vicriviroc to CCR5 expressed in cells by quantifying the amount of [^{125}I]-RANTES that was displaced by a specific concentration of vicriviroc. Radiolabeled ligand binding is a common technique used in the GPCR field to measure ligand-binding affinity. Here we demonstrate that we can perform these experiments on live cells. This assay was used to measure the binding affinity of vicriviroc to CCR5 mutants in a collaborative project with the Moore Lab at Weill Cornell Medical College [103].

2.7. CCR5 NABBs

2.7.1. Expression and Purification of Zap1.

This protocol is described in detail elsewhere [100]. In brief, the zap1 construct (pE28-zap1) was expressed in BL21 (DE3) rosetta2 cells. The cells were harvested after reaching an OD_{600} ~1.2. Cells pellets were resuspended in homogenization buffer and then put through a French press. The cell extract was incubated with 1% Triton X-100, DNAse I, and 5 mM $MgSO_4$ for 30 min. and then spun down on a Beckman centrifuge for 45 minutes at 16,500 at 4°C. The supernatant was filtered with a 0.45 or 0.65 μm syringe filters and then put into a super loop to be separated on an AKTA explorer FPLC. The supernatant was loaded onto a Ni column, washed once with buffer T, washed with 10 column volumes of buffer C and 10 column volumns of buffer ND. Zap1 was eluted from the Ni column with an increasing gradient of Buffer E over 10 column volumes. The zap1 fractions were collected from the Ni column and concentrated to about 5 mL using an Amicon Ultra. The concentrated zap1 was then loaded into a superloop and injected onto a Superdex 200 26/60 pg column. The sample was eluted from the column with buffer G. Fractions of zap1 were collected and a SDS-PAGE gel was run to determine which peak contained monomeric full-length zap1.

2.7.2. Incorporating CCR5 into Nanoscale Apolipoprotein Bound Bilayers (NABBs).

This procedure was adapted from Banerjee et al. and Knepp et al. [100,104]. Forty-eight hours post-transfection of HEK293T cells with CCR5, the cells were harvested and

solubilized in buffer N. Lysate was then centrifuged and the supernatant was bound to sepharose beads conjugated to the 1D4 mAb overnight at 4°C. The next day the beads were washed three times with buffer N and then eluted from the beads in two 30-minute elutions with buffer M. The purified CCR5 was then combined with zap1 and POPC, the ratio of zap1 to lipids was 1:75, in a buffer containing 1.5% sodium cholate, 0.33% DM, 15 mM Tris-HCl (pH 7.0), 75 mM $(NH_4)_2SO_4$, and 7.5% glycerol. This mixture incubated for 30 minutes on ice and was then put on a 1 mL column packed with detergent-removing resin (Pierce). The NABBs were then eluted from the column with NABB buffer, fractions were collected, and NABB containing fractions were identified by measuring the absorbance at 280 nm.

2.8. Evaluation of Antibodies

2.8.1. Dot Blot Analysis of Anti-Rhodamine Antibodies.

A 3 $in.^2$ piece of PVDF membrane was washed in MeOH and then allowed to air dry. When the membrane was dry 5 μL of rhodamine-labeled peptide samples were pipette onto the membrane in a grid drawn with a pencil. Peptide dilutions were made in ddH_2O. The membrane was then allowed to air dry and then blotted with primary and secondary antibodies as described for Western Blot analysis. The primary anti-rhodamine antibodies were all used at a dilution of 1:2000. The three antibodies tested in this manner were a mouse monoclonal antibody from Acris (cat.#: AM08431PU-N), a rabbit polyclonal antibody from Molecular Probes (cat.# A-6397), and a mouse monoclonal antibody from Abcam (cat.# ab9093). A representative data set is shown in Figure 2-6.

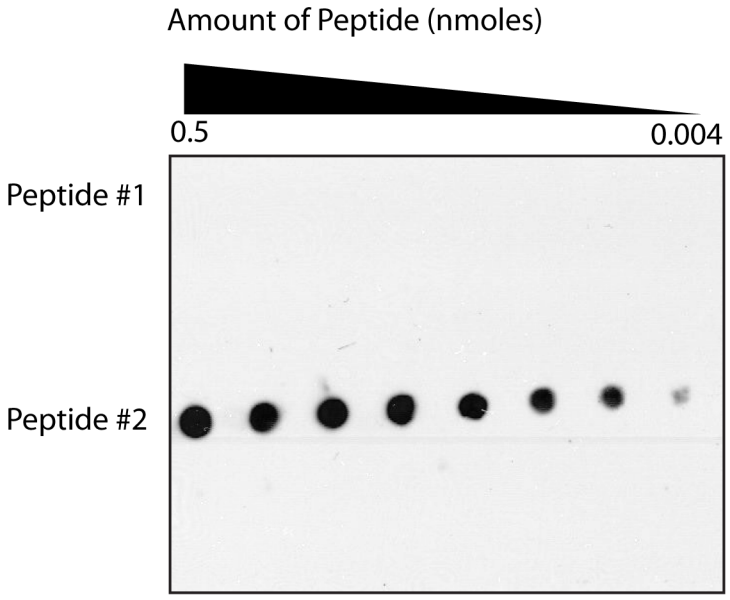

Figure 2-6. Dot blot analysis of anti-rhodamine antibodies. It is important to have a sensitive detection antibody for the photocrosslinking experiments. Here is one example of how we test an antibody's reactivity through a dot blot analysis. A dilution series of two tetramethylrhodamine (TAMRA) labeled peptides were bound to a PVDF membrane using a dot blot apparatus. Peptide #1 is a TAMRA-labeled analogue of the pepducin ATI-2341. Peptide #1 is conjugated directly to TAMRA via an amide bond whereas peptide #2, TAMRA-glucagon, contains an aminohexanoyl linker between the TAMRA and the peptide. The results show that the Abcam anti-rhodamine antibody (cat.# ab9093) is able to detect peptide #2, but not peptide #1 on a dot blot. This suggests that a linker between the fluorophore and peptide is required for detection of the fluorophore when it is directly conjugated to a peptide. This might indicate that the antibody is unable to react with the fluorophore on peptide #1 due to steric hindrance by the peptide.

2.8.2. Evaluation of Antibodies to Heterotrimeric G protein Subunits, Chemokines, and HIV Envelope Protein (gp120).

Antibodies reacting with heterotrimeric G protein subunits, chemokines, and gp120 were evaluated either by dot blot analysis or SDS-PAGE followed by Western Blot detection. For evaluation of G protein antibodies, HEK293T cell pellets or membrane preparations were solubilized in 1% Triton X-100 with protease inhibitors for 1 hour at 4°C. Lysates were then run on an SDS-PAGE gel, which was then transferred to a PVDF membrane for Western Blot analysis. The primary antibodies used in this study are described below. The secondary antibodies were all directly conjugated to HRP and used at a dilution of 1:10,000. All primary G protein antibodies were obtained from Santa Cruz Biotechnology Inc.. A goat polyclonal antibody to $G_{\alpha i\text{-}1/2/3}$ (cat.# sc-26716) was used at a 1:200 dilution. A rabbit polyclonal antibody to $G_{\alpha i\text{-}1}$ (cat.# sc-391) was used at a 1:50 dilution. A rabbit polyclonal antibody to G_{β} (cat.# sc-378) was used at a 1:3000 dilution. The Western Blot evaluating the G protein antibodies is shown in Figure 2-7B. The bands detected at approximately 37 kDa correlate to the heterotrimeric G protein subunits. The $G_{\alpha i\text{-}1/2/3}$ antibody did not detect any proteins suggesting either it does not recognize any proteins in these samples or the protein levels are too low to detect. The $G_{\alpha i\text{-}1}$ antibody detected protein only in the whole cell lysate sample and not in the membrane preparations. This might suggest that this G protein alpha subunit is not bound to the membrane or there is not enough protein present to detect with this antibody. The G_{β} antibody was able to detect the G protein beta subunit in all lanes, which indicates that the G protein beta subunit is present in all of these samples. We were unable to determine

what the bands at the higher molecular weights are. It is possible that they could be aggregated protein samples or complexes that did not dissociate in the denaturing gel.

Antibodies that react with gp120, an HIV envelope protein, were obtained from Dr. John Moore's Lab at Weill Cornell Medical College. The Moore Lab also provided purified JRFL gp120. The pure gp120 was diluted in 1X NuPAGE LDS sample buffer containing 10 mM DTT and ~1% DM. A known amount of gp120 was then run on a SDS-PAGE gel, transferred to a PVDF membrane, and immunoblotted with the following primary antibodies. The mouse PA-1 antibody (Progenics Pharmaceuticals Inc.) was used at a dilution of 1:1000, sheep D7324 antibody from Aalto Bioreagents was used at a dilution of 1:133, and mouse ARP3119 (National Institute for Biological Standards and Control (NIBSC), Centralised Facility for AIDS Reagents, Hertfordshire, UK) was used at a dilution of 1:2000. The appropriate secondary antibody conjugated to HRP was used for detection at a dilution of 1:10,000. An antibody to the chemokine SDF-1α was tested with the same procedure. This antibody was a rabbit polyclonal antibody from Cell Signaling (cat.# 3740) and was used at a dilution of 1:1000. A representative data set is shown in Figure 2-7.

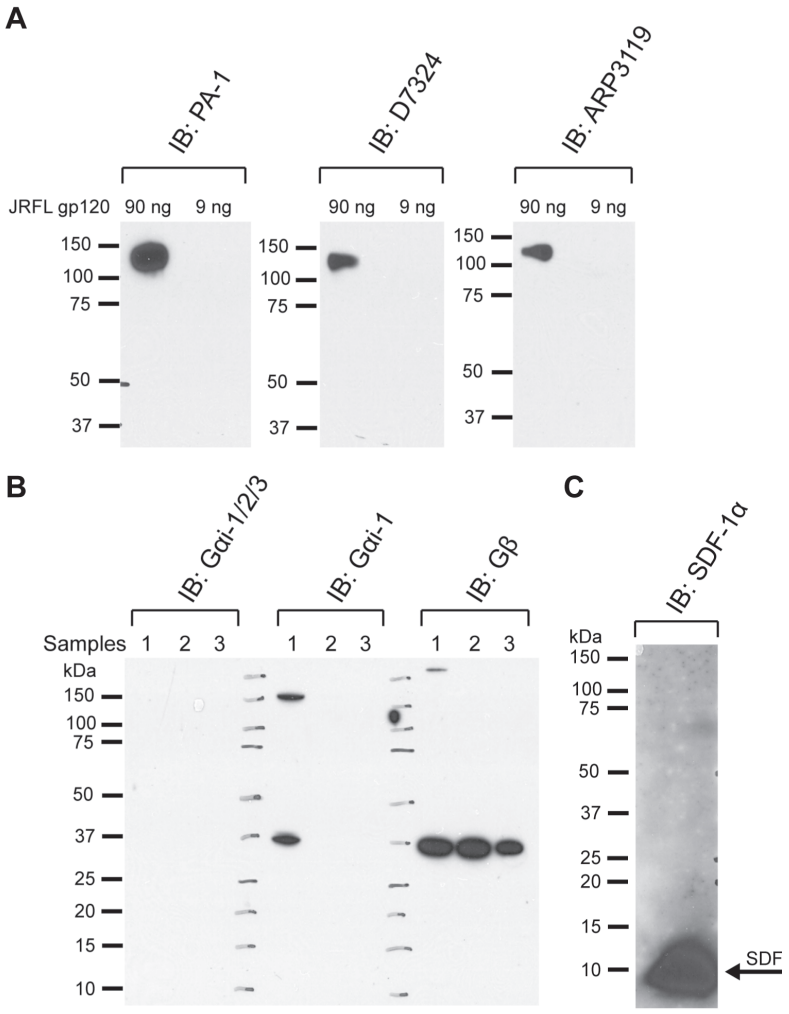

Figure 2-7. Evaluation of antibodies to G protein subunits, chemokines and gp120. Here we have evaluated the ability of several commercial antibodies to detect purified gp120 (A), G protein subunits from cell extract (B), and SDF-1α obtained from a commercial source (C) on a Western Blot after being run on a denaturing gel. In panel B, sample 1 is lysate from HEK 293T cells, sample 2 is solubilized membranes prepared from HEK 293T cells, and sample 3 is solubilized membranes prepared from HEK 293 T cells transfected with WT rhodopsin. The purpose of testing these antibodies was to determine whether they could be used to identify crosslinks between a receptor and one of these binding partners. These blots display the reactivity of each of the antibodies with the denatured proteins in these samples.

2.9. Photocrosslinking Studies

2.9.1. Photocrosslinking of Rhodamine-labeled Pepducin to CXCR4.

(This work was done in collaboration with Anchor Therapeutics in Cambridge, MA [31].) HEK293T cells heterologously expressing CXCR4 were incubated with 3 μM of a rhodamine-labeled analogue of ATI-2341 containing photo-leucine at one position (ATI-2766) in 1X Hank's Buffered Salt Solution (HBSS; pH 7.5) containing 20 mM HEPES and 0.2% BSA for 10 minutes at 37°C. Following incubation the pepducin-containing buffer was aspirated and 1.5 mL of HBSS buffer with 20 mM HEPES and 0.2% BSA was added. The plate was put under a Maxima ML-3500S UV-A light (Spectronics Corporation) for 5 to 15 minutes and then the cells were scraped and transferred to an eppendorf tube. The cells were spun down and washed three times with 1 mL of 1X DPBS containing protease inhibitors. The cells were solubilized in 1 mL of CHAPSO buffer for 1 hour at 4°C in the dark. The lysate was spun down and the supernatant was transferred to one tube for SDS-PAGE analysis and another tube for immunopurification with 1D4 sepharose beads. The lysate nutated with the 1D4 sepharose at 4°C in the dark overnight and the next day the unbound lysate was removed and beads were washed three times with CHAPSO buffer. Samples were then eluted from the beads with 1% SDS for 1 hour at 37°C on a shaker. Both the lysate and immunopurified samples were run on a SDS-PAGE. After the gels were run they were imaged on a typhoon 9400 fluorescence scanner and then transferred to a PVDF membrane for immunoblotting with the 1D4 antibody. (typhoon settings: emission 580 Bp 30 Cy3, TAMRA, Alexafluor546; PMT 560; laser Green 532)

> Note: To detect a photocrosslink between a GPCR and a rhodamine-labeled ligand using fluorescence requires significantly more crosslinked complexes than using the anti-fluorescein antibody to detect a fluorescein labeled ligand.

2.9.2. Photocrosslinking of Fluorescein-tagged (FL-tagged) Ligands to Heterologously Expressed GPCRs in live cells.

HEK293T cells expressing WT receptor or receptor UAA mutants were incubated with 50 or 100 nM of the FL-tagged ligand in 1X HBSS pH 7.5 containing 20 mM HEPES and 0.2% BSA for 10 minutes at 37°C in a 5% CO_2 atmosphere. For competition studies, the FL-labeled ligand was co-incubated with the competitor at the concentration indicated. Following incubation the cells were put under a Maxima ML-3500S UV-A light (Spectronics Corporation) in a 4°C cold room on ice for 15 minutes or otherwise indicated. After UV light exposure the cells were scraped in 1X PBS containing the protease inhibitors aprotinin and leupeptin and spun down in a tabletop centrifuge at 3000xg for 5 minutes. Cell pellets were then solubilized in detergent and analyzed by SDS-PAGE and Western Blot detection as described above.

2.9.3. Photocrosslinking of Cells Expressing CCR5 UAA mutants to [^{3}H]-maraviroc.

Two days post-transfection, HEK293T cells were suspended in 1X DPBS. Cells were then spun down and resuspended in 1X HBSS pH 7.5 containing 20 mM HEPES with 0.2% BSA and 100 nM [^{3}H]-maraviroc. Cell suspensions were then incubated for 2 hours at 37°C on a nutator. After the incubation, cell suspensions were transferred to a 24-well plate and exposed to a Maxima ML-3500S UV-A light (Spectronics Corporation) in a 4°C cold room on ice for 15 minutes. After UV light exposure, cells were transferred to eppendorf tubes, pelleted, and supernatant removed. Cell pellets were then stored at -20°C until further analysis. For analysis, cell pellets were solubilized in detergent and the receptors were immunopurified from the lysate using the 1D4-sepharose. The purified

samples were then separated on a SDS-PAGE gel and detected on a Western Blot with the 1D4 antibody as described above.

2.9.4. Quantification of [^{3}H]-maraviroc Bound and Crosslinked to CCR5 UAA mutants.

After the PVDF membrane was exposed to film, the membrane was then cut into segments to quantify the amount of tritium present. The membrane was cut between each lane to separate each sample; in addition, each sample was cut into three different molecular weight segments as specified. Each of these membrane segments were then transferred to individual vials with scintillation fluid and counted on a LKB Wallac 1209 Rackbeta Liquid Scintillation Counter (Perkin Elmer). To quantify the amount of [^{3}H]-maraviroc that was bound to each of the CCR5 UAA mutants, 15 μL of the original eluted sample from the 1D4 mAb sepharose beads was transferred directly into a vial with Ecoscint A scintillation fluid (National Diagnostics). All of the scintillation vials were mixed thoroughly before being counted on the LKB Wallac Beta Liquid Scintillation Counter. Each vial was counted over 10 minutes. After counting, the counts per minute (cpm) per cm^2 of PVDF membrane was then calculated for each membrane segment by dividing the cpm for a particular sample by the area of the membrane segment in cm^2. The amount of [^{3}H]-maraviroc each CCR5 UAA was able to bind was normalized to the other mutants by setting the WT sample as 100% and then calculating for the UAA mutants what percentage they were of WT.

Note: It is important to perform the 1D4 Western Blot using the same PVDF membrane that is cut for beta-scintillation counting because all the

wash steps involved in performing the Western Blot remove all the [^{3}H]-maraviroc that is non-specifically bound to the PVDF membrane. There is a lot of [^{3}H]-maraviroc carried over to the SDS-PAGE because any uncrosslinked maraviroc stays bound to CCR5 until the receptor becomes denatured on the SDS-PAGE gel. A tritium gradient is then detected on the PVDF membrane if no washing steps are performed before the scintillation counting. The washing steps used for the Western Blot works well to remove a small molecule that does not bind well to the PVDF membrane, but other steps may need to be taken if the tritiated ligand has higher binding affinity to the PVDF membrane.

2.10. Preparation and Digestion of CCR5 for MS Analysis

2.10.1. Cyanogen Bromide (CNBr) and Trypsin Digestion of CCR5 and CCR5 Crosslinked Complexes.

HEK293T cells were transfected with WT CCR5 as described above. Forty-eight hours post-transfection the cells were scraped in 1X DPBS with aprotinin and PMSF. The cell pellet was resuspended in 6 mL of 1X HBSS pH 7.5 with 20 mM HEPES in the presence or absence of 100 nM Fluorescein-maraviroc-BzF (FL-MVC-BzF) and 0.2% BSA. Cell suspension was put into the 37°C CO_2 incubator on a nutator for 2 hours. After incubation the cell suspension was transferred to a 24-well plate and put under a Maxima ML-3500S UV-A light for 15 minutes. The cell suspension was then transferred back to a falcon tube, spun down, and supernatant removed. The cell pellets were solubilized in 1% DM in 20 mM Tris pH 7.0 with protease inhibitors for 1 hour at 4°C and sonicated with six 1 second pulses. The lysate was then spun down at full speed on a tabletop centrifuge and the supernatant was bound to 1D4-sepharose beads overnight at 4°C. The next day the beads were washed threes times with 1% DM in 20 mM Tris pH 7 and samples were eluted with 1D5 peptide in 1% DM in two 1 hour elutions in an eppendorf spin filter on ice. The purified receptor was reduced by incubating in 17 mM DTT for 1 hour at 56°C and then alkylated with 0.1M iodoacetamide for 1 hour at room temperature in the dark. The protein was precipitated with 10% TCA at 4°C for 10 minutes then spun down at 14,000 rpm for 2 minutes. The precipitated pellet was washed by bath sonication in 95% ethanol three times. After the last wash all the ethanol was removed and resuspended in a CNBr solution. The CNBr solution contained 500 molar excess of CNBr per methionine

in the sample in approximately 80% TFA. The samples were then kept in the dark for 24 hours with the sonicator on for approximately 12 hours. After CNBr digestion, the samples were dried as much as possible in the hood with a stream of argon. Then a hole was punched in the top of the eppendorf tube, wrapped in parafilm and put into speedvac. Once dry, the pellet was then suspended in 100 µL of ddH_2O, sonicated, and dried on a speedvac. The samples were then digested further with trypsin by the Proteomics Facility at Rockefeller University or by following the protocol adapted from the Proteomics facility. In brief, the dried samples from the CNBr digestion were then dissolved in 20 µL of 6M urea in 200 mM ammonium bicarbonate. Samples were then reduced and alkylated again as described above. Then ammonium bicarbonate buffer was added to both samples to reduce the urea concentration to below 1 M. Trypsin Gold (Promega) was then added to the samples for a final concentration of 0.2 µg of trypsin per 1 µg of sample protein. The samples were then kept at 37°C for 36 hours on a shaker. Following digestion, formic acid was added to the samples so that the final concentration of formic acid was 10% to terminate the trypsin reaction. The digested sample then either went through a second purification as described below or was submitted to the Proteomics Facility at Rockefeller University for LC-MS/MS analysis.

2.10.2. Immunopurification with anti-Fluorescein (anti-FL) Antibody.

HEK293T cells heterologously expressing WT CCR5 were crosslinked to a fluorescein labeled analogue of maraviroc containing benzophenone (FL-MVC-bp) as described above. After crosslinking the cell pellets were solubilized in 1% DM in 20 mM Tris pH 7.5 containing protease inhibitors for 1 hour at 4°C on a nutator. The lysate was then

spun down and the supernatant was bound to protein A dynabeads (Invitrogen) that were pre-bound to a rabbit polyclonal anti-fluorescein antibody (abcam #ab19491) as described by the manufacturer. The samples incubated with the beads overnight at 4°C. The next day the unbound fraction was removed and the beads were washed 3 times with the 1% DM buffer. The samples were then eluted either in 50 mM glycine pH 2.5 for 1 hour at room temperature if being submitted for mass spectrometry analysis or eluted in 1X NuPAGE LDS sample buffer containing DTT for 1 hour at 37°C for Western Blot analysis.

2.10.3. Liquid Chromatography – Tandem Mass Spectrometry (LC-MS/MS) Analysis of Digested Protein Samples.

Protein samples were digested as described above and submitted to the Proteomics Resource Center at Rockefeller University for LC-MS/MS analysis. Prior to the analysis, the samples were cleaned up with C18 Stage (stop-and-go-extraction) Tips. The tips were first washed with 70% acetonitrile containing 2% formic acid and then conditioned with 2% formic acid in HPLC-grade water. The samples were loaded onto the tips, washed with 2% formic acid in water, and eluted using 70% acetonitrile and 2% formic acid mixture. Samples were subsequently dried using a speed vac and resuspended in 5% acetonitrile and 2% formic acid mixture. One third of each sample was loaded onto a C18 PepMap1000 micro-precolumn (300 μm I.D., 5 mm length, 5 μm beads Thermo Scientific) at a flow-rate of 5 μL/min., and then injected onto an analytical C18 column (75 μm I.D., 3 μm beads, Nikkyo Technos Co.) at a flow rate of 300 nL/min. The gradient was 125 minutes long in the range of 5-45% B (buffer A was 0.1% formic acid

in water, and buffer B was 0.1% formic acid in acetonitrile.) Eluted peptides were electrosprayed directly into the LTQ-Orbitrap XL mass spectrometer from Thermo Scientific, that operates in a 300-1800 m/z mass range. Tandem mass spectrometry was performed by collision-induced dissociation using nitrogen as a collision gas. The resulting spectra were then analyzed using Proteome Discoverer software (Thermo Scientific) to identify the peptides in the sample.

2.11. Imaging of Fluorescent-SDF-1α Binding to Cells.

(Performed with Dr. Joelle Goulding at the University of Nottingham in Dr. Stephen Hill's Lab) HEK GloSensor cells (Promega) stably expressing a CXCR4 construct containing a SNAP-tag at the N-terminus (Cisbio) were grown on 8-chamber coverslips. Prior to imaging, the cells were labeled with the SNAP-substrate 488 at 0.5 μM for 1 hour at room temperature and were then washed with 1X HBSS containing 2% BSA. After labeling the cells were incubated with 10 nM SDF-1α-RED (Cisbio) in 1X HBSS with 2% BSA for 10 minutes at 37°C in the presence or absence of a 30-minute pre-incubation with 100 nM SDF-1α or 10 μM AMD3100. The cells were then imaged on a Zeiss LSM 710 laser scanning confocal microscope with an argon 488 laser with a band pass 493-603 filter for the SNAP label and a Helium Neon 633 laser with a band pass 638-737 filter for the SDF-1α-RED. A representative data set is shown in Figure 2-8.

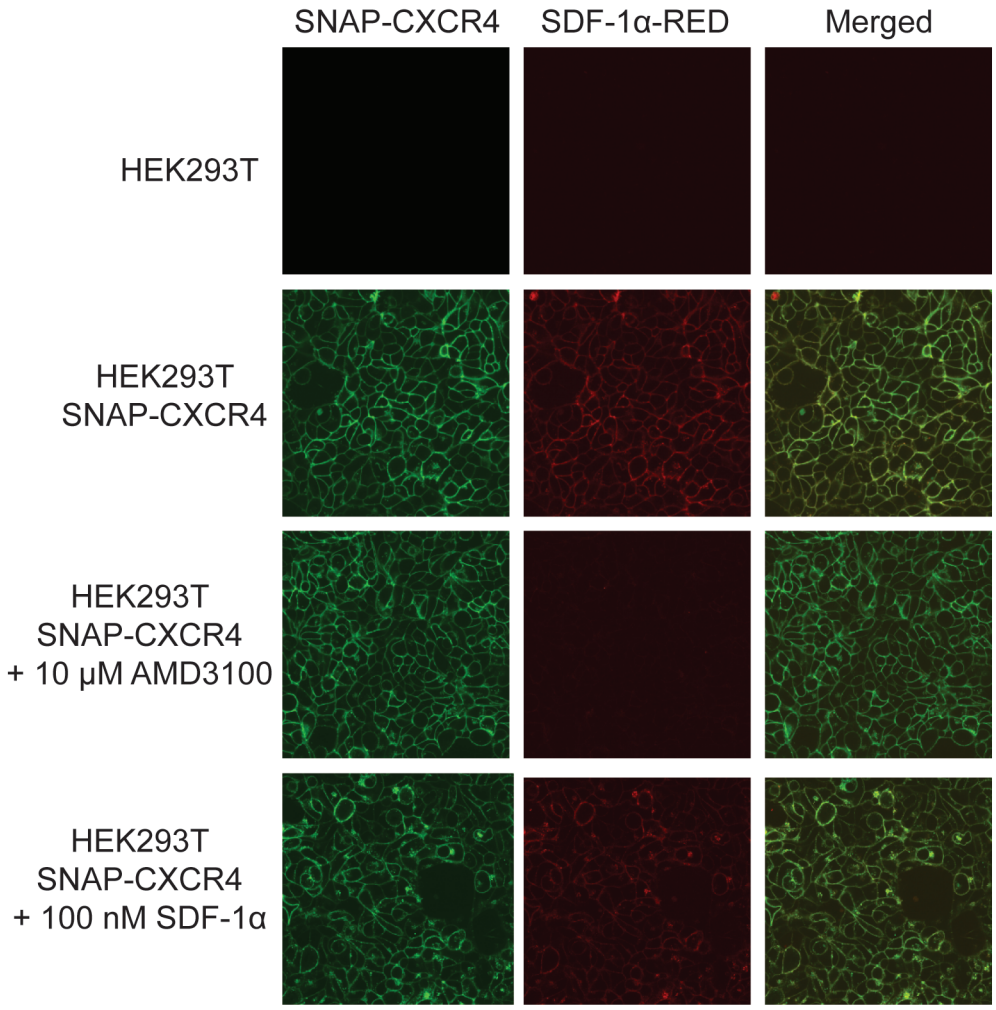

Figure 2-8. Imaging of fluorescent-SDF-1α binding to cells. This figure shows that we were able to detect specific binding of SDF-1α-RED to live cells expressing CXCR4. Minimal background was detected to untransfected cells. In addition, the binding of SDF-1α-RED to CXCR4 expressing cells was shown to be specific as it could be competed off with unlabeled SDF-1α and AMD3100, a CXCR4-specific inhibitor.

CHAPTER 3: Results

3.1. Investigating Ligand Binding Sites on CXCR4

3.1.1. Photocrosslinking Studies of the CXCR4-T140 complex.

We used the CXCR4-T140 complex to validate the targeted photocrosslinking technology for identifying GPCR-ligand binding interfaces. The site-directed crosslinking technology relies on a specific and sensitive detection method to identify both binding partners in the crosslinked complex. We accomplish this by attaching a unique antibody reactive tag on each complex component. CXCR4 contains a C-terminal C9 epitope tag for mAb 1D4, and T140 is labeled with fluorescein (Figure 3-1A). The fluorescein tag is used for specific detection by immunoblot analysis using an anti-fluorescein antibody. Fluorescein was directly conjugated to Lys 8 on T140, which does not interfere with binding to CXCR4 [105,106]. Thus, fluorescein-T140 (FL-T140) is a suitable ligand to validate the application of the site-directed crosslinking technology.

First, to optimize conditions for crosslinking and detection of the FL-T140/CXCR4 complex, we used a T140 analogue containing fluorescein and BzF at position 10 (FL-T140-BzF). This T140 derivative has been reported to crosslink to CXCR4 and serves as a positive control [107]. We also demonstrated that FL-T140-BzF

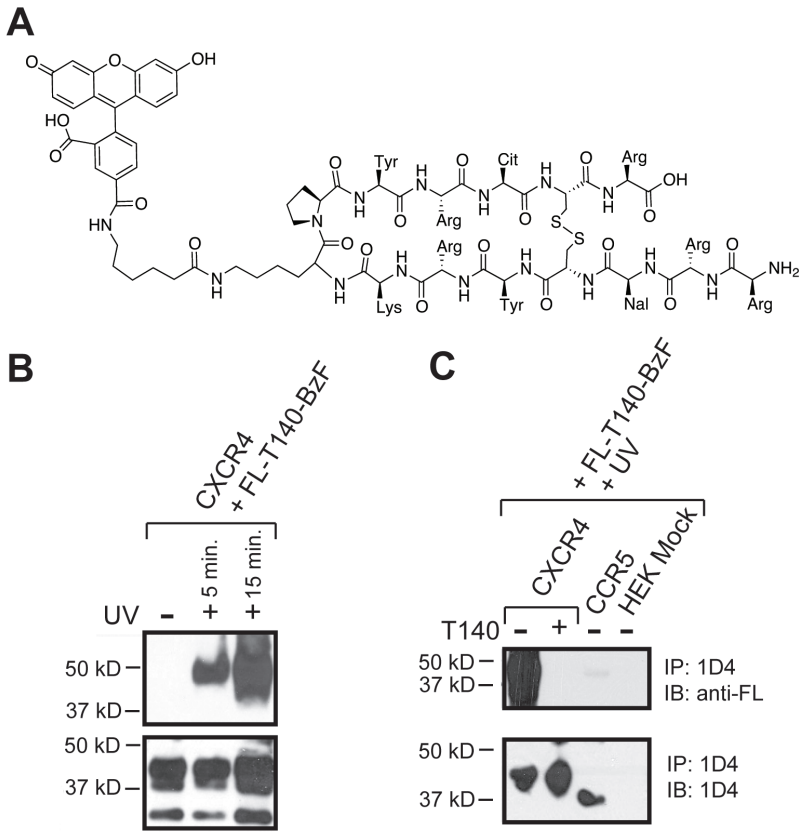

Figure 3-1. FL-T140-BzF crosslinks specifically to CXCR4. (A) Chemical structure of FL-T140. (B) Western blot analysis of FL-T140-BzF crosslinked to HEK293T cells transfected with CXCR4. Cells were solubilized in detergent and the lysate was immunopurified with Sepharose beads conjugated to the 1D4 antibody. Samples were eluted from the beads and loaded onto two SDS-PAGE gels that were transferred and blotted with either the monoclonal 1D4 antibody or anti-fluorescein polyclonal antibody. The UV-dependent anti-fluorescein band at the molecular mass of CXCR4 indicates FL-T140-BzF is crosslinked to CXCR4. (C)This crosslink is shown to be specific as no crosslink is detected when 100-fold excess of unlabeled T140 is present. In addition, no crosslink is detected to HEK293T cells transfected with CCR5 or in mock-transfected cells. Adapted with permission from (Grunbeck, A., et al. (2011) *Biochemistry 50*, 3411-3413). Copyright (2011) American Chemical Society.

crosslinks specifically to CXCR4 in cell culture. CXCR4-transfected HEK293T cells were incubated with FL-T140-BzF prior to UV light exposure. Following UV exposure, the cells were solubilized in detergent and CXCR4 was immunopurified from the lysate using sepharose beads conjugated to the 1D4 mAb. An immunoblot of the purified samples showed a UV-treatment-dependent band on the anti-fluorescein blot at the molecular mass of the receptor (Figure 3-1B & C). This indicates the existence of a covalent complex between FL-T140-BzF and CXCR4, which was not detected if a 100-fold excess of unlabeled T140 was present. Additionally, no crosslink was detected in untransfected cells or to CCR5, another chemokine receptor with high homology to CXCR4, demonstrating the specificity of T140 for CXCR4. The fluorescein moiety also proved to be a specific and sensitive detection tag on an immunoblot using an anti-fluorescein polyclonal antibody.

For the site-specific crosslinking experiments from the side of the receptor, residues in CXCR4 were chosen for replacement with a photocrosslinking UAA based on previously reported biochemical and molecular modeling data. The CXCR4 schematic shows the sites, which when mutated to an Ala, caused a decrease in T140 inhibition of HIV-1 entry (Figure 3-2A) [108]. Although in principle any amino acid residue can be targeted for amber codon suppression, we chose Phe residues in close proximity to these sites for replacement with BzF or azF in order to make mutations that would be the least likely to perturb the native structure of the receptor. These UAAs were incorporated one-by-one at each position using an engineered BzF or azF amino-acyl tRNA synthetase and suppressor tRNA pair that recognize an amber stop codon (UAG) on the receptor mRNA

[95]. Incorporation of BzF at the position of the amber stop codon in CXCR4 was confirmed by immunoblot to detect full-length receptor (Figure 3-2B).

Introducing UAAs into GPCRs alters the native sequence of the receptor, but the proper folding and function of the receptor can be retained, as has been reported for the incorporation of UAAs into other GPCRs, including rhodopsin and CCR5 [95,97,109]. For this experiment, we determined whether incorporation of BzF into CXCR4 affects binding to T140 by examining the crosslinking efficiency of FL-T140-BzF to each of the CXCR4 BzF-containing mutants. All of the mutants crosslinked to FL-T140-BzF, indicating that T140 is able to bind to the CXCR4 variants containing BzF (Figure 3-2C). Each of the CXCR4 BzF mutants were then tested for UV-induced crosslinking to FL-T140. HEK293T cells expressing the CXCR4 BzF mutants were incubated with FL-T140 and then exposed to UV light. The cells were then scraped and solubilized in detergent and the lysate was separated on a SDS-PAGE gel and subjected to immunoblot analysis.

The results from this series of experiments showed an anti-fluorescein positive band at the molecular mass of CXCR4 only when BzF was introduced at position 189 (Figure 3-3A) or when BzF was at position 10 in FL-T140-BzF (Figure 3-3B). The same crosslinking experiment was also performed in the presence of 100-fold excess of unlabeled T140. In this case no band was detected with the anti-fluorescein antibody, which demonstrates the specificity of the crosslink at position 189 for T140 (Figure 3-3C). The same results were also seen with azF at the same sites in CXCR4, although background crosslinking without UV treatment was significantly higher when using azF as compared to BzF (Figure 3-3D).

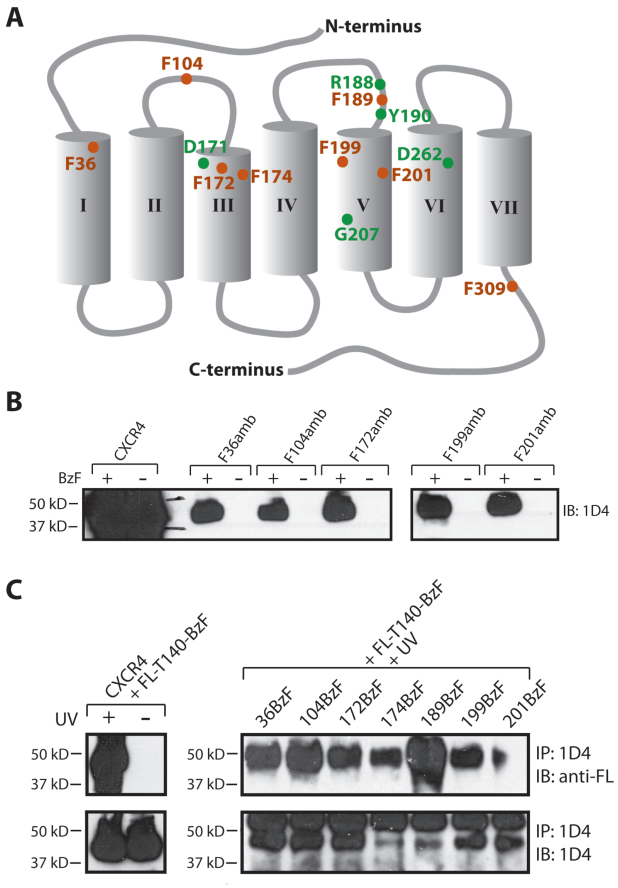

Figure 3-2. Expression analysis and ligand binding evaluation of CXCR4 UAA mutants. (A) CXCR4 schematic highlighting sites important for T140 binding (green) as determined by alanine scanning [108] and positions where a UAA was incorporated (orange). (B) CXCR4 amber mutants were co-expressed in HEK293T cells with a suppressor tRNA and BzF amino-acyl tRNA synthetase pair. Growth media either contained or did not contain 0.5 mM BzF. Full-length receptor was detected on a western blot using the 1D4 mAb, which recognizes an epitope on the C-terminus of the receptor. 1D4-positive bands are only present when BzF was added to the growth medium indicating that BzF is being incorporated at the position indicated. Similar results were obtained for F174amb and F189amb. (C) HEK293T cells expressing each of the CXCR4 BzF mutants were incubated with 100 nM FL-T140-BzF. After incubation cells were exposed to UV light for 15 minutes, solubilized in detergent, lysate separated by SDS-PAGE, and evaluated by western blot analysis. All CXCR4 BzF containing mutants were shown to crosslink to FL-T140-BzF. This indicates that incorporation of BzF at these positions does not affect binding to T140. Therefore in the crosslinking experiments shown in Figure 3-3, the data show that under the crosslinking conditions the ligand is bound to the CXCR4 UAA mutant. It follows therefore that the absence of a crosslink is most likely due to the reactive free radical being too far away from any potentially reactive group on the bound ligand. Adapted with permission from (Grunbeck, A., et al. (2011) *Biochemistry 50*, 3411-3413). Copyright (2011) American Chemical Society.

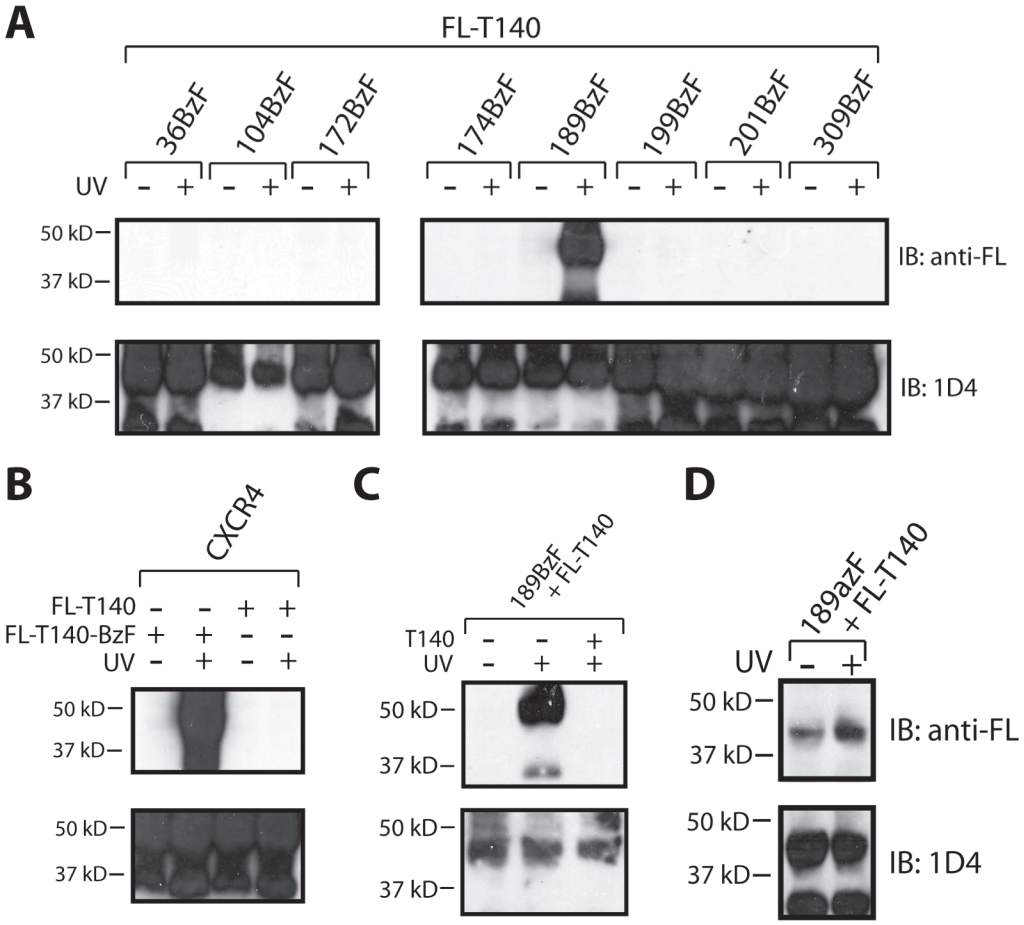

Figure 3-3. Photocrosslinking of CXCR4 UAA mutants to FL-T140. (A) Western blot analysis of lysate from HEK293T cells expressing CXCR4 BzF mutants that were exposed to UV light in presence of FL-T140. CXCR4 189BzF was the only CXCR4 BzF mutant that crosslinked to FL-T140. (B) As a positive control FL-T140-BzF was crosslinked to WT CXCR4. Background crosslinking was not detected between WT CXCR4 and FL-T140. (C) Crosslinking of CXCR4 189BzF to FL-T140 was performed in the absence and presence of a 100-fold excess of unlabeled T140. The band on the anti-fluorescein blot disappeared in the presence of excess T140. (D) Crosslinking results for CXCR4 189azF to FL-T140. Crosslink was specific for position 189, but background crosslinking, most likely due to exposure to ambient room light, was detected. Background was not detected when BzF was used as the photocrosslinker. Adapted with permission from (Grunbeck, A., et al. (2011) *Biochemistry 50*, 3411-3413). Copyright (2011) American Chemical Society.

3.1.2. Investigating the binding interaction between a pepducin and CXCR4

We investigated the binding site of the CXCR4-specific pepducin, ATI-2341, by performing a competition study to determine if this ligand has an overlapping binding site with T140 on CXCR4. HEK293T cells heterologously expressing CXCR4 were co-incubated with FL-T140-BzF and a 100-fold excess of another ligand, which included AMD3100, a CXCR4-specific small molecule inhibitor, ATI-2341, and maraviroc, a CCR5-specific small molecule inhibitor. After a 10 minute incubation at 37°C the cells were then exposed to UV light for 15 minutes. The cell lysates were then run on a SDS-PAGE gel and detected by Western Blot analysis. The blot detected with anti-fluorescein shows a disappearance of the fluorescein band at the molecular weight of CXCR4 when the cells weren't exposed to UV light or were co-incubated with unlabeled T140. A slight decrease is seen in the band on the anti-fluorescein blot when AMD3100 is present, but no change is observed with the presence of ATI-2341 or maraviroc (Figure 3-4) [31]. This suggests that ATI-2341 is unable to compete with T140 for binding to CXCR4.

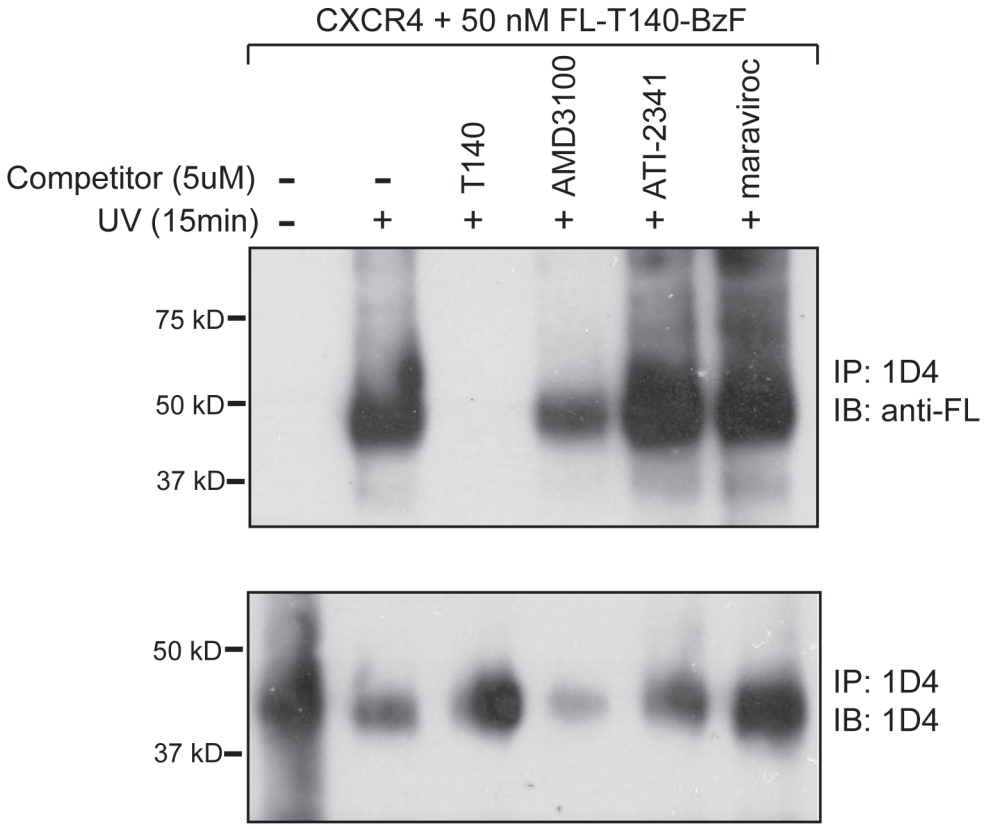

Figure 3-4. Competition of CXCR4 ligands with T140 binding. T140 binding to HEK293T cells expressing WT CXCR4 is detected using a T140 analogue labeled with fluorescein (FL) and containing *p*-benzoyl-L-phenylalanine (BzF), a photoactivatable crosslinker. A UV-dependent crosslink between FL-T140-BzF and CXCR4 is detected on a Western Blot using a polyclonal anti-fluorescein antibody. This band disappears when the experiment is performed in the presence of 100-fold excess of unlabeled T140, which indicates that the crosslink is specific for T140. There is a slight decrease in the amount of FL-T140-BzF crosslinked to CXCR4 when AMD3100, a CXCR4-specific small molecule inhibitor is present, although as can be seen on the Western Blot detected with the 1D4 antibody this sample had a slightly lower amount of CXCR4 present. This difference in receptor expression, which we believe is due to the protein amounts in the samples not being normalized, might be the reason for the detection of a decrease in FL-T140-BzF crosslinking. The band on the anti-FL Western Blot does not change if the experiment is performed in the presence of 100-fold excess of ATI-2341, or maraviroc, a CCR5-specific inhibitor. These results show that none of these ligands compete with T140 for binding to CXCR4 and therefore do not have overlapping binding sites. Adapted from (Janz, J., Ren, Y., Looby, R., Kazmi, M., Sachdev, P., Grunbeck, A., et al. (2011) *JACS* 133, 15878-15881.)

Additionally, since ATI-2341 mimics the i1 loop of CXCR4 we were interested in determining the relevance of this peptide sequence to the function of CXCR4. We mutated the residues in CXCR4, Met 63 through Leu 78, that corresponded to the sequence of ATI-2341 to the homologous sequence in CCR5. We reference the CXCR4/CCR5 chimeric receptor as CXCR4_R5i1. CCR5 has high homology to CXCR4, but ATI-2341 does not bind or activate this receptor. Therefore we can use CXCR4_R5i1 to see if the native i1 loop in CXCR4 is necessary for pepducin activity. This could indicate whether the pepducin is mimicking the active state of the receptor or if it is acting as an allosteric modulator to stimulate an active conformation of the receptor. In the first step of this project, we created the CXCR4_R5i1 construct and tested for cell surface expression of the receptor using a cell-based ELISA. HEK293T cells were transfected with the construct and plated into a 96-well plate. A conformationally sensitive antibody that recognizes an epitope on the extracellular surface of the receptor was used to detect correctly folded receptor at the plasma membrane under paraformaldehyde (PFA) treatment of the cells. The conformationally sensitive antibody for CXCR4 is 12G5 and 2D7 is specific for CCR5. Total receptor expression was determined by fixing the cells with methanol, which allows the antibody to permeate the membrane. The 1D4 antibody was used to measure total receptor expression by recognizing a linear epitope at the C-terminus of the receptors. Non-specific binding of the secondary antibody was determined by measuring binding of the secondary antibody to fixed cells without primary antibody present. The cell surface ELISA results show that relatively the same amount of WT CXCR4 and CXCR4_R5i1 was detected with the 12G5 antibody. All three receptors had relatively the same signal with the 1D4 antibody.

Also, the levels of primary antibody binding to transfected cells was significantly above what was detected for untransfected cells, which suggests that antibody binding is specific (Figure 3-5). These findings suggest that replacement of the i1 loop in CXCR4 does not affect expression of the receptor or translocation of the receptor to the plasma membrane. Further characterization of the CXCR4_R5i1 will be carried out by the Hill Lab at the University of Nottingham as discussed later in this manuscript.

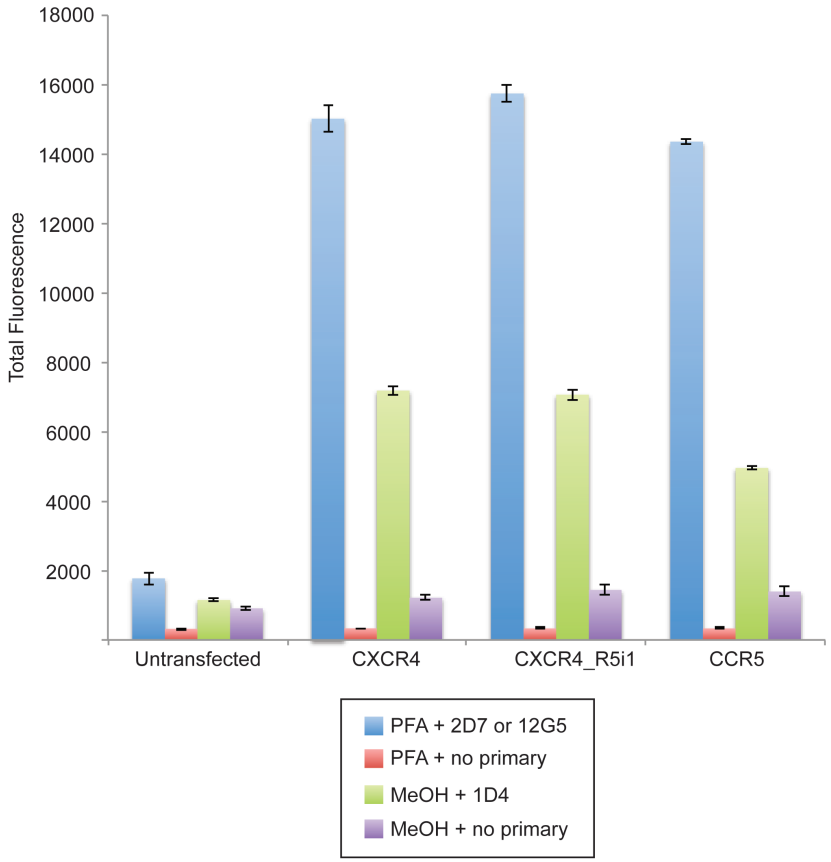

Figure 3-5. Cell surface expression of CXCR4-R5i1. A cell-based ELISA was used to measure cell surface expression of the CXCR4-CCR5 chimera CXCR4-R5i1. Untransfected HEK293T cells and cells transfected with WT CXCR4, CXCR4_R5i1, or WT CCR5 were plated into a 96-well plate. Cells were fixed with PFA for treatment with either 2D7 or 12G5, which recognize a conformational epitope on the extracellular surface of the receptor. MeOH fixation was used with the 1D4 antibody, which recognizes an epitope on the cytoplasmic side of the receptor. Non-specific binding of the secondary antibody was measured in the absence of primary antibody. The data shows similar levels of specific 1D4 and 12G5 binding for both WT CXCR4 and CXCR4_R5i1. CCR5 also showed a comparable 1D4 signal. Primary antibody binding to transfected cells was also significantly above that seen for untransfected cells indicating that antibody binding is specific. The lack of signal when no primary antibody is present also indicates that the signal is specific.

3.2. Photocrosslinking Study of CCR5-Maraviroc Complex.

We applied the targeted photocrosslinking technique to investigate the binding site of the small molecule HIV-1 inhibitor, maraviroc, on its target receptor CCR5 (Figure 3-6a). For this study we used a tritiated version of maraviroc in order to retain the native structure of the small molecule. We chose positions in CCR5 to replace with BzF or azF, based on earlier models of the maraviroc-binding site, with the expectation that a loss-of-function phenotype would not be observed. These earlier studies proposed models of the maraviroc binding-site in CCR5 based on scanning mutagenesis, molecular dynamics simulations, or structure-activity relationship studies[110-112]. Some of this work was based on studies of other structurally related CCR5 pharmacophores such as TAK-779[113,114]. From this earlier data, we chose 8 positions in CCR5 for additional study (Figure 3-6b). Our aim was to create a set of CCR5 UAA mutant receptors that would bind maraviroc normally and in addition contain reactive side chains that might crosslink upon UV excitation.

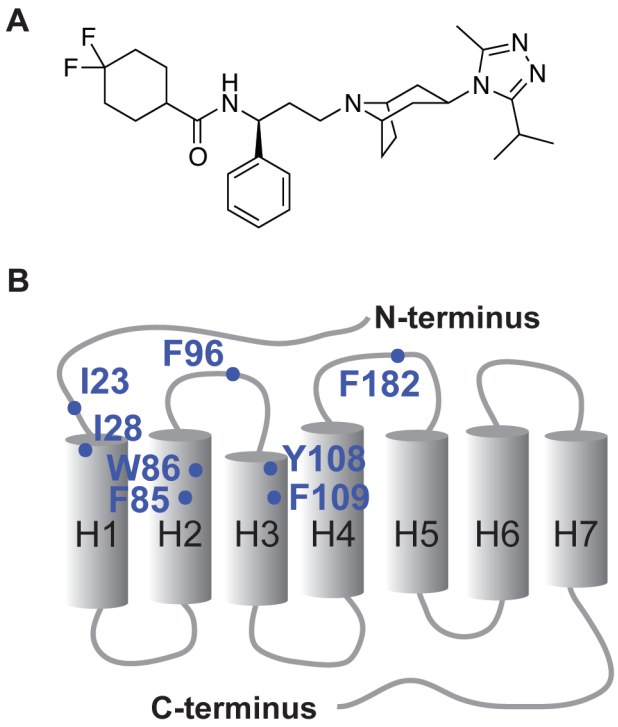

Figure 3-6. Targeted photocrosslinking was employed to study the binding site of maraviroc on CCR5. (A) Chemical structure of the CCR5-specific HIV-1 entry inhibitor maraviroc. (B) A schematic of the CCR5 structure showing in blue the positions in the receptor where BzF and azF were introduced. Adapted with permission from (Grunbeck, A., et al. (2012) *ACS Chem. Biol. 7*, 967-972). Copyright (2012) American Chemical Society.

3.2.1. Functional Characterization of CCR5 UAA mutants

3.2.1.a. [^{3}H]-maraviroc binding

To evaluate whether the CCR5 UAA mutants retain binding to maraviroc we performed ligand-binding experiments with [^{3}H]-maraviroc. These experiments were performed in parallel with the photocrosslinking studies. After cells expressing the CCR5 UAA mutants were incubated with [^{3}H]-maraviroc, exposed to UV light, lysed in detergent, and receptors were immunopurified, a portion of the eluted samples were put into vials with scintillation fluid and counted on a beta-scintillation counter. The amount of tritium detected in each of the samples was then plotted on a bar graph (Figure 3-7). All of the CCR5 UAA mutants show relatively the same amount of [^{3}H]-maraviroc binding when both BzF and azF is incorporated at the position indicated, except for residue Trp 86. The CCR5 W86BzF mutant shows significantly decreased levels of binding to maraviroc as compared to CCR5 W86azF. Most of the CCR5 UAA mutants retain about 50% of binding to maraviroc as compared to WT. It is important to note that these differences could be a result of a difference in receptor expression level in addition to a change in ligand binding affinity. The relative expression levels of the CCR5 BzF and azF mutants are depicted in the Western Blot shown in Figure 3-9. The Western Blot shows total receptor expression in the cell lysate as detected with the 1D4 antibody. As can be seen in this figure the expression levels vary significantly between different mutants, such as between CCR5 Y108BzF and CCR5 F109BzF. The [^{3}H]-maraviroc

binding data appears to correlate with the relative expression level differences seen on the Western Blot, although the Western Blot does not give any information about the amount of correctly folded or functional receptor that is expressed in the cell. We expect that the population of receptors expressed in the cell is heterogeneous and it is unknown what percentage of these overexpressed proteins is actually folded correctly. This is another factor that could play into the differences in the amount of [^{3}H]-maraviroc that is able to bind each CCR5 UAA mutant.

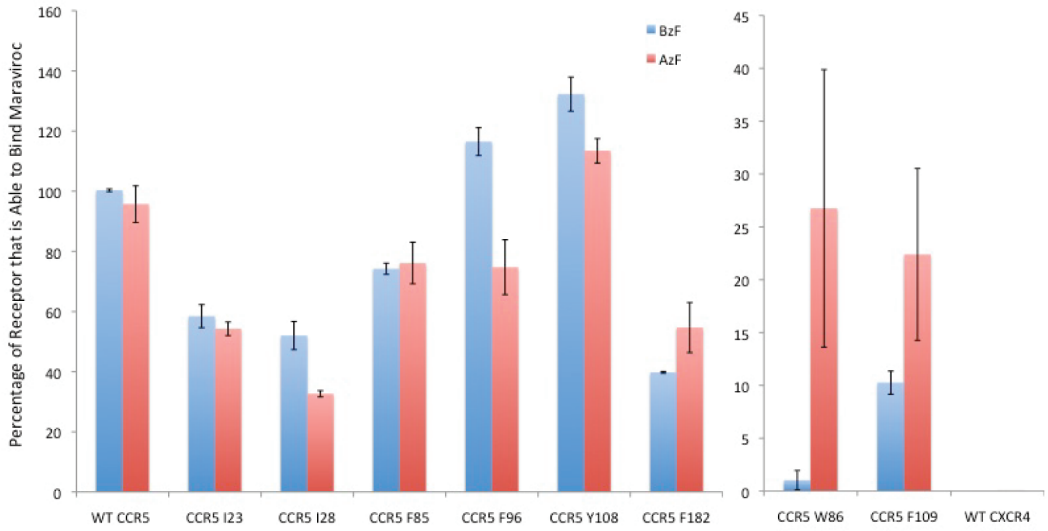

Figure 3-7. [^{3}H]-maraviroc binding. CCR5 UAA mutants retain binding to maraviroc. Each of the CCR5 UAA mutants was measured for their ability to bind maraviroc under the conditions of the crosslinking experiments. In brief, after the HEK293T cells expressing the CCR5 UAA mutants were incubated with [^{3}H]-maraviroc, exposed to UV light and then solubilized in detergent, the receptors were then immunopurified from the lysate using sepharose beads conjugated to the 1D4 mAb. The beads were then washed, samples were eluted using SDS, and the amount of tritium in the elution was quantified. The [^{3}H]-maraviroc detected in the elution was determined to be a result of being specifically bound to the purified receptor. This was supported by no tritium was detected in the sample with the homologous receptor, CXCR4, which is unable to bind maraviroc. Therefore the amount of tritium in the eluted samples was quantified for each CCR5 UAA mutant to determine the amount of [^{3}H]-maraviroc that was specifically bound. The values were then normalized to each other by setting the amount of tritium that was bound to WT CCR5 as an equivalent to 100% binding. The error bars are a result of averaging the values obtained from the sample that was exposed to UV light with the sample that was not. The differences in binding between the mutants are a result of varied expression levels of each of the mutants and differences in binding affinity for maraviroc. This graph shows that all of the mutants retain significant binding to maraviroc except for the CCR5 W86BzF mutant. Adapted with permission from (Grunbeck, A., et al. (2012) *ACS Chem. Biol. 7*, 967-972). Copyright (2012) American Chemical Society.

3.2.1.b. Calcium Flux assay

Another method to evaluate whether CCR5 UAA mutants retain their native structure and function is through live cell-based calcium flux assays. This is a high-throughput assay where cells are loaded with a calcium-dependent fluorescent dye. The change in cytoplasmic calcium levels is measured in response to treatment of cells with the chemokine RANTES. A RANTES dose-response curve is then plotted versus the change in fluorescence that was recorded upon addition of the ligand. We can then use these plots to calculate the RANTES EC_{50}. This was carried out for a few CCR5 BzF mutants (Table 3-1). These mutants were found to have RANTES EC_{50} values that are comparable to WT CCR5, which suggests that replacing F85, Y108, or F109 in CCR5 with BzF does not significantly alter the receptor's function or RANTES binding capabilities.

Table 3-1. The effective RANTES concentration at 50% stimulation of intracellular calcium flux.

	RANTES EC_{50}
CCR5	9.8 ± 6.3
CCR5 F85BzF	14 ± 3.1
CCR5 Y108BzF	6.5 ± 1.9
CCR5 F109BzF	6.9 ± 3.7

3.2.2. Photocrosslinking CCR5 UAA Mutants to [^{3}H]-maraviroc.

We expressed each of the selected CCR5 amber mutants in HEK293T cells under conditions designed to incorporate either BzF or azF at the position of interest. Cells expressing the CCR5 UAA mutants were incubated with [^{3}H]-maraviroc and then exposed to UV light. Cells were lysed in detergent buffer solution and receptors were immunopurified using 1D4 mAb. The immunopurified material was then run on an SDS-PAGE gel to separate out any tritiated ligand that was not covalently bound to the receptor. After transferring proteins to a PVDF membrane and measuring receptor expression by immunoblot analysis, the PVDF membrane was then cut into strips to partition each sample. Each sample strip was cut further into segments and the amount of radioactivity in each segment was measured (Figure 3-8).

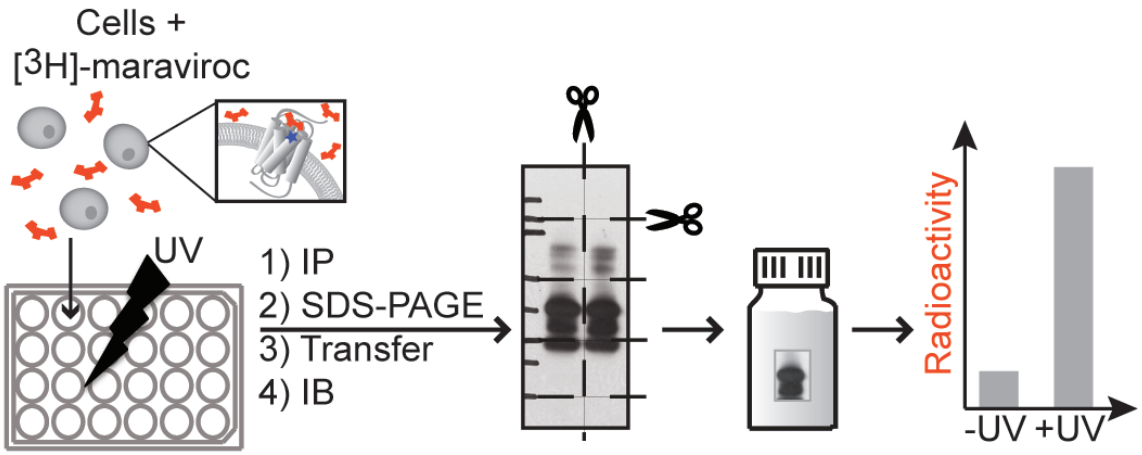

Figure 3-8. Experimental scheme for the targeted photocrosslinking technology using a radiolabeled ligand. The first step involves incubating HEK293T cells expressing the CCR5 UAA mutants with [^{3}H]-maraviroc. After incubation the cells were exposed to 365-nm UV light in a 24-well plate format. The cells were then lysed in detergent buffer solution and receptors were immunopurified, run on an SDS-PAGE gel, transferred to a PVDF membrane, and immunoblotted to determine receptor expression. The sample lanes were then cut from the PVDF membrane and each sample lane was cut into three different molecular weight segments. These membrane segments were then put into scintillation vials with scintillation fluid and then counted on a beta-scintillation counter to quantify the amount of radioactivity in each segment. Adapted with permission from (Grunbeck, A., et al. (2012) *ACS Chem. Biol.* *7*, 967-972). Copyright (2012) American Chemical Society.

These experiments showed that 3 of the 8 positions in CCR5 engineered to contain either azF or BzF were able to form a covalent bond with [^{3}H]-maraviroc upon UV illumination (Figure 3-9). Among the positions tested, different patterns of reactivity were noted for CCR5 containing azF versus BzF. Significant tritium was detected in the CCR5-maraviroc complex when either Ile 28 or Trp 86 was replaced by azF. However, when BzF was incorporated at position Ile 28, only a slight increase above background was detected. A significant increase in tritium levels was detected, however, when BzF was incorporated at position Phe 109, a site that did not crosslink when azF was present.

For these 4 mutants (CCR5 I28azF; CCR5 W86azF; CCR5 I28BzF; CCR5 F109BzF) the elevated levels of tritium were detected only in the 25-50 kDa gel fraction, which includes CCR5 with an apparent molecular mass of approximately 37 kDa. Since the molecular mass of maraviroc is under 500 Da, tritium only appears in the 25-50 kDa fraction if the [^{3}H]-maraviroc is covalently bound to CCR5. These crosslinking results were also found to be UV-treatment-specific (Figure 3-10).

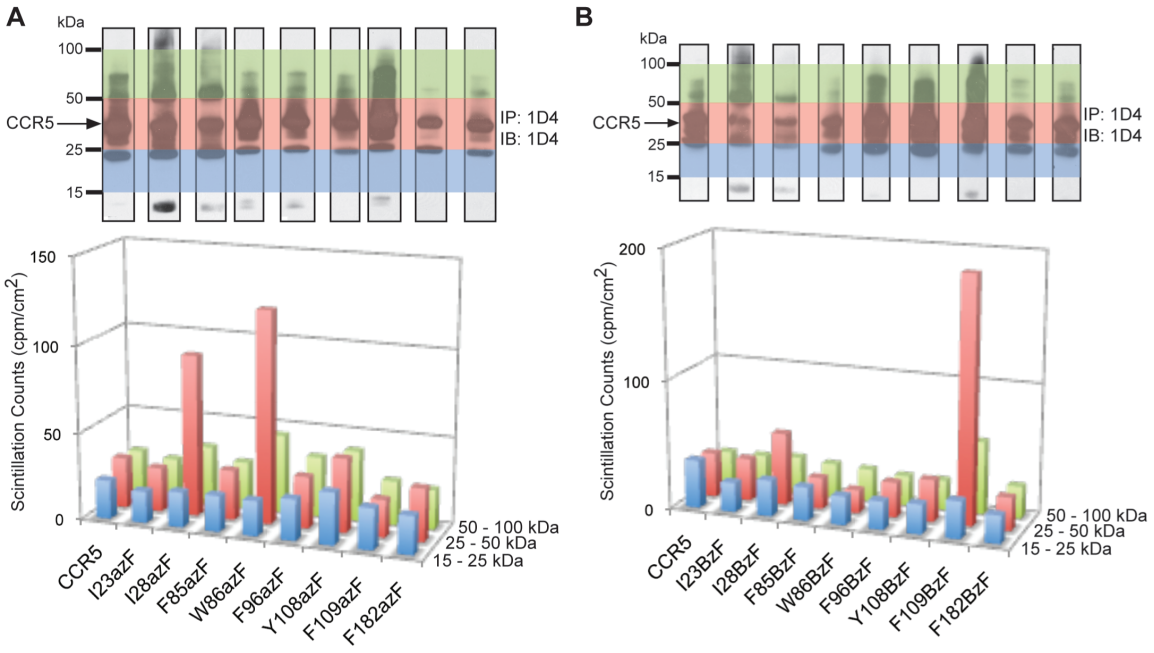

Figure 3-9. Photocrosslinking results with CCR5 azF and BzF replacement mutants. (A) CCR5 azF mutants were tested for crosslinking to [^{3}H]-maraviroc. Receptor expression is shown by immunoblot analysis with the 1D4 antibody. Note that the exposure for each sample is not normalized across all lanes. Each lane corresponds to the mutant shown in the bar graph directly below. The colors highlighted on the Western Blot designate where the membrane was cut for scintillation counting and correlate with the colors in the bar graph. The bar graph reports the amount of tritium detected in the PVDF segments indicated. All of these samples represent the CCR5 azF mutants that were exposed to UV light in the presence of [^{3}H]-maraviroc. The membrane segment of interest is the 25-50 kDa segment (red), which contains CCR5. The CCR5 band is indicated with the arrow at 37 kDa. The other strong band at 25 kDa is the light chain from the 1D4 mAb, which was used for immunopurification. Positions 28 and 86 were the only two sites found to have significantly higher tritium levels in the 25-50 kDa segment. (B) The same positions in CCR5 were also tested for crosslinking using BzF. This data set is displayed as in panel a. Positions 28 and 109 were found in this crosslinking scan to have significantly higher tritium levels in the 25-50 kDa segment. Adapted with permission from (Grunbeck, A., et al. (2012) *ACS Chem. Biol. 7*, 967-972). Copyright (2012) American Chemical Society.

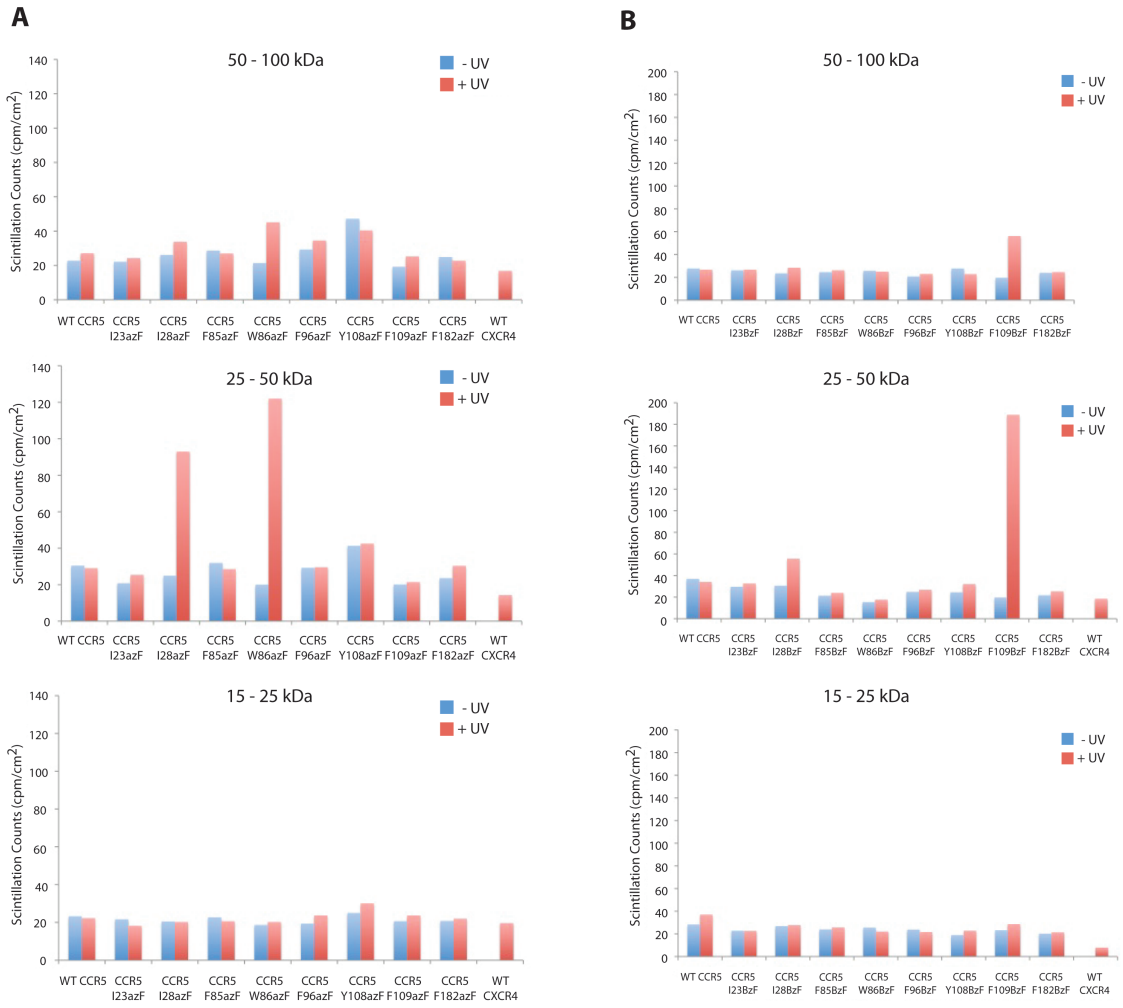

Figure 3-10. Photocrosslinking results with CCR5 UAA mutants. The data set is from the same experiment that is shown in Figure 3-9, except here we include the control sample for each mutant that was not exposed to UV light. The three bar graphs shown here display the amount of tritium detected in the 50 – 100 kDa segment (top), 25 – 50 kDa segment (middle), and 15 – 25 kDa segment (bottom). Panel (A) is the data for azF and shows that the elevated levels of tritium detected in the 25 – 50 kDa segment for the I28azF and W86azF mutants is UV-specific. Panel (B) displays the data when BzF is introduced into CCR5. This data shows that the elevated levels of tritium detected in the 25 – 50 kDa segment for the I28BzF and F109BzF mutants is UV-specific. These results support the conclusion that the increases in tritium levels at the molecular weight of the receptor are a result of a covalent crosslink between the UAA at the positions specified in CCR5 and [^{3}H]-maraviroc. Adapted with permission from (Grunbeck, A., et al. (2012) *ACS Chem. Biol. 7*, 967-972). Copyright (2012) American Chemical Society.

3.2.3. Digestion of CCR5 and MS analysis

The targeted photocrosslinking technique enables the identification of the exact position in the receptor that is involved in the formation of the covalent crosslink with the ligand. To identify the site of the crosslink in maraviroc we optimized a chemical and enzymatic digestion strategy to detect peptide fragments of CCR5 by mass spectrometry. CCR5 was expressed in HEK293T cells, lysed in a detergent containing buffer and immunopurified with the 1D4 mAb. The purified receptor was reduced and alkylated and then precipitated with TCA. The receptor was digested with cyanogen bromide (CNBr) and trypsin and then analyzed by LC-MS/MS by the Proteomics Facility at Rockefeller University. The CCR5 peptides detected resulted in approximately 50% sequence coverage. Most of these peptides were identified by performing a non-specific search, which indicates that the receptor was not digested at locations predicted for CNBr and trypsin digestion. CNBr hydrolyzes peptide bonds at the carboxyl side of Met residues and trypsin cleaves peptide bonds at the carboxyl end of Arg and Lys. Some of the peptides identified seemed to be more likely digested by chymotrypsin, which cleaves peptide bonds at the C-terminal side of Phe, Tyr, and Trp. This is not entirely uncommon as most trypsin samples are reported to have some level of chymotrypsin activity. Although these peptides were not identified when the sample was only digested with chymotrypsin, which might suggest that the concentration of enzyme used could be important to obtain particular digestion patterns or the digestion of CCR5 is not very reproducible. Further experiments need to be performed to obtain a very robust and reproducible digestion protocol for CCR5. The peptides listed in Table 3-2 were detected

in two separate trypsin digestions of the same CNBr-treated sample. The peptide of interest is highlighted in red as this peptide contains Phe 109, which is a position that had high crosslinking efficiency with [^{3}H]-maraviroc.

Table 3-2. The peptide fragments detected by LC-MS/MS after digestion of CCR5 with CNBr and trypsin.

Peptides[a]	Modification[b]	Expectation Value[c]
$_{LGM288}$THCCINPIIYAFVGEK$_{305FRN}$	C3(Carbamidomethyl); C4(Carbamidomethyl)	1.6E-07
$_{ASL162}$PGIIFTR$_{168SQK}$		2.4E-06
$_{IDR127}$YLAVVHAVFALK$_{138ART}$		2.4E-06
$_{VFA160}$SLPGIIFTR$_{168SQK}$		7.0E-05
$_{YLL71}$NLAISDLFFLL$_{81TVP}$		4.7E-05
$_{KCC327}$SIFQQEAPERA$_{337SSV}$		2.5E-05
$_{QLL105}$TGLYFIGFF$_{113SGI}$		0.0033
$_{FCK325}$CCSIFQQEAPERA$_{337SSV}$	C1(Carbamidomethyl); C2(Carbamidomethyl)	0.0013
$_{AVF159}$ASLPGIIFTR$_{168SQK}$		0.0012
$_{KCC327}$SIFQQEAPER$_{336ASS}$		0.0010
$_{LVM211}$VICYSGILK$_{219TLL}$	C3(Carbamidomethyl)	0.00044
$_{FAS161}$LPGIIFTR$_{168SQK}$		0.00011
$_{FCK323}$CCSIFQQEAPER$_{334ASS}$	C1(Carbamidomethyl); C2(Carbamidomethyl)	0.00011

[a] The peptides were identified using Proteome Discoverer 1.3 and Mascot. The peptide sequence in the larger font is the one identified. The numbers and letters on either side indicate the position of the peptide within the protein and the adjacent amino acids.

[b] The modifications are indicated in parentheses next to the residue they modify.

[c] The expectation value was determined by Mascot and "is a measure of the number of matches with scores equal to or better than the score values that are expected to occur only by chance" according to the Mascot definition. A smaller expectation values indicates a better match.

3.2.4. Fluorescein as a Purification Handle

An additional CCR5-maraviroc photocrosslinking study was performed using a fluorescein-labeled maraviroc analogue (FL-maraviroc). A version of this ligand was also synthetized to contain a benzophenone group (FL-MVC-bp). Dr. Martin Teintze from Montana State University provided both of these maraviroc analogues. A panel of CCR5 BzF containing mutants was examined for crosslinking to FL-maraviroc as described for

the CXCR4-FL-T140 crosslinking experiments. HEK293T cells expressing each of these mutants were exposed to UV light in the presence of FL-maraviroc. After solubilization of the cells, the receptors were immunopurified and run on an SDS-PAGE gel. The crosslinks were then detected by Western Blot analysis using an antibody that reacts with fluorescein. The results from this experiment identified two bands on the anti-fluorescein blot at the molecular weight of CCR5, which were present when BzF was introduced at position Ile 23 and Phe 109 (Figure 3-11). These bands were not detected when 100-fold excess of maraviroc was present during the crosslinking experiment. Since FL-maraviroc has a molecular weight of less than 1 kDa, detection of a fluorescein positive band at 37 kDa on a denaturing gel indicates that the ligand is covalently bound to the receptor.

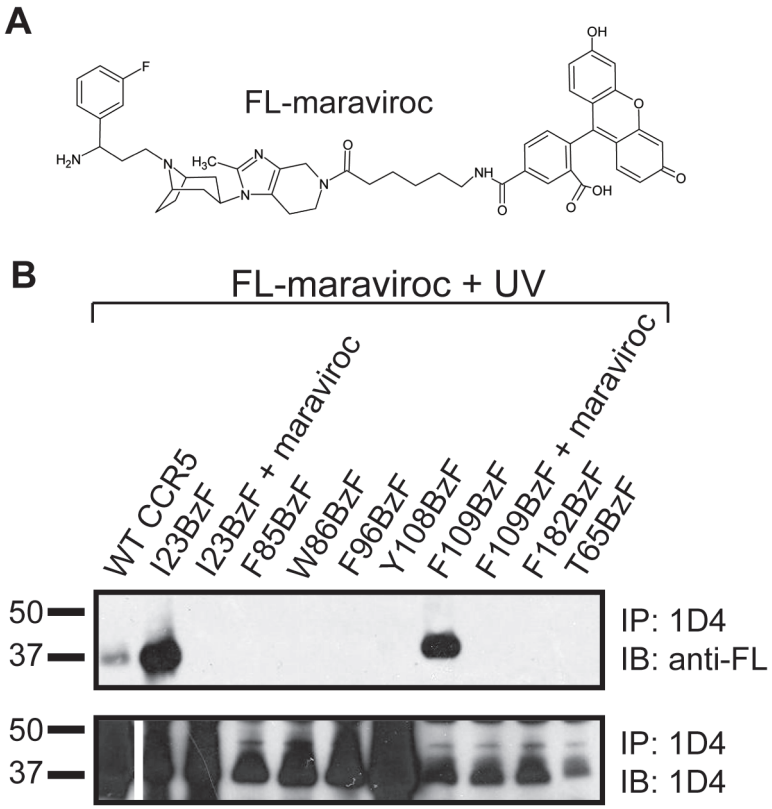

Figure 3-11. Photocrosslinking of CCR5 BzF mutants to FL-maraviroc. (A) The structure of the fluorescein-maraviroc (FL-maraviroc) analogue. (B) The CCR5 BzF mutants were examined for their crosslinking potential to FL-maraviroc. Receptor expression is probed on a Western Blot using the 1D4 antibody, which recognizes an epitope at the C-terminus of the receptor. Two sites (Ile 23 and Phe 109) were found to crosslink specifically to FL-maraviroc as shown by the bands on the anti-fluorescein (anti-FL) blot at the molecular weight of CCR5.

Another advantage of using a fluorescein-labeled ligand in this context is the fluorescein moiety has the potential to be used as a purification tag. This is particularly beneficial for preparing samples for mass spectrometry analysis where the fluorescein-containing peptides can be purified post-digestion of the crosslinked receptor-ligand complex. We tested the ability of the anti-fluorescein antibody to purify two receptor-ligand crosslinked complexes, CXCR4-(FL-T140-BzF) and CCR5-(FL-MVC-bp). For the immunopurification step the anti-fluorescein antibody was pre-bound to protein G magnetic Dynabeads. Cells expressing CXCR4 or CCR5 were exposed to UV light in the presence or absence of the cognate ligand containing a fluorescein and benzophenone group. The cell lysates were bound to the anti-fluorescein beads overnight at 4°C and then samples were eluted and run on a SDS-PAGE gel. The presence of receptor and ligand were then detected via Western Blot analysis. The 1D4 immunoblot shows bands corresponding to CXCR4 (~40kDa) and CCR5 (~37 kDa) only when the fluorescein-labeled ligand was present (Figure 3-12). These bands are also shown to contain fluorescein as is seen by the bands on the anti-fluorescein immunoblot. The bands detected on both blots above 50 kDa are either antibody that eluted from the beads or receptor aggregates. These results suggest that the anti-fluorescein beads are able to specifically purify the crosslinked receptor-(FL-ligand) complex.

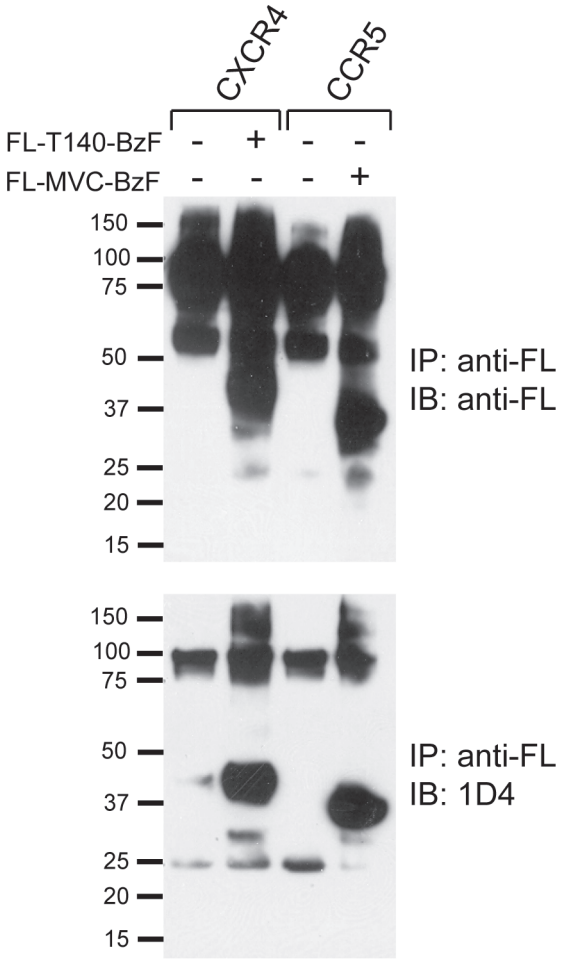

Figure 3-12. Immunopurification with anti-fluorescein (anti-FL) antibody. HEK293T cells expressing CXCR4 or CCR5 were exposed to UV-light in the absence or presence of FL-T140-BzF or FL-MVC-bp as indicated. Cells were solubilized in detergent and the lysate was incubated with Dynabead pre-bound to the anti-FL antibody. Samples were eluted from the beads and run on an SDS-PAGE gel and immunoblotted. The bands on the 1D4 immunoblot are only present in the lanes that contained the FL-labeled ligand. In addition, these bands are also shown to be anti-FL positive. This indicates that the crosslinked receptor-FL-ligand complex can be specifically purified with the anti-FL antibody.

CHAPTER 4: Discussion

4.1. Ligand Binding Sites on CXCR4

4.1.1. Binding interaction with the cyclic-peptide inhibitor T140.

The CXCR4-T140 complex proved to be an ideal model system to validate the targeted photocrosslinking strategy. Previously, CXCR4-T140 complex models were developed using mutagenesis and crosslinking techniques, which included chemical- and photocrosslinking using a T140 analogue containing BzF. These strategies required digestion of CXCR4 to determine the site in the receptor that was covalently bound to the T140 analogue [108,115]. These experiments were only able to resolve a peptide fragment of CXCR4 that was bound to T140. CXCR4-T140 complex models derived from these studies differ from the crystal structure of CXCR4 bound to CVX15, a 16-residue peptide with high homology to T140 [23]. The difference between the CXCR4-T140 complex models and the crystal structure of the CXCR4-CVX15 complex result from the inability of earlier crosslinking techniques to identify the exact site in CXCR4 that crosslinked with T140. We were able to identify the precise site of crosslinking between CXCR4 and T140 by introducing BzF at a specific position in CXCR4 expressed in cells using amber codon suppression. Out of the 8 sites in CXCR4 that were tested, position 189 was the

only location found to form a UV-dependent covalent crosslink with FL-T140. This crosslink was detected when Phe 189 was replaced with both BzF and azF, although the presence of a UV-independent crosslink with azF might suggest activation of this molecule by ambient room light. These results suggest that Phe 189 in CXCR4 is within close proximity to the T140 binding site, whereas the other CXCR4 residues examined are not.

These findings were evaluated in the context of the crystal structure of CXCR4 bound to CVX15, a 16-residue peptide with high homology to T140, to verify the application of this technology to identify residues in CXCR4 that are within close proximity to the T140 binding site. Assuming that T140 has a similar binding site as CVX15, Phe 189 immediately stands out from the other sites as being within crosslinking distance to the ligand (Figure 4-1A&B). Since the crystal structure is limited to a single static image, Dr. Huber carried out computational modeling to predict the possible orientations of BzF at each of these sites (Figure 4-1C). He calculated the distance between the center-of-mass of the reactive carbonyl in BzF to the nearest atom in the CVX15 peptide for each of the possible orientations of BzF at each position. BzF at position 189 was the only site to have a reasonably high probability of being within 2 to 5 Å from the peptide – all other potential carbonyl-CVX15 atom pairs were greater than 5 Å apart (Figure 4-1D).

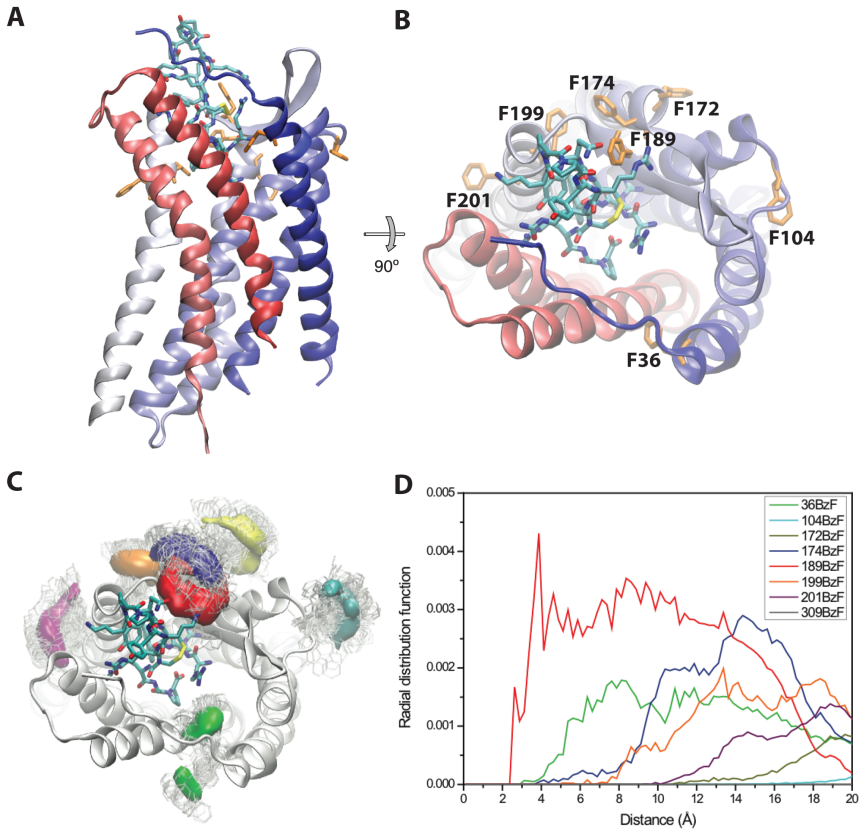

Figure 4-1. Molecular modeling of CXCR4 BzF mutants. (A) Crystal structure of CXCR4 bound to CVX15 (cyan) with residues replaced with UAAs highlighted in orange [23]. N-terminus of receptor is highlighted in blue and fades to red at the C-terminus. (B) A 90° rotation of the structure in A, which shows a view from the extracellular side of the receptor. (C) Crystal structure of CXCR4 (grey) bound to CVX15 (stick representation). The side-chain modeling determined 100 potential orientations of BzF at each site examined in the crosslinking experiments, and are highlighted on the structure in stick form. The colored density maps indicate the location of the BzF carbonyl for all potential orientations of BzF at each position. Position 309 is not shown because this view is from the extracellular side of the receptor. (D) A graph of the radial distribution function *versus* the distance. Distance measurements were made from the carbonyl in BzF to the closest atom in the CVX15 peptide. The graph for position 309 is not visible on this plot because the distance to the ligand is greater than 20 Å. This graph shows that for position 189, CVX15 has the highest probability of being within the reactive radius of 3.1 Å from the carbonyl group in BzF [42]. This supports the data that position 189 is the most likely site to form a crosslink out of the positions examined. From this model, the predicted crosslink site on the ligand is Arg 11, which is conserved in both CVX15 and T140. Note this crosslink is independent of the methionine "magnet" effect [116]. Adapted with permission from (Grunbeck, A., et al. (2011) *Biochemistry 50*, 3411-3413). Copyright (2011) American Chemical Society.

Comparison of the photocrosslinking results to the crystal structure of CXCR4 bound to the homologous T140 peptide ligand, CVX15, has validated our results and enabled us to estimate the distance dependency of the photocrosslinking reaction. The CXCR4-CVX15 crystal structure shows that Phe 189 is within extracellular loop 2 of CXCR4, which borders the main ligand-binding pocket of CXCR4, and lies within close proximity of the bound CVX15 ligand. The main ligand-binding pocket for family A GPCRs is defined as the pocket between the extracellular segments of transmembrane helices III, V, and VI [117]. This suggests that T140 has a similar binding site to CVX15, which is what we would expect due to their structural similarity. The CXCR4-CVX15 crystal structure was also used for the side chain modeling study, which estimated that BzF needs to be within 3 Å of its target in order to form a UV-dependent covalent crosslink. This result agrees with other reports that the minimum required distance to form a crosslink with a benzophenone group is approximately 3 Å [42,118]. Since we observed the same crosslinking profile when azF was used as the photoactivable probe we estimate that the phenylazide group has the same distance requirements as benzophenone in this context.

Through analysis of the complex structure of CXCR4 and CVX15, we propose that the site of the crosslink from the BzF at position 189 in CXCR4 is Arg 11 in T140. This residue is conserved in both the CVX15 and T140 peptides and is the residue in the peptide sequence that is within 3 Å of the photoreactive carbonyl in BzF at position 189. The suggestion that benzophenone is reacting with Arg rather than a Met goes against other reports that benzophenone favors reaction with Met. This phenomenon is described as the methionine “magnet” effect [116].

From this study we concluded that this cell-based photocrosslinking method can be used to identify the residues in a GPCR that are within a precise distance from a bound ligand. We showed that incorporating either BzF or azF into the receptor results in the same crosslinking sites and that fluorescein serves as a very sensitive and specific epitope tag. We also demonstrated that the crosslinking results agreed with a crystal structure of a similar complex and this enabled us to estimate the distance dependency of the photocrosslinking reaction to be approximately 3 Å. We plan to use this methodology to map residues in CXCR4 that line the binding site of other CXCR4-specific ligands, such as the native chemokine ligand SDF-1α and the CXCR4-specific pepducin ATI-2341. In addition, we have applied this targeted photocrosslinking strategy to identify a ligand binding site on another chemokine receptor, CCR5, which will be discussed in the following sections.

4.1.2. Investigating the binding site of the agonist pepducin ATI-2341

Pepducins are a novel GPCR ligand with an undefined mechanism of action. One hypothesis about the mechanism of action of ATI-2341 is that the pepducin mimics the active conformation of the i1 loop of CXCR4. An alternative hypothesis is that the pepducin binds to an allosteric site on CXCR4 to initiate the active state, which could potentially be mimicking a dimer interface or inhibiting dimerization. One way to differentiate between these two hypotheses is through the identification of the location of the pepducin-binding site. We were unable to directly apply the targeted photocrosslinking strategy to investigate the pepducin binding site because at the time we

did not have ATI-2341 labeled with a sensitive detection tag. An anti-rhodamine antibody did not recognize the rhodamine-labeled ATI-2341 analogue on a dot blot, as shown in Figure 2-6. This peptide was detected using fluorescence, but a significant amount of protein was required to detect a specific signal above background [31]. As an alternative we investigated whether ATI-2341 had an overlapping binding site with T140 through a competition study using FL-T140-BzF as a probe. The results showed that crosslinking of FL-T140-BzF to CXCR4 was completely inhibited by unlabeled T140 and partially inhibited by AMD3100. This might indicate that AMD3100 and T140 have similar binding modes. On the other hand, ATI-2341 and maraviroc, a CCR5-specific inhibitor, had no effect on crosslinking of FL-T140-BzF to CXCR4. These results suggest that ATI-2341 does not bind in a similar region as T140. In addition, since T140 is suggested to bind within the conserved main ligand-binding pocket for Family A GPCRs these competition results are also in agreement with other reports that ATI-2341 is a CXCR4-allosteric modulator.

We would like to further investigate the binding mode of ATI-2341 using the CXCR4_R5i1 receptor. The cell surface ELISA showed that this chimeric receptor is expressed at the plasma membrane and at similar levels as WT CXCR4. We now plan to evaluate the ligand binding properties and downstream signaling of this receptor in collaboration with Dr. Stephen Hill's Lab at the University of Nottingham. Chemokine binding will be determined by imaging cells expressing CXCR4_R5i1 in the presence of a fluorescent SDF-1α analogue as described in the methods section. Previously, we were able to show that we can measure specific binding of fluorescent SDF-1α to cells expressing CXCR4 labeled with a SNAP-tag (Figure 2-8). For this study a SNAP-tagged

version of CXCR4_R5i1 will be constructed to enable co-visualization of receptor expression and chemokine binding. The Hill lab will carry out the fluorescence microscopy to measure chemokine binding. In addition, they will evaluate CXCR4 mediated inhibition of forskolin induced cAMP production in HEK Glosensor cells stably expressing CXCR4_R5i1. This Glosensor cell line from Promega stably expresses a luciferase construct containing a cAMP-binding domain. The increase in cAMP production leads to an increase in luciferase activity. From these two experiments we can then infer whether the i1 loop of CXCR4 is necessary for receptor activation. We can then use this information to formulate a new hypothesis about the mechanism of action of pepducins.

4.2. Maraviroc Binding Site on CCR5.

CCR5 is an attractable target for anti-HIV therapeutics because the absence of CCR5 at the cell surface, which is seen with the genetic Δ32 variant of CCR5, has little to no impact on immune function. In addition, cells expressing this variant are protected against HIV-1 infection. These findings directed the development of small molecule HIV therapeutics to target CCR5. Maraviroc is one of the small molecule HIV-1 entry inhibitors, which targets CCR5, that was identified from a small molecule screen at Pfizer. Out of the molecules identified from this screen, maraviroc showed the highest CCR5 specificity and most potent pharmacological activity [19]. Maraviroc is suggested to

be an allosteric modulator of CCR5 and has shown to have inverse agonist activity, which indicates that when maraviroc is bound to CCR5 the functional activity of CCR5 is decreased to below basal levels [119]. Maraviroc is the first GPCR-specific HIV-1 entry inhibitor to be approved by the FDA for therapeutic use, but its precise receptor-drug binding site interactions have not been defined and the mechanism for how the drug blocks HIV-1 entry remains controversial. The clinical relevance of co-receptor blocker agents and the increasing frequency of maraviroc resistant viruses also signify the importance of investigating the binding interactions between CCR5 and maraviroc[120]. Understanding the precise binding orientation of maraviroc could contribute to the design of additional HIV-1 co-receptor blockers. In addition, recent advances in structural studies have confirmed that the arrangement and disposition of the 7-helix bundle of family A GPCRs is conserved. Since maraviroc is hypothesized to bind within a pocket in the 7-transmembrane helical domain of CCR5, determining the allosteric binding site for maraviroc could facilitate the design of other GPCR allosteric regulators.

Currently, there is no high-resolution structure of CCR5 and despite significant effort, including extensive receptor mutagenesis and medicinal chemistry that has created hundreds of small molecule CCR5 ligands, the precise binding site of maraviroc is not known experimentally. We have applied the targeted photocrosslinking technique to identify the amino acid residues in CCR5 that are within close proximity to the bound maraviroc.

We adapted the targeted photocrosslinking method that was previously described for the identification of residues in CXCR4 that were within about 3 Å of FL-T140. The obvious limitation of this earlier work was that in essence we mapped the binding site of

a fluorescein-labeled analogue of T140, and not T140 itself. In the current work, we aimed to devise a strategy to study maraviroc binding without altering the structure of maraviroc. We therefore optimized the targeted photocrosslinking technology in a small-scale cell-based system so that radioactivity could be used to detect the presence of maraviroc. This allowed us to use a tritiated version of maraviroc, which retained its native chemical structure and its pharmacological properties.

The elevated levels of tritium that are detected in the 25-50 kDa gel fractions are a result of a direct UV-dependent crosslink between the UAA incorporated into CCR5 and [^{3}H]-maraviroc. Significantly higher tritium counts were detected in this molecular weight segment when azF was introduced at position Ile 28 and Trp 86 and when BzF was introduced at position Phe 109. The crosslinking patterns observed with BzF and azF may differ as a result of either the structural orientation or reactivity of their unique side chains. The photoreactive group in benzophenone is a carbon radical, which reacts preferentially with C-H bonds. On the other hand the reactive group in phenylazides upon photoactivation is a phenylnitrene, which react more non-specifically with the target molecule. The differences in the reactivities of these photoreactive molecules could result in different preferences for reaction with maraviroc in addition to altering the occurrence of intramolecular crosslinks. Alternatively, the structural difference between the azido and benzoyl functional groups might also have had differing effects on ligand affinity for the mutant CCR5.

We performed ligand-binding experiments with [^{3}H]-maraviroc to determine if introducing a UAA at any of the positions we tested altered maraviroc binding. In addition, three CCR5 BzF mutants were examined in calcium flux assays and found to

retain RANTES binding similar to WT. The only CCR5 mutant that was found to have substantially reduced maraviroc binding was when residue Trp 86 was replaced with BzF. This result suggests that CCR5 W86BzF may have failed to crosslink to maraviroc because of decreased ligand binding affinity. On the other hand, we also detected different crosslinking results at position 109 for the two crosslinkers. The binding data suggest that maraviroc is able to bind to both the CCR5 F109BzF and CCR5 F109azF mutants. Therefore, we can conclude that the difference in crosslinking between the two photoactivable groups at position 109 was a result of a difference in reactivity of the photoactivatable crosslinking groups. Other relevant factors that might affect the reactivity of these crosslinking groups include the chemical bonds of maraviroc near to the reactive moiety and the specific spatial orientation of the side chain.

We then applied our crosslinking results to evaluate a newly predicted structure of the CCR5-maraviroc complex, which was created by our collaborators in Dr. Goddard's Lab at Caltech. They generated a CCR5-maraviroc complex model using the GEnSeMBLE structure prediction methodology, which is a Monte Carlo based method aimed at sampling all reasonable packings of the 7-helix bundle (they examined 10 trillion) and selecting an ensemble of 100 low-energy packings likely to play a role in binding of various ligands and in the activation process[121]. The lowest 20 of these structures were used to predict the most stable CCR5-maraviroc complex, which was used to understand the experimental observations. Dr. Huber calculated 100 different conformations of the BzF and azF side chains at each of the eight positions in CCR5 that were tested in the crosslinking studies, as was done in the CXCR4-T140 study. Distance measurements were then made from either the carbonyl in BzF, or the nitrogen adjacent

to the phenyl ring in azF, to the nearest possible non-hydrogen atom in maraviroc. He then calculated a probability distribution for the side chain at each of the indicated positions to come within 3 Å of contacting a non-hydrogen atom in maraviroc (Figure 4-2). According to the predicted structures, the only positions in CCR5 with a reasonable probability of being within 3 Å of the bound maraviroc were Trp 86, Tyr 108, and Phe 109.

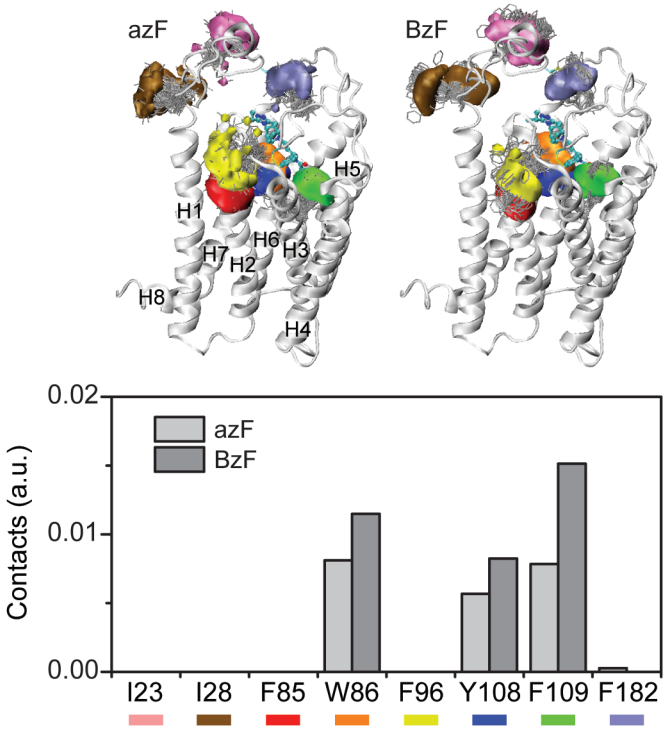

Figure 4-2. Interpretation of crosslinking data according to a molecular model of the CCR5-maraviroc complex. The crosslinking experiments identified three positions in the receptor that were able to crosslink to maraviroc when replaced by either azF or BzF. These results suggest that these three positions in CCR5 are within about 3 Å from the bound maraviroc. We modeled 100 different conformations of the azF and BzF side chains at each of the positions tested in the crosslinking experiments in the context of this CCR5-maraviroc model. We then measured the distance from the reactive group in the photocrosslinker, which is the carbonyl in BzF or the nitrogen adjacent to the phenyl ring in azF, to the nearest non-hydrogen atom in maraviroc. The top panel in this figure displays the CCR5-maraviroc model with the side chain predictions at each of the positions in CCR5 that were replaced with a UAA. The colored densities represent the location of the reactive group in azF (left) and BzF (right) and the colors coordinate with the colored boxes under the residue names listed below the bar graph. The bar graph shows the probability of the side chains at the indicated position to be within 3 Å of contacting a non-hydrogen atom in maraviroc. In this model only Trp 86, Tyr 108, and Phe 109 are found to be within 3 Å of the bound maraviroc. Experimentally, crosslinking was also found between CCR5 I28BzF and maraviroc. Adapted with permission from (Grunbeck, A., et al. (2012) *ACS Chem. Biol. 7*, 967-972). Copyright (2012) American Chemical Society.

The experimental crosslinking data are consistent with the predictions based on the Trp 86 and Phe 109 positions in the CCR5-maraviroc complex. On the other hand, the predicted model suggested that Tyr 108 would be within crosslinking distance of bound maraviroc, but no experimental crosslink was observed under the conditions tested. This discrepancy between predictions based on the complex model and the experimental data could mean that the complex model is not entirely correct (although the other sites were accurately predicted). One possible explanation is that the CCR5 receptor might adopt a different low-energy conformation for Y108BzF and Y108azF mutants. This is plausible because the Goddard lab has found that the Y108A mutant does adopt different transmembrane bundle packing when bound to maraviroc. If the CCR5-maraviroc complex for the UAA-containing protein does not change, a second possibility for the discrepancy could be that the photocrosslinkers at position 108 were not able to react due to *either* a suboptimal orientation of the side chain *or* the lack of an appropriate target bond in maraviroc. Both of these possible explanations are plausible because Tyr 108 side chain lies in a tight region near maraviroc, whereas both Trp 86 and Phe 109 reside in a more open region. Thus, to accommodate the BzF and azF UAAs at the Tyr 108 position, maraviroc may have to move to a different (but may be proximal to original) binding site not accessible to the photocrosslinkers. The computational methods can be used to test these suggestions, but we have not yet done so. In addition, position 28, which formed crosslinks in both the CCR5 I28azF and CCR5 I28BzF mutants, was not identified in the model to be within crosslinking distance of maraviroc. This result again could indicate limitations of the model. However, given the location of Ile 28 in

the N-terminal tail of CCR5, we favor the possibility that the experimental crosslink could suggest an additional maraviroc-binding site, which has also been predicted before by others and us[104,111]. The location of Ile 28, is consistent with a maraviroc "docking site" on the extracellular surface of CCR5 and might be relevant for understanding its mechanism of action with respect to its function as an HIV-1 entry blocker. To further evaluate the exact orientation of maraviroc in the CCR5 ligand-binding pocket, we would like to identify the locations of the crosslinks on the maraviroc molecule.

We plan to use mass spectrometry to identify the site of the crosslink on maraviroc. We have optimized a two-step digestion method of CCR5 for mass spectrometry analysis. This protocol has led to detection of approximately 50% of CCR5's sequence. Out of the peptides that were identified only one contains a site in CCR5 that was identified to crosslink to maraviroc. The sequence of this peptide is TGLYFIGFF, where the central Phe is Phe 109. We would now like to apply this digestion method to a protein sample containing a crosslinked complex of CCR5 F109BzF and maraviroc. Additionally, we plan to digest and analyze crosslinked samples of CCR5 with FL-MVC-bp and CCR5 F109BzF with FL-maraviroc. These complexes have been shown to result in covalent complexes upon UV-light exposure. We have also shown that the fluorescein moiety can be used as a purification tag. Therefore an advantage of using these crosslinked complexes for mass spectrometry analysis is that after digestion of the protein samples the peptide fragment that is crosslinked to the FL-ligand can be purified. This has the potential to clean up the mass spectra and improve identification of the crosslinked site.

Another possibility is to perform the crosslinking experiment with a maraviroc sample where 50% of the ligand is deuterated. This would aid in the identification of the mass peak that corresponds to the peptide crosslinked to maraviroc because there would be two mass peaks present that are separated by the mass difference between maraviroc and deuterated maraviroc. We have obtained a deuterated version of maraviroc from ALSACHIM, where the hydrogens on the two methyl groups have been replaced with deuterium. One potential pitfall in the use of a deuterated ligand is if the position of the deuterium is at the location required for the hydrogen abstraction step of the crosslinking reaction. This could result in a decrease in crosslinking efficiency with the deuterated ligand due to the increased bond strength of a carbon-deuterium bond as compared to a carbon-hydrogen bond.

To our knowledge, this is the first demonstration of a direct chemical crosslink between a GPCR and its native small-molecule ligand. We show that the targeted photocrosslinking technology using UAA mutagenesis can be applied to identify the binding-site of a small molecule ligand and that tritium is a sensitive detection tag for small-scale cell-based assays. We used the crosslinking results to evaluate a model of the CCR5-maraviroc complex and we confirmed that maraviroc binds within the transmembrane helix bundle. This method should prove to be valuable for obtaining structural information about the binding site of GPCR allosteric modulators. In principle, the method should be applicable to any receptor-ligand complex where the receptor can be heterologously expressed in mammalian cells in culture and isotopically-labeled ligands are available.

CHAPTER 5: Conclusions and Future Perspectives

5.1. Targeted Photocrosslinking Strategy

We have established a live-cell targeted photocrosslinking technique for the identification of residues in a GPCR that are within a precise distance from a ligand-binding pocket. The targeted photocrosslinking strategy is unique compared to prototypical photoaffinity ligand studies, as the location of the crosslinker in the receptor is known prior to ligand binding and UV illumination. We have described the introduction of two UAAs containing distinct photoactivatable groups, BzF and azF, into the HIV-1 co-receptors, CCR5 and CXCR4. Each of the receptor UAA mutants were examined for UV-specific crosslinking to either a fluorescein labeled peptide ligand or a tritiated small molecule ligand. In these studies we demonstrated the necessity of a chromatography step under denaturing conditions and a sensitive detection tag on both the receptor and ligand for identification of a UV-induced covalent complex. The application of the photocrosslinking strategy to the CXCR4-T140 complex enabled us to validate our results with a crystal structure and estimate the distance dependency of the photocrosslinking reaction mechanism. In the CCR5-maraviroc study we identified different crosslinking profiles with the two UAAs, which demonstrated the utility of applying two photoactivatable probes with a different size and reactivity. We also exhibited the bigger picture applications of photocrosslinking studies by evaluating a molecular model of the complex with the crosslinking data.

In the future, we would like to expand the targeted photocrosslinking technique in several ways. The first is to further analyze a crosslinked GPCR UAA-ligand complex using mass spectrometry and identify the location of the crosslink on the ligand. Additionally, we would like to apply the targeted photocrosslinking strategy to identify the binding interactions between GPCRs and their other binding partners. Advancing the photocrosslinking technique in these ways will bring this chemically-precise strategy to its full potential of creating a structural model of a GPCR signaling complex in its native environment.

5.1.1. MS analysis to identify site of crosslink in ligand

Mass spectrometry analysis is the obvious choice for a high sensitivity technique to detect the location of the crosslink in the ligand. As a proof-of-principle experiment, we would like to identify the location of the crosslink on maraviroc in the CCR5 F109BzF-maraviroc crosslinked complex. We have optimized a two-step digestion method of CCR5, which involves CNBr treatment followed by trypsin digestion, to detect a peptide fragment in the receptor that contains Phe 109. We plan to perform this experiment using either FL-maraviroc or deuterated maraviroc, as described in the discussion section. In theory, we could also analyze the CCR5 I28azF-maraviroc complex with mass spectrometry as well to prove or disprove our hypothesis of a second maraviroc-binding site, although the digestion steps would need to be altered to allow for detection of the receptor fragment containing Ile 28. Analysis of the mass spectrometry results could be complicated as the fragmentation profile of maraviroc is unknown, but if

the site of attachment in the maraviroc molecule is identified we can infer the orientation of maraviroc in the binding site.

5.1.2. Detecting crosslinks to other GPCR binding partners

Both T140 and maraviroc are extracellular GPCR ligands with inhibitory properties. These two ligands facilitate formation of receptor-ligand complexes at the plasma membrane because the ligand can be added at saturating concentrations and neither T140 nor maraviroc are reported to induce receptor internalization. Stabilizing GPCR complexes prior to UV illumination is optimal for increasing the yield of crosslinked complexed, which improves signal-to-noise in the detection step. Other examples of CCR5- and CXCR4-binding molecules that can be added to cells at specific concentrations and are interesting to study with targeted photocrosslinking are native chemokine ligands, HIV-1 envelope proteins, and pepducins. We have tested antibodies to SDF-1α and the HIV-1 envelope protein gp120 and shown that these antibodies recognize the protein on a denaturing gel (Figure 2-7 A&C). Each of these antibodies reacted with epitopes in the native sequence of the protein. Detection could also be improved by introducing an engineered antibody epitope, such as a FLAG or HA tag. For the pepducin, we have an analogue with a rhodamine label, which was detected on a SDS-PAGE gel with fluorescence, but the anti-rhodamine antibodies we tested did not recognize this label. Therefore a pepducin analogue containing a fluorescein-label or radiolabel will need to be synthesized for targeted photocrosslinking studies.

GPCRs are transmembrane proteins and another component of their signaling complexes are the cytoplasmic binding partners, such as G proteins and β-arrestin. Investigating the binding interactions with cytoplasmic proteins in a live cell complex is a bit more involved because these proteins need to be co-expressed rather than added extracellularly. We have tested several G protein antibodies that recognize either the α or β subunit of G proteins expressed endogenously in HEK293T cells (Figure 2-7B). To improve detection of the G protein subunits with an engineered antibody epitope, the G protein will need to be heterologously expressed in addition to the GPCR UAA mutants. Identifying the binding interactions between a receptor and G protein could facilitate our understanding of ligand functional selectivity and G protein subtype specificity.

5.2. Insights into the Structure and Function of GPCR-ligand Complexes.

Adapted from (Grunbeck, A. and Sakmar, T.P. "Probing GPCR-Ligand Interactions with Targeted Photoactivatable Crosslinkers," *in preparation.*)

Over the past five years there has been a significant increase in the number of solved GPCR crystal structures and the rate of newly available structures is increasing dramatically as enabling technologies have become disseminated. These structures provide atomic-level information about one static structure of a receptor, usually in complex with a ligand or drug. The conditions required for standard crystallography techniques are not always amenable for the analysis of every receptor-ligand complex. Photoactivatable crosslinking studies are one alternative approach to gain structural information about these complexes. The distance dependency of these photolytic

reactions allows for the precise mapping of biological interactions. In fact, targeted photocrosslinking and crystallography are complementary methods because the systematic interpretation of crosslinking data requires knowledge of structure. The availability of a single structure of a GPCR in complex with a ligand can facilitate cell-based photocrosslinking studies with large numbers of ligands or ligand analogues. The only limiting factor is the problem of detecting a crosslink in cases where appropriately labeled ligands are not readily available.

Since the origins of photocrosslinking fifty years ago, many studies have been performed to investigate the interactions between GPCRs and their ligands. However, the recent coincident advances in the structural biology of GPCRs and unnatural amino acid mutagenesis of GPCRs has led to a resurgence of interest in targeted photocrosslinking to probe receptor ligand-binding sites. By interpreting targeted crosslinking data in light of available crystal structures more accurate models of receptor-ligand complexes can be created. The complementarity of these two structural techniques has the potential to advance our understanding of the structure and function of GPCR-ligand interactions.

References

(1) Gilman, A. G. (1987) G proteins: transducers of receptor-generated signals. *Annu Rev Biochem*, *56*, 615.

(2) Pierce, K. L.; Premont, R. T.; Lefkowitz, R. J. (2002) Seven-transmembrane receptors. *Nature reviews. Molecular cell biology*, *3*, 639.

(3) Marinissen, M. J.; Gutkind, J. S. (2001) G-protein-coupled receptors and signaling networks: emerging paradigms. *Trends Pharmacol Sci*, *22*, 368.

(4) Overington, J. P.; Al-Lazikani, B.; Hopkins, A. L. (2006) How many drug targets are there? *Nature Reviews Drug Discovery*, *5*, 993.

(5) Heller, J.; Ostwaldt (1972) RHODOPSIN - CONFORMATIONAL-CHANGES IN A MEMBRANE PROTEIN. *Annals of the New York Academy of Sciences*, *195*, 439.

(6) Hudson, B. D.; Smith, N. J.; Milligan, G. (2011) Experimental challenges to targeting poorly characterized GPCRs: uncovering the therapeutic potential for free fatty acid receptors. *Advances in pharmacology (San Diego, Calif.)*, *62*, 175.

(7) Esche, C.; Stellato, C.; Beck, L. A. (2005) Chemokines: Key players in innate and adaptive immunity. *Journal of Investigative Dermatology*, *125*, 615.

(8) Bleul, C. C.; Farzan, M.; Choe, H.; Parolin, C.; Clark-Lewis, I.; Sodroski, J.; Springer, T. A. (1996) The lymphocyte chemoattractant SDF-1 is a ligand for LESTR/fusin and blocks HIV-1 entry. *Nature*, *382*, 829.

(9) Oberlin, E.; Amara, A.; Bachelerie, F.; Bessia, C.; Virelizier, J. L.; ArenzanaSeisdedos, F.; Schwartz, O.; Heard, J. M.; ClarkLewis, I.; Legler, D. F.;

Loetscher, M.; Baggiolini, M.; Moser, B. (1996) The CXC chemokine SDF-1 is the ligand for LESTR/fusin and prevents infection by T-cell-line-adapted HIV-1. *Nature*, *382*, 833.

(10) Oppermann, M. (2004) Chemokine receptor CCR5: insights into structure, function, and regulation. *Cellular Signalling*, *16*, 1201.

(11) Cheng, Z. J.; Zhao, J.; Sun, Y.; Hu, W.; Wu, Y. L.; Cen, B.; Wu, G. X.; Pei, G. (2000) beta-arrestin differentially regulates the chemokine receptor CXCR4-mediated signaling and receptor internalization, and this implicates multiple interaction sites between beta-arrestin and CXCR4. *J Biol Chem*, *275*, 2479.

(12) Balistreri, C. R.; Caruso, C.; Grimaldi, M. P.; Listi, F.; Vasto, S.; Orlando, V.; Campagna, A. M.; Lio, D.; Candore, G. (2007) CCR5 receptor - Biologic and genetic implications in age-related diseases. *Biogerontology: Mechanisms and Interventions*, *1100*, 162.

(13) Deng, H.; Liu, R.; Ellmeier, W.; Choe, S.; Unutmaz, D.; Burkhart, M.; Di Marzio, P.; Marmon, S.; Sutton, R. E.; Hill, C. M.; Davis, C. B.; Peiper, S. C.; Schall, T. J.; Littman, D. R.; Landau, N. R. (1996) Identification of a major co-receptor for primary isolates of HIV-1. *Nature*, *381*, 661.

(14) Dragic, T.; Litwin, V.; Allaway, G. P.; Martin, S. R.; Huang, Y. X.; Nagashima, K. A.; Cayanan, C.; Maddon, P. J.; Koup, R. A.; Moore, J. P.; Paxton, W. A. (1996) HIV-1 entry into CD4(+) cells is mediated by the chemokine receptor CC-CKR-5. *Nature*, *381*, 667.

(15) Feng, Y.; Broder, C. C.; Kennedy, P. E.; Berger, E. A. (1996) HIV-1 entry cofactor: Functional cDNA cloning of a seven-transmembrane, G protein-coupled receptor. *Science*, *272*, 872.

(16) Balter, M. (1996) A second coreceptor for HIV in early stages of infection. *Science*, *272*, 1740.

(17) Donzella, G. A.; Schols, D.; Lin, S. W.; Este, J. A.; Nagashima, K. A.; Maddon, P. J.; Allaway, G. P.; Sakmar, T. P.; Henson, G.; De Clercq, E.; Moore, J. P. (1998) AMD310, a small molecule inhibitor of HIV-1 entry via the CXCR4 co-receptor. *Nat. Med.*, *4*, 72.

(18) Seibert, C.; Sakmar, T. P. (2004) Small-molecule antagonists of CCR5 and CXCR4: A promising new class of anti-HIV-1 drugs. *Curr. Pharm. Des.*, *10*, 2039.

(19) Dorr, P. K.; Todd, K.; Irvine, R.; Robas, N.; Thomas, A.; Fidock, M.; Sultan, H.; Mills, J.; Perruccio, F.; Burt, K.; Rickett, G.; Perkins, H.; Griffin, P.; Macartney, M.; Hamilton, D.; Westby, M.; Perros, M. (2005) Site-Directed Mutagenesis Studies of CCR5 Reveal Differences in the Interactions between the Receptor and Various CCR5 Antagonists. *Abstracts of the Interscience Conference on Antimicrobial Agents and Chemotherapy*, *45*, 261.

(20) Wu, L. J.; LaRosa, G.; Kassam, N.; Gordon, C. J.; Heath, H.; Ruffing, N.; Chen, H.; Humblias, J.; Samson, M.; Parmentier, M.; Moore, J. P.; Mackay, C. R. (1997) Interaction of chemokine receptor CCR5 with its ligands: Multiple domains for HIV-1 gp120 binding and a single domain for chemokine binding. *Journal of Experimental Medicine*, *186*, 1373.

(21) Mirzabekov, T.; Bannert, N.; Farzan, M.; Hofmann, W.; Kolchinsky, P.; Wu, L. J.; Wyatt, R.; Sodroski, J. (1999) Enhanced expression, native purification, and characterization of CCR5, a principal HIV-1 coreceptor. *Journal of Biological Chemistry*, *274*, 28745.

(22) Tamamura, H.; Hori, A.; Kanzaki, N.; Hiramatsu, K.; Mizumoto, M.; Nakashima, H.; Yamamoto, N.; Otaka, A.; Fujii, N. (2003) T140 analogs as CXCR4 antagonists identified as anti-metastatic agents in the treatment of breast cancer. *FEBS Lett.*, *550*, 79.

(23) Wu, B., Chien, E.Y., Mol, C.D., Fenalti, G., Liu, W., Katritch, V., Abagyan, R., Brooun, A., Wells, P., Bi, F.C., Hamel, D.J., Kuhn, P., Handel, T.M., Cherezov, V., Stevens, R.C. (2010) Structures of the CXCR4 Chemokine GPCR with Small-Molecule and Cyclic Peptide Antagonists. *Science*, *330*, 1066.

(24) Covic, L.; Misra, M.; Badar, J.; Singh, C.; Kuliopulos, A. (2002) Pepducin-based intervention of thrombin-receptor signaling and systemic platelet activation. *Nat Med*, *8*, 1161.

(25) Tchernychev, B.; Ren, Y.; Sachdev, P.; Janz, J. M.; Haggis, L.; O'Shea, A.; McBride, E.; Looby, R.; Deng, Q.; McMurry, T.; Kazmi, M. A.; Sakmar, T. P.; Hunt III, S.; Carlson, K. E. (2010) Identification and characterization of CXCR4-derived pepducins: Reverse engineering of novel chemotactic agonists. *Proc. Natl. Acad. Sci.*

(26) Leff, P. (1995) THE 2-STATE MODEL OF RECEPTOR ACTIVATION. *Trends in Pharmacological Sciences*, *16*, 89.

(27) Park, J. H.; Scheerer, P.; Hofmann, K. P.; Choe, H. W.; Ernst, O. P. (2008) Crystal structure of the ligand-free G-protein-coupled receptor opsin. *Nature*, *454*, 183.

(28) Hoffmann, C.; Zurn, A.; Bunemann, M.; Lohse, M. J. (2008) Conformational changes in G-protein-coupled receptors - the quest for functionally selective conformations is open. *British Journal of Pharmacology*, *153*, S358.

(29) Salon, J. A.; Lodowski, D. T.; Palczewski, K. (2011) Significance of G Protein-Coupled Receptor Crystallography for Drug Discovery. *Pharmacological Reviews*, *63*, 901.

(30) Christopoulos, A.; Kenakin, T. (2002) G protein-coupled receptor allosterism and complexing. *Pharmacol Rev*, *54*, 323.

(31) Janz, J. M.; Ren, Y.; Looby, R.; Kazmi, M. A.; Sachdev, P.; Grunbeck, A.; Haggis, L.; Chinnapen, D.; Lin, A. Y.; Seibert, C.; McMurry, T.; Carlson, K. E.; Muir, T. W.; Hunt, S., 3rd; Sakmar, T. P. (2011) Direct interaction between an allosteric agonist pepducin and the chemokine receptor CXCR4. *J Am Chem Soc*, *133*, 15878.

(32) Congreve, M.; Marshall, F. (2010) The impact of GPCR structures on pharmacology and structure-based drug design. *Br J Pharmacol*, *159*, 986.

(33) Keov, P.; Sexton, P. M.; Christopoulos, A. (2011) Allosteric modulation of G protein-coupled receptors: a pharmacological perspective. *Neuropharmacology*, *60*, 24.

(34) Unal, H.; Karnik, S. S. (2012) Domain coupling in GPCRs: the engine for induced conformational changes. *Trends Pharmacol Sci*, *33*, 79.

(35) Singh, A.; Thornton, E. R.; Westheimer, F. H. (1962) The photolysis of diazoacetylchymotrypsin. *J Biol Chem*, *237*, 3006.

(36) Chowdhry, V.; Westheimer, F. H. (1979) Photoaffinity labeling of biological systems. *Annu Rev Biochem*, *48*, 293.

(37) Fleet, G. W. J.; Porter, R. R.; Knowles, J. R. (1969) Photoaffinity Labelling of Antibodies with Aryl Nitrene as Reactive Group. *Nature*, *224*, 511.

(38) Nakayama, T. A.; Khorana, H. G. (1990) Synthesis of a New Photoactivatable Analogue of 11-*cis*-Retinal. *J. Org. Chem.*, *1990*, 4953.

(39) Nakayama, T. A.; Khorana, H. G. (1990) Orientation of retinal in bovine rhodopsin determined by cross-linking using a photoactivatable analog of 11-cis-retinal. *J. Biol. Chem.*, *265*, 15762.

(40) Galardy, R. E.; Craig, L. C.; Jamieson, J. D.; Printz, M. P. (1974) Photoaffinity labeling of peptide hormone binding sites. *J Biol Chem*, *249*, 3510.

(41) Bayley, H.; Knowles, J. R. (1978) Photogenerated reagents for membrane labeling. 2. Phenylcarbene and adamantylidene formed within the lipid bilayer. *Biochemistry*, *17*, 2420.

(42) Dorman, G.; Prestwich, G. D. (1994) Benzophenone photophores in biochemistry *Biochemistry*, *33*, 5661.

(43) Gritsan, N. P.; Gudmundsdottir, A. D.; Tigelaar, D.; Zhu, Z.; Karney, W. L.; Hadad, C. M.; Platz, M. S. (2001) A laser flash photolysis and quantum chemical study of the fluorinated derivatives of singlet phenylnitrene. *J Am Chem Soc*, *123*, 1951.

(44) Ganjian, I.; Pettei, M. J.; Nakanishi, K.; Kaissling, K. (1978) A photoaffinity-labelled insect sex pheromone for the moth *Antheraea polyphemus*. *Nature*, *271*.

(45) Vogt, R. G.; Prestwich, G. D.; Riddiford, L. M. (1988) Sex pheromone receptor proteins. Visualization using a radiolabeled photoaffinity analog. *J Biol Chem*, *263*, 3952.

(46) Nishikori, K.; Noshiro, O.; Sano, K.; Maeno, H. (1980) Characterization, solubilization, and separation of two distinct dopamine receptors in canine caudate nucleus. *J Biol Chem*, *255*, 10909.

(47) Kuno, T.; Tanaka, C. (1981) Identification of the D-1 dopamine receptor subunit in rat striatum after photoaffinity labeling. *Brain research*, *230*, 417.

(48) Takayanagi, I.; Yoshioka, M.; Takagu, K.; Tamura, Z. (1976) Photoaffinity labeling of the beta-adrenergic receptors and receptor reserve for isoprenaline. *European journal of pharmacology*, *35*, 121.

(49) Darfler, F. J.; Marinetti, G. V. (1977) Synthesis of a photoaffinity probe for the beta-adrenergic receptor. *Biochem Biophys Res Commun*, *79*, 1.

(50) Wrenn, S. M., Jr.; Homcy, C. J. (1980) Photoaffinity label for the beta-adrenergic receptor: synthesis and effects on isoproterenol-stimulated adenylate cyclase. *Proc Natl Acad Sci U S A*, *77*, 4449.

(51) Rashidbaigi, A.; Ruoho, A. E. (1981) Iodoazidobenzylpindolol, a photoaffinity probe for the beta-adrenergic receptor. *Proc Natl Acad Sci U S A*, *78*, 1609.

(52) Lavin, T. N.; Heald, S. L.; Jeffs, P. W.; Shorr, R. G.; Lefkowitz, R. J.; Caron, M. G. (1981) Photoaffinity labeling of the beta-adrenergic receptor. *J Biol Chem*, *256*, 11944.

(53) Burgermeister, W.; Hekman, M.; Helmreich, E. J. (1982) Photoaffinity labeling of the beta-adrenergic receptor with azide derivatives of iodoccyanopindolol. *J Biol Chem*, *257*, 5306.

(54) Burgermeister, W.; Nassal, M.; Wieland, T.; Helmreich, E. J. (1983) A carbene-generating photoaffinity probe for beta-adrenergic receptors. *Biochimica et biophysica acta*, *729*, 219.

(55) Gorman, J. J.; Folk, J. E. (1980) Transglutaminase amine substrates for photochemical labeling and cleavable cross-linking of proteins. *J Biol Chem*, *255*, 1175.

(56) Moseley, J. M.; Findlay, D. M.; Martin, T. J.; Gorman, J. J. (1982) Covalent cross-linking of a photoactive derivative of calcitonin to human breast cancer cell receptors. *J Biol Chem*, *257*, 5846.

(57) Stadel, J. M.; Goodman, D. B.; Galardy, R. E.; Rasmussen, H. (1978) Synthesis and characterization of 2-nitro-5-aziodobenzoylglycyloxytocin, an oxytocin photoaffinity label. *Biochemistry*, *17*, 1403.

(58) Zhou, A. T.; Bessalle, R.; Bisello, A.; Nakamoto, C.; Rosenblatt, M.; Suva, L. J.; Chorev, M. (1997) Direct mapping of an agonist-binding domain within the parathyroid hormone/parathyroid hormone-related protein receptor by photoaffinity crosslinking. *Proc Natl Acad Sci U S A*, *94*, 3644.

(59) Bregman, M. D.; Levy, D. (1977) Labeling of glucagon binding components in hepatocyte plasma membranes. *Biochem Biophys Res Commun*, *78*, 584.

(60) Bregman, M. D.; Cheng, S.; Levy, D. (1978) Synthesis and properties of a photoaffinity probe for the glucagon receptor in hepatocyte plasma membranes. *Biochimica et biophysica acta*, *539*, 489.

(61) Carney, D. H.; Glenn, K. C.; Cunningham, D. D.; Das, M.; Fox, C. F.; Fenton, J. W., 2nd (1979) Photoaffinity labeling of a single receptor for alpha-thrombin on mouse embryo cells. *J Biol Chem*, *254*, 6244.

(62) Ramachandran, J.; Muramoto, K.; Kenez-Keri, M.; Keri, G.; Buckley, D. I. (1980) Photoaffinity labeling of corticotropin receptors. *Proc Natl Acad Sci U S A*, *77*, 3967.

(63) Demoliou, C. D.; Epand, R. M. (1980) Synthesis and characterization of a heterobifunctional photoaffinity reagent for modification of tryptophan residues and its application to the preparation of a photoreactive glucagon derivative. *Biochemistry*, *19*, 4539.

(64) Johnson, G. L.; MacAndrew, V. I., Jr.; Pilch, P. F. (1981) Identification of the glucagon receptor in rat liver membranes by photoaffinity crosslinking. *Proc Natl Acad Sci U S A*, *78*, 875.

(65) Gorka, J.; McCourt, D. W.; Schwartz, B. D. (1989) Automated synthesis of a C-terminal photoprobe using combined Fmoc and t-Boc synthesis strategies on a single automated peptide synthesizer. *Peptide research*, *2*, 376.

(66) Nakamoto, C.; Behar, V.; Chin, K. R.; Adams, A. E.; Suva, L. J.; Rosenblatt, M.; Chorev, M. (1995) Probing the bimolecular interactions of parathyroid hormone with the human parathyroid hormone/parathyroid hormone-related protein receptor. 1. Design, synthesis and characterization of photoreactive benzophenone-containing analogs of parathyroid hormone. *Biochemistry*, *34*, 10546.

(67) Suva, L. J.; Flannery, M. S.; Caulfield, M. P.; Findlay, D. M.; Juppner, H.; Goldring, S. R.; Rosenblatt, M.; Chorev, M. (1997) Design, synthesis and utility of novel benzophenone-containing calcitonin analogs for photoaffinity labeling the calcitonin receptor. *The Journal of pharmacology and experimental therapeutics*, *283*, 876.

(68) Kauer, J. C.; Erickson-Viitanen, S.; Wolfe, H. R., Jr.; DeGrado, W. F. (1986) p-Benzoyl-L-phenylalanine, a new photoreactive amino acid. Photolabeling of calmodulin with a synthetic calmodulin-binding peptide. *J Biol Chem*, *261*, 10695.

(69) Herblin, W. F.; Kauer, J. C.; Tam, S. W. (1987) Photoinactivation of the mu opioid receptor using a novel synthetic morphiceptin analog. *European journal of pharmacology*, *139*, 273.

(70) Li, Y. M.; Marnerakis, M.; Stimson, E. R.; Maggio, J. E. (1995) Mapping peptide-binding domains of the substance P (NK-1) receptor from P388D1 cells with photolabile agonists. *J Biol Chem*, *270*, 1213.

(71) Kage, R.; Leeman, S. E.; Krause, J. E.; Costello, C. E.; Boyd, N. D. (1996) Identification of methionine as the site of covalent attachment of a p-benzoyl-phenylalanine-containing analogue of substance P on the substance P (NK-1) receptor. *J Biol Chem*, *271*, 25797.

(72) Boyd, N. D.; Kage, R.; Dumas, J. J.; Krause, J. E.; Leeman, S. E. (1996) The peptide binding site of the substance P (NK-1) receptor localized by a photoreactive analogue of substance P: presence of a disulfide bond. *Proc Natl Acad Sci U S A*, *93*, 433.

(73) Dong, M.; Wang, Y.; Pinon, D. I.; Hadac, E. M.; Miller, L. J. (1999) Demonstration of a direct interaction between residue 22 in the carboxyl-terminal half of secretin and the amino-terminal tail of the secretin receptor using photoaffinity labeling. *J Biol Chem*, *274*, 903.

(74) Dong, M.; Wang, Y.; Hadac, E. M.; Pinon, D. I.; Holicky, E.; Miller, L. J. (1999) Identification of an interaction between residue 6 of the natural peptide ligand and a

distinct residue within the amino-terminal tail of the secretin receptor. *J Biol Chem*, *274*, 19161.

(75) Dong, M.; Asmann, Y. W.; Zang, M.; Pinon, D. I.; Miller, L. J. (2000) Identification of two pairs of spatially approximated residues within the carboxyl terminus of secretin and its receptor. *J Biol Chem*, *275*, 26032.

(76) Zang, M.; Dong, M.; Pinon, D. I.; Ding, X. Q.; Hadac, E. M.; Li, Z.; Lybrand, T. P.; Miller, L. J. (2003) Spatial approximation between a photolabile residue in position 13 of secretin and the amino terminus of the secretin receptor. *Mol Pharmacol*, *63*, 993.

(77) Tan, Y. V.; Couvineau, A.; Van Rampelbergh, J.; Laburthe, M. (2003) Photoaffinity labeling demonstrates physical contact between vasoactive intestinal peptide and the N-terminal ectodomain of the human VPAC1 receptor. *J Biol Chem*, *278*, 36531.

(78) Tan, Y. V.; Couvineau, A.; Laburthe, M. (2004) Diffuse pharmacophoric domains of vasoactive intestinal peptide (VIP) and further insights into the interaction of VIP with the N-terminal ectodomain of human VPAC1 receptor by photoaffinity labeling with [Bpa6]-VIP. *J Biol Chem*, *279*, 38889.

(79) Tan, Y. V.; Couvineau, A.; Murail, S.; Ceraudo, E.; Neumann, J. M.; Lacapere, J. J.; Laburthe, M. (2006) Peptide agonist docking in the N-terminal ectodomain of a class II G protein-coupled receptor, the VPAC1 receptor. Photoaffinity, NMR, and molecular modeling. *J Biol Chem*, *281*, 12792.

(80) Ceraudo, E.; Murail, S.; Tan, Y. V.; Lacapere, J. J.; Neumann, J. M.; Couvineau, A.; Laburthe, M. (2008) The vasoactive intestinal peptide (VIP) alpha-Helix up to C terminus interacts with the N-terminal ectodomain of the human VIP/Pituitary adenylate

cyclase-activating peptide 1 receptor: photoaffinity, molecular modeling, and dynamics. *Molecular endocrinology (Baltimore, Md.)*, *22*, 147.

(81) Schwyzer, R.; Caviezel, M. (1971) p-Azido-L-phenylalanine: a photo-affinity 'probe' related to tyrosine. *Helvetica chimica acta*, *54*, 1395.

(82) Escher, E. (1977) Isolation and structure analysis of a photoproduct of the new photoaffinity label p-nitrophenylalanine. *Helvetica chimica acta*, *60*, 339.

(83) Escher, E. H.; Nguyen, T. M.; Robert, H.; St-Pierre, S. A.; Regoli, D. C. (1978) Photoaffinity labeling of the angiotensin II receptor. 1. Synthesis and biological activities of the labeling peptides. *J Med Chem*, *21*, 860.

(84) Escher, E. H.; Guillemette, G. (1979) Photoaffinity labeling of the angiotensin II receptor. 3. Receptor inactivation with photolabile hormone analogues. *J Med Chem*, *22*, 1047.

(85) Escher, E.; Laczko, E.; Guillemette, G.; Regoli, D. (1981) Biological activities of photoaffinity labeling analogues of kinins and their irreversible effects on kinin receptors. *J Med Chem*, *24*, 1409.

(86) Suchanek, M.; Radzikowska, A.; Thiele, C. (2005) Photo-leucine and photo-methionine allow identification of protein-protein interactions in living cells. *Nat Methods*, *2*, 261.

(87) Cai, K.; Itoh, Y.; Khorana, F. C. (2001) Mapping of contact sites in complex formation between transducin and light-activated rhodopsin by covalent crosslinking: Use of a photoactivatable reagent. *Proceedings of the National Academy of Sciences of the United States of America*, *98*, 4877.

(88) Karnik, S. S.; Sakmar, T. P.; Chen, H. B.; Khorana, H. G. (1988) Cysteine residues 110 and 187 are essential for the formation of correct structure in bovine rhodopsin. *Proc Natl Acad Sci U S A*, *85*, 8459.

(89) Ward, S. D.; Hamdan, F. F.; Bloodworth, L. M.; Wess, J. (2002) Conformational changes that occur during M3 muscarinic acetylcholine receptor activation probed by the use of an in situ disulfide cross-linking strategy. *J Biol Chem*, *277*, 2247.

(90) Anthony-Cahill, S. J.; Griffith, M. C.; Noren, C. J.; Suich, D. J.; Schultz, P. G. (1989) Site-specific mutagenesis with unnatural amino acids. *Trends in biochemical sciences*, *14*, 400.

(91) Chin, J. W.; Martin, A. B.; King, D. S.; Wang, L.; Schultz, P. G. (2002) Addition of a photocrosslinking amino acid to the genetic code of Escherichiacoli. *Proc Natl Acad Sci U S A*, *99*, 11020.

(92) Chin, J. W.; Santoro, S. W.; Martin, A. B.; King, D. S.; Wang, L.; Schultz, P. G. (2002) Addition of p-azido-L-phenylalanine to the genetic code of Escherichia coli. *J Am Chem Soc*, *124*, 9026.

(93) Huang, L. Y.; Umanah, G.; Hauser, M.; Son, C.; Arshava, B.; Naider, F.; Becker, J. M. (2008) Unnatural amino acid replacement in a yeast G protein-coupled receptor in its native environment. *Biochemistry*, *47*, 5638.

(94) Umanah, G.; Huang, L. Y.; Schultz, P. G.; Naider, F.; Becker, J. M. (2009) Incorporation of the unnatural amino acid p-benzoyl-L-phenylalanine (Bpa) into a G protein-coupled receptor in its native context. *Advances in experimental medicine and biology*, *611*, 333.

(95) Ye, S. X.; Kohrer, C.; Huber, T.; Kazmi, M.; Sachdev, P.; Yan, E. C. Y.; Bhagat, A.; RajBhandary, U. L.; Sakmar, T. P. (2008) Site-specific incorporation of keto amino acids into functional G protein-coupled receptors using unnatural amino acid mutagenesis. *J. Biol. Chem.*, *283*, 1525.

(96) Coin, I.; Perrin, M. H.; Vale, W. W.; Wang, L. (2011) Photo-cross-linkers incorporated into G-protein-coupled receptors in mammalian cells: a ligand comparison. *Angewandte Chemie (International ed. in English)*, *50*, 8077.

(97) Ye, S. X.; Huber, T.; Vogel, R.; Sakmar, T. P. (2009) FTIR analysis of GPCR activation using azido probes. *Nat. Chem. Biol.*, *5*, 397.

(98) Grunbeck, A.; Huber, T.; Sachdev, P.; Sakmar, T. P. (2011) Mapping the ligand-binding site on a G protein-coupled receptor (GPCR) using genetically encoded photocrosslinkers. *Biochemistry*, *50*, 3411.

(99) Navratilova, I.; Sodroski, J.; Myszka, D. G. (2005) Solubilization, stabilization, and purification of chemokine receptors using biosensor technology. *Analytical Biochemistry*, *339*, 271.

(100) Banerjee, S.; Huber, T.; Sakmar, T. P. (2008) Rapid incorporation of functional rhodopsin into nanoscale apolipoprotein bound bilayer (NABB) particles. *Journal of Molecular Biology*, *377*, 1067.

(101) Rashtchian, A. (1995) Novel methods for cloning and engineering genes using the polymerase chain reaction. *Current opinion in biotechnology*, *6*, 30.

(102) Staudinger, R.; Wang, X. H.; Bandres, J. C. (2001) Allosteric regulation of CCR5 by guanine nucleotides and HIV-1 envelope. *Biochemical and Biophysical Research Communications*, *286*, 41.

(103) Berro, R.; Yasmeen, A.; Abrol, R.; Trzaskowski, B.; Abi-Habib, S.; Grunbeck, A.; Lascano, D.; Goddard, W. A.; Klasse, P. J.; Sakmar, T. P.; Moore, J. P. (2013) Use of G-protein coupled and uncoupled CCR5 conformers by CCR5 inhibitor-resistant and -sensitive human immunodeficiency virus type 1 variants. *in preparation*.

(104) Knepp, A. M.; Grunbeck, A.; Banerjee, S.; Sakmar, T. P.; Huber, T. (2011) Direct measurement of thermal stability of expressed CCR5 and stabilization by small molecule ligands. *Biochemistry*, *50*, 502.

(105) Oishi, S.; Masuda, R.; Evans, B.; Ueda, S.; Goto, Y.; Ohno, H.; Hirasawa, A.; Tsujimoto, G.; Wang, Z. X.; Peiper, S. C.; Naito, T.; Kodama, E.; Matsuoka, M.; Fujii, N. (2008) Synthesis and application of fluorescein- and biotin-labeled molecular probes for the chemokine receptor CXCR4. *ChemBioChem*, *9*, 1154.

(106) Nomura, W.; Tanabe, Y.; Tsutsumi, H.; Tanaka, T.; Ohba, K.; Yamamoto, N.; Tamamura, H. (2008) Fluorophore labeling enables imaging and evaluation of specific CXCR4-ligand interaction at the cell membrane for fluorescence-based screening. *Bioconjugate Chem.*, *19*, 1917.

(107) Wilkinson, R. A., Pincus, S.H., Shepard, J.B., Walton, S.K., Bergin, E.P., Labib, M., Teintze, M. (2010) Novel compounds containing multiple guanide groups which bind the HIV co-receptor CXCR4. *Antimicrob. Agents Chemother.*

(108) Trent, J. O.; Wang, Z. X.; Murray, J. L.; Shao, W. H.; Tamamura, H.; Fujii, N.; Peiper, S. C. (2003) Lipid bilayer simulations of CXCR4 with inverse agonists and weak partial agonists. *J. Biol. Chem.*, *278*, 47136.

(109) Ye, S. X.; Zaitseva, E.; Caltabiano, G.; Schertler, G. F. X.; Sakmar, T. P.; Deupi, X.; Vogel, R. (2010) Tracking G-protein-coupled receptor activation using genetically encoded infrared probes. *Nature*, *464*, 1386.

(110) Napier, C.; Sale, H.; Mosley, M.; Rickett, G.; Dorr, P.; Mansfield, R.; Holbrook, M. (2005) Molecular cloning and radioligand binding characterization of the chemokine receptor CCR5 from rhesus macaque and human. *Biochem Pharmacol*, *71*, 163.

(111) Garcia-Perez, J.; Rueda, P.; Alcami, J.; Rognan, D.; Arenzana-Seisdedos, F.; Lagane, B.; Kellenberger, E. (2011) Allosteric model of maraviroc binding to CC chemokine receptor 5 (CCR5). *J Biol Chem*, *286*, 33409.

(112) Liu, Y.; Zhou, E.; Yu, K.; Zhu, J.; Zhang, Y.; Xie, X.; Li, J.; Jiang, H. (2008) Discovery of a novel CCR5 antagonist lead compound through fragment assembly. *Molecules*, *13*, 2426.

(113) Dragic, T.; Trkola, A.; Thompson, D. A.; Cormier, E. G.; Kajumo, F. A.; Maxwell, E.; Lin, S. W.; Ying, W.; Smith, S. O.; Sakmar, T. P.; Moore, J. P. (2000) A binding pocket for a small molecule inhibitor of HIV-1 entry within the transmembrane helices of CCR5. *Proc Natl Acad Sci U S A*, *97*, 5639.

(114) Seibert, C.; Ying, W.; Gavrilov, S.; Tsamis, F.; Kuhmann, S. E.; Palani, A.; Tagat, J. R.; Clader, J. W.; McCombie, S. W.; Baroudy, B. M.; Smith, S. O.; Dragic, T.; Moore, J. P.; Sakmar, T. P. (2006) Interaction of small molecule inhibitors of HIV-1 entry with CCR5. *Virology*, *349*, 41.

(115) Boulais, P. E.; Dulude, D.; Cabana, J.; Heveker, N.; Escher, E.; Lavigne, P.; Leduc, R. (2009) Photolabeling identifies transmembrane domain 4 of CXCR4 as a T140 binding site. *Biochem. Pharm.*, *78*, 1382.

(116) Wittelsberger, A.; Thomas, B. E.; Mierke, D. F.; Rosenblatt, M. (2006) Methionine acts as a "magnet" in photoaffinity crosslinking experiments. *FEBS Lett.*, *580*, 1872.

(117) Rosenkilde, M. M.; Benned-Jensen, T.; Frimurer, T. M.; Schwartz, T. W. (2010) The minor binding pocket: a major player in 7TM receptor activation. *Trends Pharmacol. Sci.*, *31*, 567.

(118) Sato, S.; Mimasu, S.; Sato, A.; Hino, N.; Sakamoto, K.; Umehara, T.; Yokoyama, S. (2010) Crystallographic Study of a Site-Specifically Cross-Linker Protein Complex with a Genetically Incorporated Photoreactive Amino Acid. *Biochemistry*.

(119) Garcia-Perez, J.; Rueda, P.; Staropoli, I.; Kellenberger, E.; Alcami, J.; Arenzana-Seisdedos, F.; Lagane, B. (2011) New insights into the mechanisms whereby low molecular weight CCR5 ligands inhibit HIV-1 infection. *J Biol Chem*, *286*, 4978.

(120) Metz, M.; Bourque, E.; Labrecque, J.; Danthi, S. J.; Langille, J.; Harwig, C.; Yang, W.; Darkes, M. C.; Lau, G.; Santucci, Z.; Bridger, G. J.; Schols, D.; Fricker, S. P.; Skerlj, R. T. (2011) Prospective CCR5 small molecule antagonist compound design using a combined mutagenesis/modeling approach. *J Am Chem Soc*, *133*, 16477.

(121) Abrol, R.; Bray, J. K.; Goddard, W. A., 3rd (2011) BiHelix: Towards de novo Structure Prediction of an Ensemble of G protein-Coupled Receptor Conformations. *Proteins: Structure, Function, and Bioinformatics*, *In press*.